A STUDY ON NEW GRAPHITE INTERCALATION COMPOUNDS OF FLUORINE AND METAL FLUORIDES

MASAYUKI KAWAGUCHI

1984

A STUDY ON NEW GRAPHITE INTERCALATION COMPOUNDS OF FLUORINE AND METAL FLUORIDES

MASAYUKI KAWAGUCHI

1984

Preface

Since Scaufhautl first reported a graphite intercalation compound at 1841, many investigations have been done mainly in the fundamental fields. Recently, a growing interest has been taken in graphite intercalation compounds of fluorides since it was found that some of them have an unique property of a high electrical conductivity. Most of them are, however, hygroscopic and unstable in air, which makes it difficult to apply them to a wide variety of practical fields.

The main purpose of this study is the preparation of a new stable graphite intercalation compound, which was attempted in a ternary system with fluorine and metal fluoride such as AlF_3, FeF_3, MgF_2, CuF_2 or LiF. The intercalation reaction is based on the reaction of fluorine with metal fluoride, for which a further extensive work is necessary. The results included in this thesis are only the first step for this type of intercalation compounds. It is desirable that the more precise study is made concerning the crystal structure, physical properties, electrochemical behavior and so on.

The present study has been carried out under the direction of Professor Nobuatsu Watanabe in Kyoto University.

The author wishes to thank Professor Nobuatsu Watanabe and Assistant, Dr. Tsuyoshi Nakajima for their helpful advices and discussion, and students, Messrs. Akira Izumi, Takashi Kawasaki, Hitoshi Ando and Hidetoshi Watanabe for their excellent assistance in the experimental work.

Further, thanks are given to Assistant Professor Koichiro Nakanishi, Assistant, Dr. Hidekazu Touhara and all members of general physical chemistry laboratory for their kind encouragement and support during the work.

The author also wishes to express his thanks to Mr. Noriyuki

Tanaka for his helpful advice in making Wien bridge and to Dr. Fujinobu Nakamura for his assistance in NMR measurement.

Masayuki Kawaguchi

Department of Industrial Chemistry
Faculty of Engineering
Kyoto University
Yoshida, Sakyo-ku, Kyoto, Japan

11 December, 1983

Contents

GENERAL INTRODUCTION

1. Review of the Studies on Graphite Intercalation Compounds (GIC's)

Graphite with amphoteric nature has an ability to intercalate various species between its layers stacked with van der Waals bond. The compound thus formed is called graphite intercalation compound (GIC). A lot of chemical species have been intercalated into graphite since Scaufhautl first reported a GIC containing sulfate ion in 1841,[1] which was characterized more fully by Brodie in 1859.[2] Brodie also investigated graphite oxide with a covalent bond. Graphite-alkali metal compounds were reported by Fredenhagen in 1926[3] and in recent years have been investigated on their electronic structure[4,5,6] and catalytic behavior.[7,8,9] Ruff and Bretschneider reported carbon monofluoride, $(CF)_n$, in 1933,[10] which is a covalent compound of graphite and practically used as an active mass of lithium battery[11,12,13,14] or solid lubricant.[15,16,17,18] The X-ray diffraction study on GIC began in 1930s, and the study of their physical properties in the late 1940s. Since it was found that some of GIC's have high electrical conductivity[19,20] or superconductivity,[21] the study on GIC has diffused widely both in the fundamental and practical aspects.

1.1 Structure of GIC

As is shown in Figure 1, graphite has a layered structure of hexagonal carbon network planes stacked with van der Waals bond. The distance between adjacent carbon planes is ca. 3.35 Å and the interlayer spaces are flexible for intercalating some chemical species in a periodic sequence. This intercalated species is called intercalant. The stage of GIC is defined as the number of graphite layers held between two intercalant layers (Figure 2).

The distance in direction of c-axis between one intercalant layer and the neighbor is called identity period (I_c).

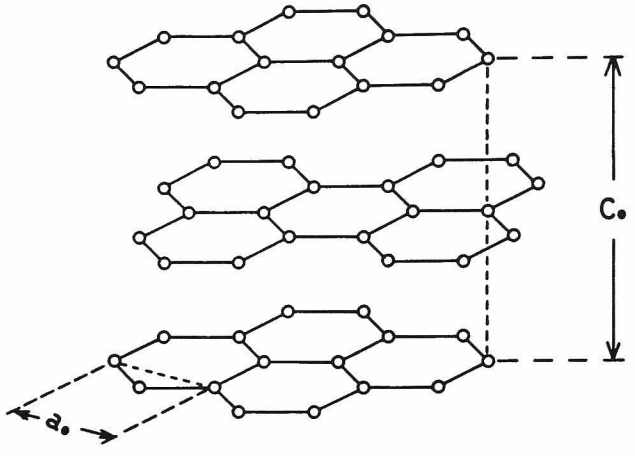

Fig. 1 The hexagonal network planes of graphite.
The spacing between adjacent carbon planes is 3.35 Å.
a_0 = 2.46 Å
c_0 = 6.7 Å

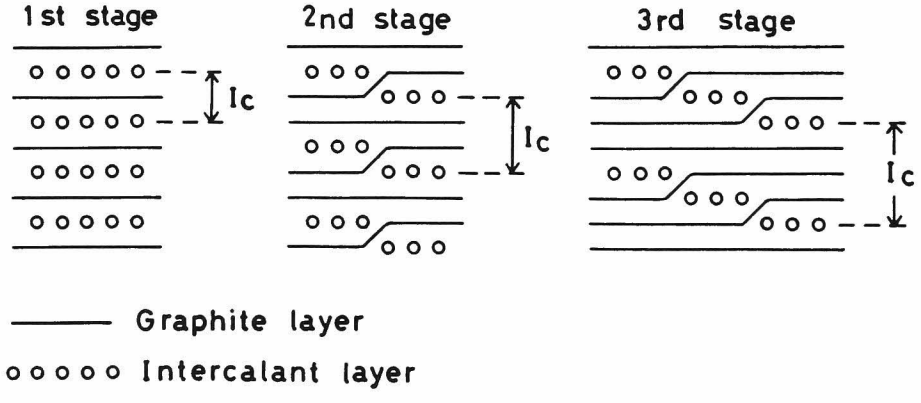

Fig. 2 A staging model proposed by Hérold and co-workers.[22)]
I_c: Identity period in direction of c-axis

1.2 Classification of GIC

In order to be intercalated into graphite layers, the chemical species must have a high vapor pressure and a strong chemical interaction with graphite. GIC's are classified into two categories, depending on the chemical bond between intercalated species and graphite. One is a nonconducting intercalation compound having a covalent bond between carbon and intercalant. In this case, host graphite loses aromatic property and electrical conductivity. Graphite fluorides, $(CF)_n$ and $(C_2F)_n$, and graphite oxide are included in this type of intercalation compound. Poly (carbon monofluoride), $(CF)_n$ is a white, nonconducting compound, made by fluorination of graphite in the temperature range, 420-630°C,[23] and a first stage compound with a chair arrangement of the sp^3-hybridized carbon sheets.[24] Recently, Watanabe et al. found a new type of graphite fluoride, poly (dicarbon monofluoride), $(C_2F)_n$,[25] which is a gray, nonconducting compound prepared by fluorination of graphite at 350-400°C with a second stage structure also having a zig-zag carbon sheets.

Another group is a compound with planar graphite layers after intercalation. These GIC's have a weak ionic bond between carbon and intercalants, and in many cases, have high electrical conductivities. They are further classified into two groups according to whether an intercalant gives the electron to graphite or accepts it from graphite. The former is called a donor-type compound accomodating an electropositive species such as alkali metal[26,27] between graphite layers. The latter is an acceptor-type compound containing Lewis acid (halogen,[28,29] metal halide,[30,31] oxyhalide[32]), acidic oxide (N_2O_5, SO_3)[33,34] or strong Brönsted acid (H_2SO_4, HNO_3).[35,36] (Table 1)

Table 1 Classification of graphite intercalation compounds.

Covalent compound		
Intercalant	GIC	
Fluorine	Graphite fluoride	$(CF)_n$, $(C_2F)_n$
Oxygen	Graphite oxide	$C_8O_2(OH)_2$, etc.
Electroconductive compound		
Type	Intercalant	GIC
Donor-type	Alkali metal	LiC_6, KC_8, RbC_8, CsC_8
	Alkaline earth metal	CaC_8, SrC_6, BaC_6
Acceptor-type	Halogen	C_8Cl, C_8Br, $C_{8.7}IF_5$
	Acid	C_5HNO_3, $C_8H_2SO_4$
	Metal fluoride	C_8AsF_5, $C_{21}TiF_4$
	Metal chloride	$C_9AlCl_{3.3}$, $C_{4.7}FeCl_2$
	Metal bromide	$C_9AlBr_3 \cdot Br_2$, $C_{14.2}FeBr_{2.1}$
	Metal oxide	$C_{6.8}CrO_3$

1.3 Physical Properties and Applications of GIC

1.3.1 High Electrical Conductivity

A high electrical conductivity is the most characteristic feature of GIC. The large increase in conductivity of intercalated graphite results from a charge transfer between an intercalant and graphite layers. In the band structure of graphite, the valence band slightly overlaps with conduction band so that graphite may have some conductive electrons and the same number of holes. In case of a donor type compound, graphite accepts the conductive electron from an intercalant to form an n-type conduc-

tor. On the other hand, in case of the acceptor type, the hole increases in valence band so as to produce a p-type conductor. With increasing carrior concentration, the electrical conductivity increases in both cases.

Many GIC's have been studied for the purpose of developing an electroconductive material.[37,38] One example was a composite wire consisting of copper sheath and graphite-SbF_5 compound, prepared by Vogel.

1.3.2 Active Mass of Lithium Battery

Only graphite fluoride, $(CF)_n$, is now commercially used as an active mass of lithium battery using nonaqueous electrolyte.[11,12,13,14] A new graphite fluoride, $(C_2F)_n$, has also high possibilities as a cathode material because it shows a higher discharge potential by 0.2-0.3 V than $(CF)_n$ on galvanostatic discharge of 0.5 mA/cm^2.[39,40] Electroconductive GIC's such as $C_{21}TiF_4$ and $C_{25}AuCl_3$ have been tested,[41] however, the discharge characteristics were inferior to those of $(CF)_n$ or $(C_2F)_n$ with regard to flatness and discharge potential.

1.3.3 Chemical Reagent, Catalyst

Several investigations have indicated that GIC's may become useful as chemical reagents.[42,43,44] The advantages of GIC arise from slow release of an intercalant, thus moderating its activity or from specific, stereochemical effects peculiar to graphite.

It was also reported that potassium-graphite compound had a high catalytic activity for isomerization reaction of olefin,[45] exchange reaction between H_2 and D_2,[46] or addition of hydrogen.[47]

2. Purpose of the Present Study

Though many applications have been attempted as described above, only a few GIC's are now in practical use. Except a non-conducting compound, $(CF)_n$ or $(C_2F)_n$, most of GIC's are hygroscopic and unstable in air, which makes it difficult to put them in practical applications. Most intercalation compounds require encapsulation to ensure chemical stability.

The purpose of the present study is to prepare a stable GIC from graphite and fluorine with metal fluoride having a high melting or boiling point, and to investigate the electrical conductivity, discharge characteristics in batteries and catalytic behavior for preparation of $(C_2F)_n$.

3. Scope of the Present Study

In Chapter 1 are described the preparation of GIC's from several kinds of graphite, fluorine and metal fluorides (AlF_3, FeF_3, MgF_2, CuF_2, LiF), and the results analysed by means of elemental analyses, X-ray diffractometry, ESCA, ^{19}F-NMR and DTA.

In Chapter 2, intercalation mechanism is discussed on the basis of the reaction between metal fluoride and fluorine and thermogravimetric curves on intercalation reaction.

Chapter 3 deals with the electrical conductivities of GIC's. The conductivities and stability are compared with regard to crystallinity of host graphite or metal fluorides.

In Chapter 4, discharge characteristics of GIC's are discussed in comparison with those of $(CF)_n$ and $(C_2F)_n$. The discharge reaction is considered from the results of analyses of discharge products.

Chapter 5 deals with $(C_2F)_n$ prepared via GIC. The reaction rate, composition and crystallinity of the products are compared

with those of $(C_2F)_n$ prepared by the conventional method.

References

1) P.Schaufhautl, J. Prakt. Chem., 21, 155 (1841).
2) B.C.Brodie, Philos. Trans. R. Soc., 149, 249 (1859).
3) K.Fredenhagen and G.Cadenbach, Z. Anorg. Allgem. Chem., 158, 249 (1926).
4) T.Inoshita, K.Nakao and H.Kimimura, J. Phys. Soc. Jpn., 43, 1237 (1977).
5) N.A.W.Holzwarth, S.Rabii, and L.A.Girifalco, Phys. Rev. B, 18, 5190 (1978).
6) H.Suematsu, K.Higuchi and S.Tanuma, J. Phys. Soc. Jpn., 48, 1541 (1980).
7) J.M.Lalancette, G.Rollin and P.Dumas, Can. J. Chem., 50, 3058 (1972).
8) M.Ichikawa, Y.Inoue and K.Tamaru, J. Chem. Soc. Chem. Comm., 1972, 928 (1972).
9) J.M.Lalancette and R.Roussel, Can. J. Chem., 54, 2110 (1976).
10) O.Ruff and O.Bretschneider, Z. Anorg. Allgem. Chem., 217, 1 (1934).
11) N.Watanabe and M.Fukuda, U. S. Pat., 3,536,532 (1970); N.Watanabe and M.Fukuda, ibid., 3,700,502 (1972).
12) M.Fukuda and T.Iijima, Prog. Batt. Solar Cells, 1, 26 (1978).
13) J.Watanabe, H.Ogawa and R.Okazaki, ibid., 1, 39 (1978).
14) J.Watanabe, E.Kawakubo, T.Shinagawa and Y.Kajikawa, ibid., 3, 74 (1980).
15) R.L.Fusaro and H.E.Sliney, ASLE Trans., 13, 56 (1970).
16) H.Gisser, M.Petronio and A.Shapiro, Lubr. Eng., 28, 161 (1972).
17) R.L.Fusaro and H.E.Sliney, ASLE Trans., 16, 189 (1973).
18) C.Martin, J.Sullean and M.Roussel, Wear, 34, 215 (1975).
19) F.L.Vogel, J. Mat. Sci., 12, 982 (1977).

20) G.M.T.Foley, C.Zeller, E.R.Falardeau and F.L.Vogel, Solid State Commun., 24, 371 (1977).
21) N.B.Hannay, T.H.Geballe, B.T.Matthias, K.Andres, P.Schmidt and D.MacNair, Phys. Rev. Lett., 14, 225 (1965).
22) N.Daumas and A.Hérold, C. R. Acad. Sci. Ser. C, 268, 373 (1969).
23) P.Kamarchik and J.L.Margrave, Acc. Chem. Res., 11, 296 (1978).
24) V.K.Mahajan, R.B.Badachhape and J.L.Margrave, Inorg. Nucl. Chem. Lett., 10, 1103 (1974).
25) Y.Kita, N.Watanabe and Y.Fujii, J. Am. Chem. Soc., 101, 3832 (1979).
26) J.M.Lalancette, G.Rollin and A.P.Giraitis, Can. J. Chem., 50, 3058 (1972).
27) F.Hulliger, Phys. Chem. Mater. Layered Struct., 5, 52 (1976).
28) J.G.Hooley, Carbon, 11, 225 (1973).
29) A.Hérold, Mater. Sci. Eng., 31, 1 (1977).
30) W.Rüdorff, E.Stumpp, W.Spriessler and F.W.Siecke, Angew. Chem., 75, 130 (1963).
31) E.Stumpp, Mater. Sci. Eng., 31, 53 (1977).
32) H.P.Boehm and J.N.Meussdoerffer, Carbon, 9, 521 (1971).
33) H.Fuzellier and A.Hérold, C. R. Acad. Sci. Ser. C, 267, 607 (1968).
34) M.Bagouin, H.Fuzellier and A.Hérold, ibid., 262, 1074 (1966).
35) S.Aronson, C.Frishberg and G.Frankel, Carbon, 9, 715 (1971).
36) D.E.Nixon, G.S.Parry and A.R.Ubbelohde, Proc. R. Soc. London, Ser. A, 291, 324 (1966).
37) A.R.Ubbelohde, Carbon, 14, 1 (1976).
38) F.L.Vogel, G.M.T.Foley, C.Zeller, E.R.Falardeau and J.Gan, Mater. Sci. Eng., 31, 261 (1977).
39) N.Watanabe, Solid St. Ionics, 1, 87 (1980).
40) N.Watanabe, R.Hagiwara, T.Nakajima, H.Touhara and K.Ueno, Electrochimica Acta, 27, 1615 (1982).

41) M.Armand and P.Touzain, Mater. Sci. Eng., 31, 319 (1977).
42) H.B.Kagan, Pure Appl. Chem., 46, 177 (1976).
43) R.Setton, Mater. Sci. Eng., 31, 303 (1977).
44) M.S.Whittingham, L.B.Ebert, in "Physics and Chemistry of Materials and Layered Structures" (F.Levy, ed.), Vol. 6, D. Reidel, Dordrecht, 1979.
45) D.M.Ottmers and H.F.Pase, Ind. Eng. Chem. Fundamentals, 5, 302 (1966).
46) K.Watanabe, T.Kondow, M.Soma, T.Onishi and K.Tamaru, J. Chem. Soc. Chem. Comm., 1972, 39 (1972).
47) K.Tamaru and Y.Iwazawa, Tanso, 1975, 23 (1975).

Chapter 1

PREPARATION OF NEW GRAPHITE INTERCALATION COMPOUNDS*

1. Introduction

Reaction of natural graphite with fluorine gas yields graphite fluorides, $(CF)_n$ and $(C_2F)_n$ at temperatures, 350-600°C.[1,2] Below 300°C, fluorine gas is, however, so inert to graphite that no graphite intercalation compound (GIC) is formed.

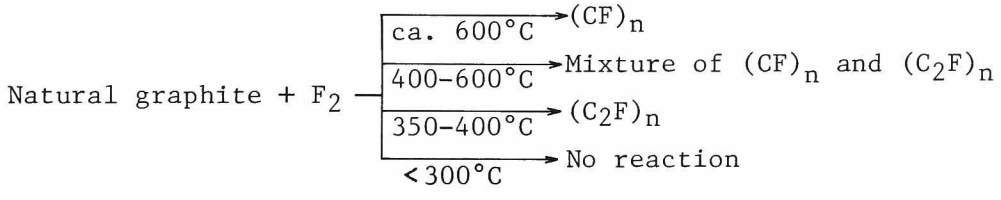

Metal fluorides hitherto intercalated into graphite have low melting or boiling points so that the preparation of GIC's are generally made at temperatures higher than the melting points. These fluorides are molecular crystal in solid state and in similar state even in the GIC's. For example, SbF_5 (mp; 8.3°C) reacts with graphite at 70°C to form a 1st stage compound, $C_{6.5}SbF_5$,[3] and a reaction of AsF_5 (mp; -80°C) with graphite gives $C_{10}AsF_5$.[4] These GIC's show high electrical conductivities,[5] however, they are very hygroscopic in moist air. On the other hand, ionic metal fluorides such as AlF_3, FeF_3, MgF_2, CuF_2 and LiF are not intercalated because they have no vapor pressure at low temperatures and no interaction with graphite.

Natural graphite + AlF_3, FeF_3, MgF_2, CuF_2 or LiF $\xrightarrow[20\text{-}400°C]{}$ No reaction

---

* Z. Naturforsch., 36b, 1419 (1981); Chem. Lett., 1981, 1045 (1981); Carbon, 20, 287 (1982); Nippon Kagaku Kaishi, 1983, 283 (1983).

In this chapter, preparation and analyses of new GIC's containing fluorine and metal fluorides described above are reported.

$$\text{Graphite} + F_2 + MF_n \longrightarrow C_xF(MF_n)_y$$

where M is Al, Fe, Mg, Cu or Li and n is 3, 2 or 1

2. Experimental

2.1 Materials

Graphite materials used were Madagascar natural graphite, petroleum coke heat-treated at 2800°C (graphitized PC), pyrolytic graphite heat-treated at 3000°C (PG), PAN-based carbon fiber heat-treated at 2800°C. Figure 1-1 shows X-ray diffraction patterns of graphitized PC and flaky natural graphite. The purity of natural graphite was more than 99.4 % after purification with hydrogen fluoride solution. Other artificial graphite had more higher purity than natural graphite.

Fluorine gas was supplied by Daikin Kogyo Co. Ltd. The purity of fluorine gas was 99.7 %. The impurity was almost nitrogen and the content of hydrogen fluoride was under 0.01 mol%. A trace amount of hydrogen fluoride in fluorine gas was removed by sodium fluoride pellets heated at 100°C. Unreacted fluorine gas was made to react with soda lime.

Metal fluorides and metals used were anhydrous aluminum fluoride (Kishida Kagaku Co. Ltd., purity: >98 %), anhydrous magnesium fluoride (Hashimoto Chemical Industries Co. Ltd., >98 %), anhydrous lithium fluoride (Nakarai Chemicals Ltd., >97 %), powdery copper (E. Merck AG., >99.7 %), and reduced iron (Nakarai Chemicals Ltd., >99 %). Anhydrous copper fluoride (Ozark Mahoning Co.) was used after further purification: the fluoride was dried under vacuum for 14 h at 20-115°C, followed by treatment in fluorine gas flow at

115°C for 12 h. Powdery copper was used after reduction in hydrogen atmosphere at 20-450°C.

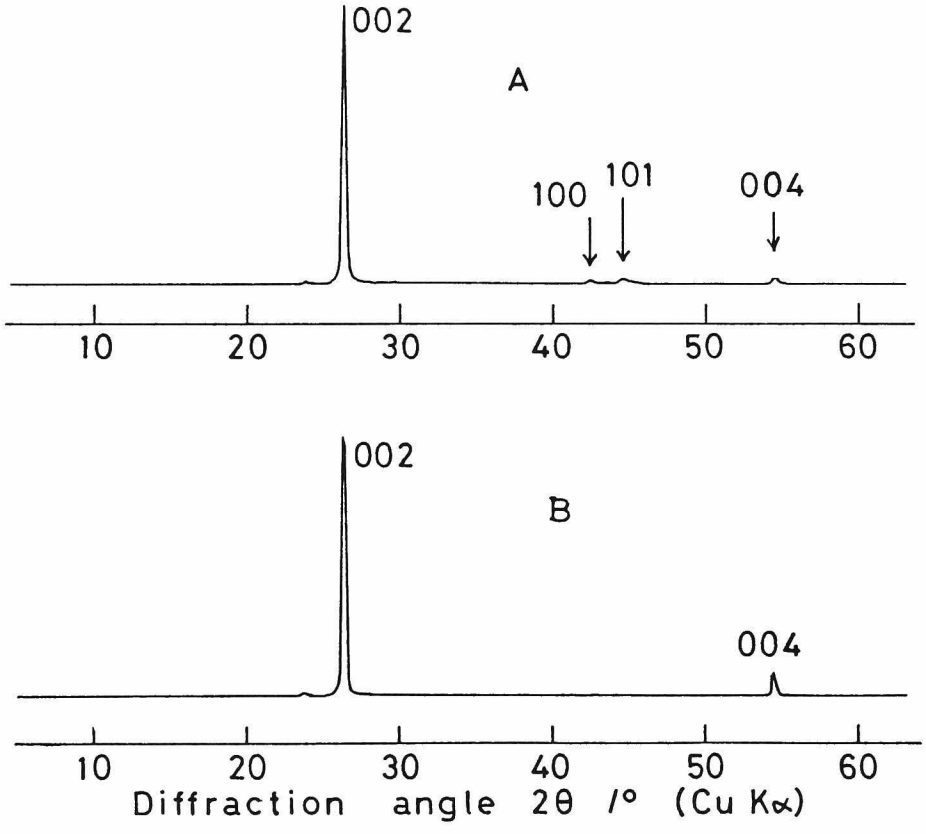

Fig. 1-1 X-ray diffraction patterns of graphitized PC (A) and flaky natural graphite (833-295 μm) (B).

2.2 Preparation of GIC

Figure 1-2 shows the fluorination apparatus, in which the reaction tube and vessel were made of nickel with copper pipe line and stainless steel valves.

A reaction vessel containing graphite and metal fluoride was placed in the reaction tube and the system was evacuated by a rotary pump at ca. 200°C for more than 12 h. Fluorine gas of 1.0×10^5 Pa (1 atm) was then introduced into the reactor and removed out of the system after ca. 30 min at the temperature. This treatment was repeated for the removal of a trace hydrogen fluoride until no hydrogen fluoride was detected in the IR gas cell connected with the reaction tube. The system was then gradually cooled down to room temperature and maintained for 0.5-7 days in fluorine atmosphere (1.0×10^5 Pa). After the reaction, fluorine gas was substituted for nitrogen and GIC formed was obtained.

A trace hydrogen fluoride was intercalated into graphite together with fluorine and metal fluoride, if it was not removed from the reaction system. Figure 1-3 is the IR spectra of fluorine gas (1.0×10^5 Pa, 1 atm) containing almost no HF (<0.01 mol%) (A), 0.01-0.02 mol% HF (B) and 1 mol% HF (C). Hydrogen fluoride of less than 0.01 mol% was undetectable. It was confirmed that no GIC containing HF was formed under this condition (Figure 1-3-A). In case of Figure 1-3-B, hydrogen fluoride was slightly intercalated into graphite, in which the amount of intercalant was several percent (wt%).

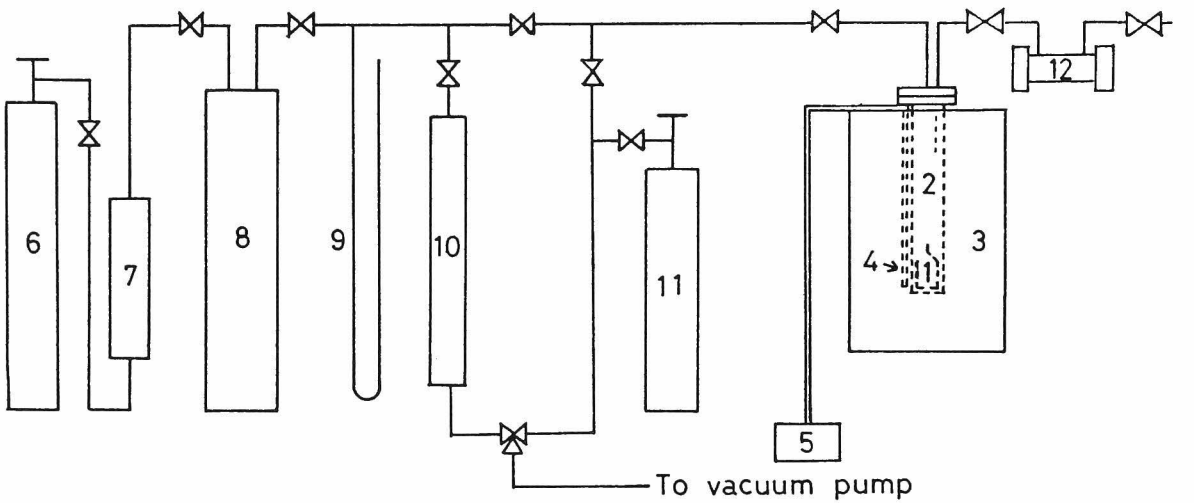

Fig. 1-2 Schematic diagram of experimental apparatus.

1. Reaction vessel
2. Reaction tube
3. Electric furnace
4. Thermocouple
5. Temperature controller
6. F_2 gas cylinder
7. HF absorber (NaF pellets heated at 100°C)
8. Buffer tank
9. Hg manometer
10. F_2 absorber (Soda lime pellets)
11. N_2 gas cylinder
12. IR gas cell

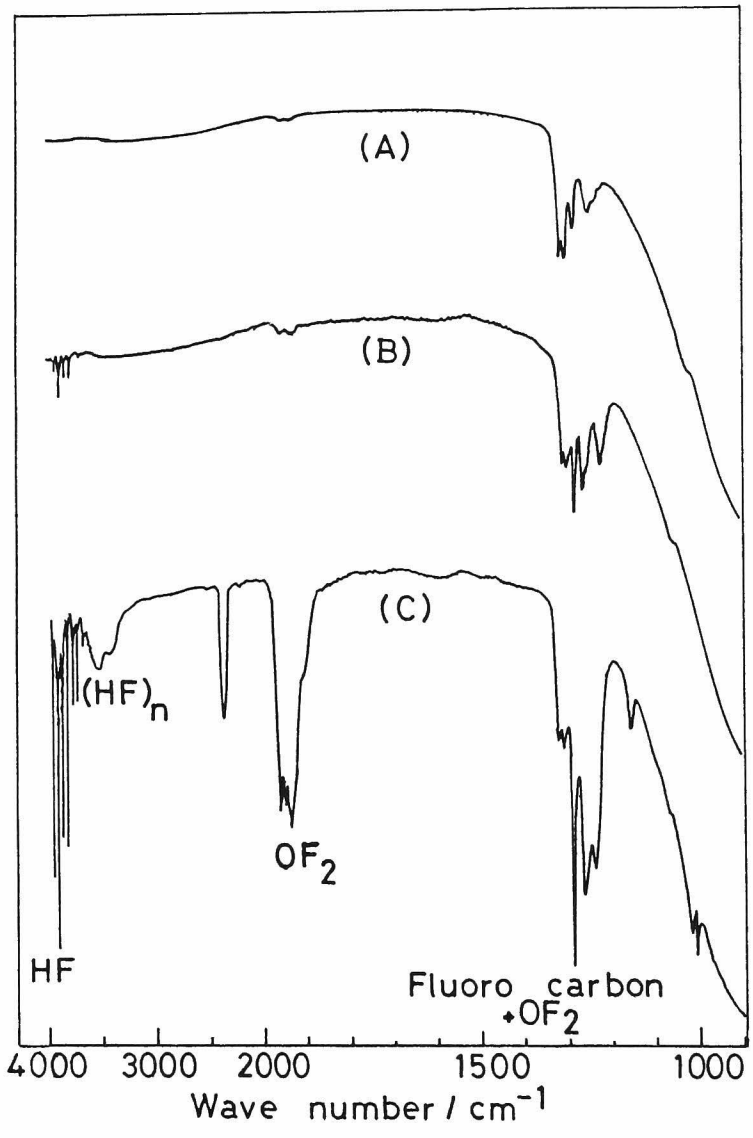

Fig. 1-3 IR spectra of fluorine gas (1.0×10^5 Pa) containing HF of < 0.01 mol% (A), 0.01-0.02 mol% (B) and 1 mol% (C).

2.3 Analyses of GIC

2.3.1 Elemental Analysis

Elemental analysis for C and F was performed at the Laboratory for Organic Elemental Microanalysis, Faculty of Pharmaceutical Science, Kyoto University. Carbon was determined by the conventional gravimetric method and fluorine was by a fluoride ion electrode after all fluorine atoms in GIC were converted into hydrogen fluoride by a oxygen flask method.[6] Al, Fe, Mg, Cu and Li were analysed by the following method. GIC was completely decomposed by heating in a Teflon container with a mixture of nitric acid (Nakarai Chemicals Ltd., purity: >99.99 %) and perchloric acid (Nakarai Chemicals Ltd., 99.99 %). Distilled water was then added to the residual solid, and the prepared solution was analysed by atomic absorption or emission method.

2.3.2 Infrared Spectroscopy (IR)

IR spectrum was observed by Shimadzu IR-27G Spectrometer using a gas cell (path way: 10 cm) with CaF_2 windows in the range of 1000 to 4000 cm^{-1}.

2.3.3 X-ray Diffractometry

X-ray diffractometry was made by Nihon Denshi X-ray diffractometer (JCX-8F). The measurement was carried out under following conditions.

X-ray: Ni filtered Cu-Kα,
Average tube voltage and current: 30 kV - 10 mA,
Scanning speed of goniometer: 2°/min,
Slit: 1° - 0.1 mm - 1°,
Time constant: 1 sec.

2.3.4 ^{19}F-NMR Spectroscopy

NMR measurement was made using Crossed Coil NMR Spectrometer (Varian WL 109) with scanning of the magnetic field under a fixed radio frequency of 15.00 MHz.

2.3.5 Photoelectron Spectroscopy (ESCA)

ESCA measurement was made by a Du Pont 650B Electron Spectrometer with Mg-Kα radiation.

Binding energies of elements were measured by placing the C_{1s} peak of graphite at 284.0 eV.

2.3.6 Differential Thermal Analysis (DTA) and Thermogravimetry (TG)

DTA was carried out by Shimadzu DT-20B under air or nitrogen atmosphere at a heating rate of 10°C/min using α-Al_2O_3 as a reference, and TG was obtained by Rigaku DTA-TG Thermal Analyser under nitrogen atmosphere at a heating rate of 10°C/min.

3. Results and Discussion

3.1 Formation of GIC, $C_xF(MF_n)_y$

Table 1-1 shows the examples of the reaction conditions and the results of elemental and X-ray diffraction analyses of GIC's, $C_xF(MF_n)_y$. Prepared GIC's were almost black in color. The GIC's contained a much larger amount of fluorine than metal fluoride, namely having much larger x than y in the composition, $C_xF(MF_n)_y$ (M: Al, Fe, Mg, Cu or Li, n: 3, 2 or 1). X was in the range of 5-12 for the compounds with the identity period, 9.4 Å, and 10-20 for those with the identity period, 12.8 Å, while y was calculated to be 0.03-0.0002, based on the values actually detected by elemental analysis.

Typical X-ray diffraction pattern is given in Figure 1-4. A large difference was not observed among the diffraction patterns of GIC's containing different metal fluorides. Broad diffraction lines were sometimes observed, suggesting that the intercalant was not strictly arranged at a lattice point. Identity period (I_c) was calculated from (00ℓ) diffraction lines to be ca. $\{9.4 + (n - 1) \times 3.35\}$ Å; n: integral number. Figure 1-4 shows the X-ray diffraction pattern of $C_{13}F(LiF)_{0.002}$ prepared from graphitized PC. The GIC (I_c = 12.75 Å) was prepared with a higher reaction rate from graphitized PC than from natural

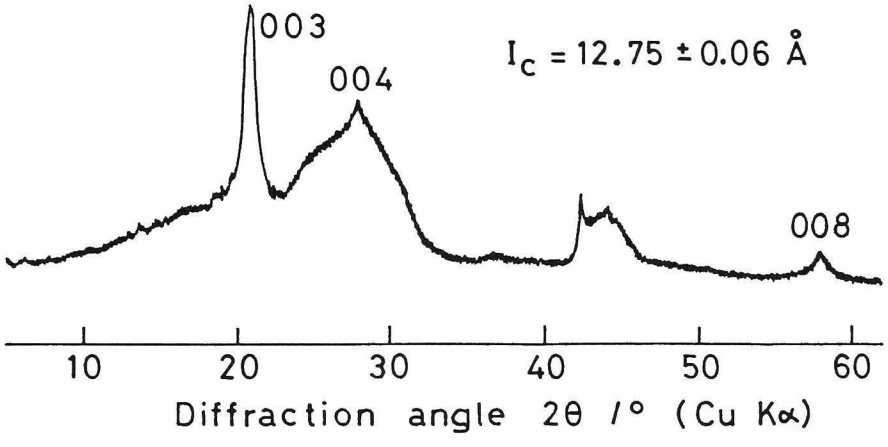

Fig. 1-4 X-ray diffraction pattern of $C_{13}F(LiF)_{0.002}$ prepared from graphitized PC.

Int.	2θ/°	d/Å	hkℓ	
vs	20.96	4.23	003	
s, br	27.84	3.20	004	
m	42.30	2.13	100	
w, br	44.06	2.05	101	I_c=12.75±0.06Å
w	57.82	1.59	008	
m	77.38	1.23	110	
w	83.62	1.16	0011	

Table 1-1 Analytical data of $C_xF(MF_n)_y$

Compound	Starting materials		Elemental analysis	Identity period
	graphite	fluoride	wt%	Å
$C_{12}F(LiF)_{0.007}$	natural graphite (833-295 μm)	LiF	C: 85.6 F: 11.3 Li: 0.03	9.38 ± 0.06
$C_{11}F(LiF)_{0.002}$	natural graphite (833-295 μm)	LiF	C: 84.4 F: 11.9 Li: 0.01	9.4
$C_{13}F(LiF)_{0.002}$	graphitized PC	LiF	C: 88.2 F: 11.0 Li: 0.01	12.75 ± 0.06
$C_{14}F(LiF)_{0.003}$	graphitized PC	LiF	C: 88.6 F: 10.3 Li: 0.011	12.8
——	PAN-based carbon fiber	LiF	C: — F: — Li: 0.01 (Intercalant; 12.3 wt%)	Mixture: 12.8, 16.1
$C_{6.7}F(CuF_2)_{0.0002}$	natural graphite (833-295 μm)	CuF_2	C: 79.5 F: 18.9 Cu: 0.01	9.42 ± 0.05

$C_{11}F(CuF_2)_{0.0005}$	graphitized PC	reduced Cu	C: 83.1 F: 11.9 Cu: 0.02 (Intercalant; 14.3 wt%)	Mixture: 9.4, 12.8
$C_{8.1}F(MgF_2)_{0.002}$	natural graphite (833-295 μm)	MgF_2	C: 82.4 F: 16.2 Mg: 0.04	9.37 ± 0.06
$C_{14}F(MgF_2)_{0.002}$	natural graphite (833-295 μm)	MgF_2	C: 86.6 F: 9.5 Mg: 0.02	12.8
$C_{12}F(MgF_2)_{0.004}$	graphitized PC	MgF_2	C: 87.8 F: 11.9 Mg: 0.06 (Intercalant; 15.0 wt%)	12.73 ± 0.13
$C_{19}F(FeF_3)_{0.0005}$	graphitized PC	reduced Fe	C: 89.1 F: 7.3 Fe: 0.01	12.8
$C_{16}F(FeF_3)_{0.01}$	natural graphite (833-295 μm)	reduced Fe	C: 89.0 F: 9.0 Fe: 0.36	Mixture: 9.4, 12.8
$C_{7.2}F(AlF_3)_{0.002}$	natural graphite (833-295 μm)	AlF_3	C: 80.7 F: 17.8 Al: 0.06	9.4
$C_{19}F(AlF_3)_{0.002}$	natural graphite (833-295 μm)	AlF_3	C: 91.9 F: 7.7 Al: 0.02	12.7

graphite. However, the lower stage GIC (I_c = 9.4 Å) was not obtained from graphitized PC but from graphite with higher crystallinity (Figure 1-5). This is probably due to the higher decomposition rate of GIC from graphitized PC, namely a smaller equilibrium constant in the following equation.

$$\text{Graphitized PC} + F_2 + MF_n \rightleftharpoons C_xF(MF_n)_y$$

Most of GIC's (I_c = 12.75 Å) prepared from natural graphite were mixed stage with large half widths of the diffraction lines or with only strong (004) diffraction line. The amount of interca-

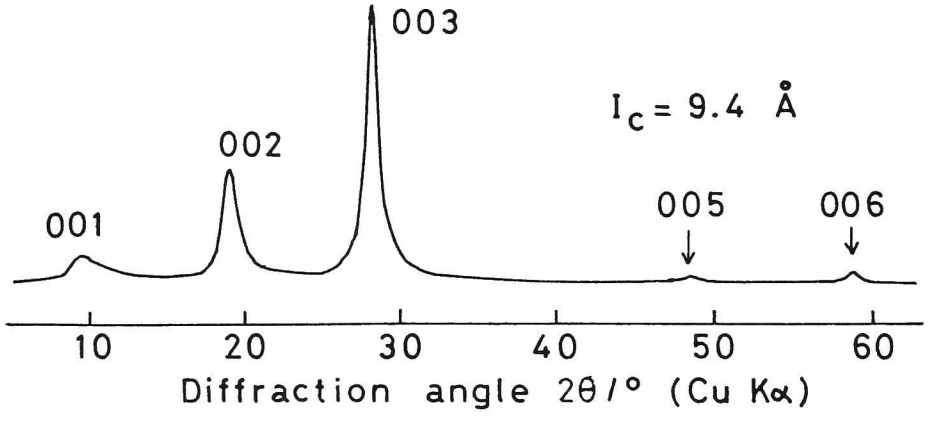

Fig. 1-5 X-ray diffraction pattern of $C_{12}F(LiF)_{0.007}$ prepared from flaky natural graphite (833-295 μm).

Int.	2θ/°	d/Å	hkℓ	
w, br	9.4	9.4	001	
m	19.02	4.66	002	
vs	28.36	3.14	003	I_c=9.38±0.06Å
w, br	48.3	1.9	005	
w	58.82	1.57	006	
vw, br	82.9	1.16	008	

lant was also smaller in GIC (I_c = 12.75 Å) prepared from natural graphite than in that (I_c = 12.75 Å) prepared from graphitized PC. It is therefore considered that Figure 1-4 shows a GIC having the higher crystallinity than that of natural graphite. It seems that the identity periods of this type GIC's are determined by the size of fluorines intercalated into graphite layers because they are almost equal to each other among the compounds prepared and most of the intercalants are fluorines. The GIC having identity period of 12.75 Å was regarded as 2nd or 3rd stage compound because no substance could be inserted into a space between graphite layers if this compound was of more higher stage than 3rd stage. If the GIC is 2nd or 3rd stage one, the intercalant must be comprised within 6.05 Å (= 12.75 - 3.35 × 2) or 2.7 Å (= 12.75 - 3.35 × 3), respectively. The peak intensity of (003) diffraction line was the highest in the diffraction lines of the GIC (I_c = 12.75 Å) as shown in Figure 1-4. This is consistent with many examples that a GIC whose identity period is near the integer times 3.35 Å has the most strongest (00 n+1) line (n: stage number). The GIC having identity period of 12.75 Å therefore might be the 2nd stage, namely that of {9.4 + (n - 1) × 3.35} Å is as "n"th stage one.

The GIC (I_c = 12.75 Å) contains two kinds of fluorines with different chemical bonds as described later in ^{19}F-NMR spectra, which suggests that one is like fluoride ion closely attached to graphite layer and another is in less ionized state in which fluorine-fluorine interaction still remains. The mole ratio of the former to the latter is ca. 2 from the ^{19}F-NMR spectra. From these results, relative intensities of (00ℓ) diffraction lines were calculated for the GIC (I_c = 12.75 Å) by using an equation for the structural factor. The following approximations were made on the calculation.

(1) Composition is $C_{10}F$ from elemental analysis.

(2) Intercalant is fluoride ion, and fluorine molecule existing

at the center between graphite layers. The ratio of the former to the latter is 2.

Peak intensity was calculated by changing the orientation of two kinds of fluorines between graphite layers, that is, the distance between the fluoride ion and the center of two adjacent graphite layers. It was indicated that the GIC (I_c = 12.75 Å) possessed the more stronger (003) diffraction line than (004) line when assumed that it was the 2nd stage, while the (004) line was stronger than (003) line in case of the 3rd stage.

3.2 Chemical Bond between Intercalated Fluorine and Graphite

NMR and ESCA spectra provide the information on the chemical interaction of intercalated fluorine with graphite.

Figure 1-6 shows ^{19}F-NMR spectra of $C_{14}F(MgF_2)_{0.002}$, $C_{11}F(LiF)_{0.002}$, $C_{7.2}F(AlF_3)_{0.002}$ and graphite fluoride, $(C_2F)_n$ prepared from flaky natural graphite (833-295 μm). Measured absorption derivatives gave the intersection points with abscissa at 0.3750 T (3750 G) for all the compounds examined. The compound $C_{14}F(MgF_2)_{0.002}$ (I_c = 12.8 Å) prepared at room temperature had a quite narrow resonance line whereas graphite fluoride $(C_2F)_n$ had a very broad one. The peak to peak width of each compound is shown in Table 1-2. The compound $C_{11}F(LiF)_{0.002}$ (I_c = 9.4 Å) prepared at a retention temperature** of 195°C showed a slightly broader width than that of $C_{14}F(MgF_2)_{0.002}$. The compound $C_{7.2}F(AlF_3)_{0.002}$ (I_c = 9.4 Å) prepared at a retention temperature** of 310°C gave a strong narrow line overlapped with a weak broad signal.

In case of solid fluoride in which every atom is completely localized at a lattice point, the nucleus of fluorine atom is

---

** Retention temperature: a temperature at which fluorine gas was introduced into a reaction system. This temperature was normally higher than that when the intercalation of fluorine and fluoride started.

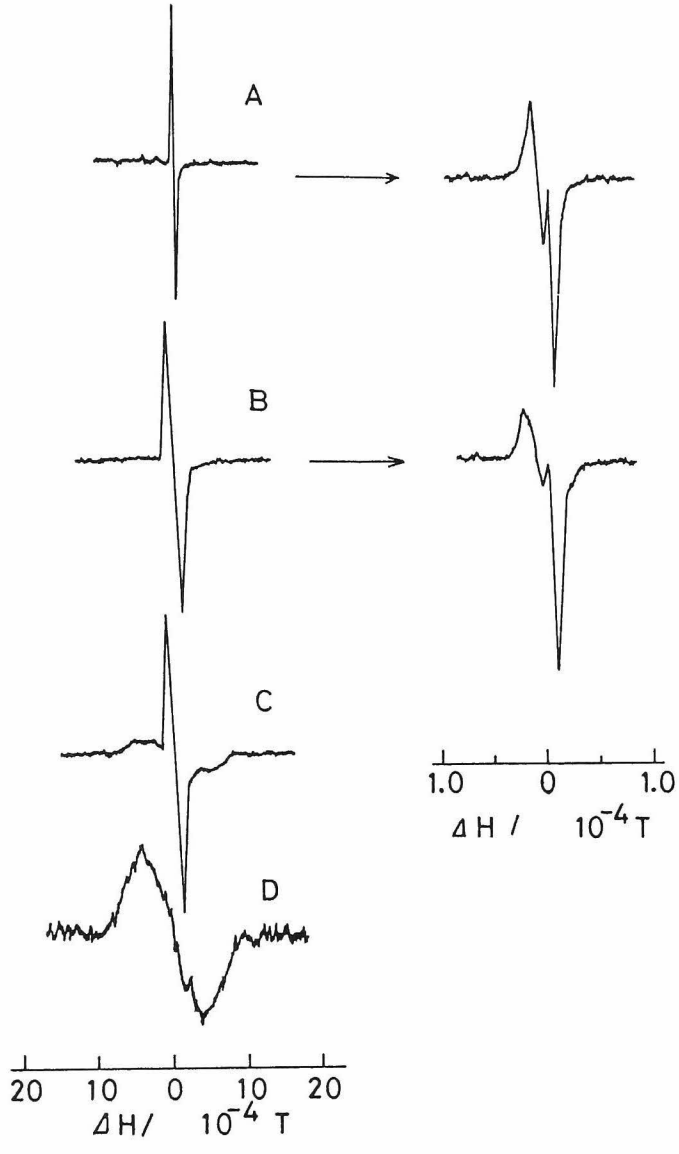

Fig. 1-6 ^{19}F-NMR spectra of $C_xF(MF_n)_y$ and graphite fluoride, $(C_2F)_n$.
Radio frequency: 15.00 MHz
(A) $C_{14}F(MgF_2)_{0.002}$ (I_c = 12.8 Å) prepared at 20°C
(B) $C_{11}F(LiF)_{0.002}$ (I_c = 9.4 Å) prepared at a retention temp.** of 195°C
(C) $C_{7.2}F(AlF_3)_{0.002}$ (I_c = 9.4 Å) prepared at a retention temp.** of 310°C
(D) Graphite fluoride, $(C_2F)_n$

Table 1-2 Peak to peak widths of ^{19}F-NMR spectra for $C_xF(MF_n)_y$.

Radio frequency: 15.00 MHz

Compound	Peak to peak width
	10^{-4} T
$C_{14}F(MgF_2)_{0.002}$ (I_c = 12.8 Å)	0.45
$C_{11}F(LiF)_{0.002}$ (I_c = 9.4 Å)	2.5
$C_{7.2}F(AlF_3)_{0.002}$ (I_c = 9.4 Å)	2.5
graphite fluoride $(C_2F)_n$	8.8

affected by the magnetic field of other surrounding nuclei directly across the space. As a result the resonance line becomes broadened. In fact, graphite fluoride with C-F covalent bonds gave a broad signal as mentioned above. The compound $C_{7.2}F(AlF_3)_{0.002}$ would contain a small amount of graphite fluoride around the surface. On the other hand, the narrow resonance lines observed for GIC's are attributed to slightly mobile fluorine atoms adsorbed chemically by carbon atoms of graphite. The peak to peak width of the compound $C_{14}F(MgF_2)_{0.002}$ was smaller than those of other GIC's, which means that the former has more mobile fluorine atoms than the latter. This mobile fluorine would contribute to increase in the electrical conductivity of GIC. When the absorption derivative was magnified along the abscissa under optimum condition, the narrow resonance lines of $C_{14}F(MgF_2)_{0.002}$ and $C_{11}F(LiF)_{0.002}$ were split into two signals

having intersection points at 0.37499 and 0.37501 T as shown in Figure 1-6. This means that the GIC's contain two kinds of mobile fluorine atoms having slightly different chemical interactions with graphite. Generally, an intercalant is not completely but partially ionized in graphite layers. The peak to peak widths were 1.3×10^{-5} T for the signal observed at the lower magnetic field and 6×10^{-6} T for that observed at the higher magnetic field. The former signal corresponds to fluorines more strongly interacting with graphite than the latter fluorines. The mole ratio of the former to the latter is estimated to be ca. 2 by comparison of each product between square of peak to peak width and peak height of the NMR signal.

In ESCA study, the kinetic energy of photoelectron, emitted from an inner shell of each element, is measured. Since the mean free path of photoelectron is at most several tens of angstroms in solid materials, only a few graphite top layers of the GIC are analysed. Accordingly the chemical bonds close to the surface of a compound are emphasized in ESCA spectra.

Figures 1-7 and 1-8 are ESCA spectra of $C_xF(MgF_2)_y$ and $C_xF(CuF_2)_y$. The spectra of (b), (c) and (d) in Figures 1-7 and 1-8 show the chemical bond around the surface of the compounds and (a) is those of a sample obtained by cleavage of PG intercalated by fluorine and metal fluoride. In C_{1s} spectra of the intercalation compounds prepared by introduction of fluorine gas into the reactor at 200-300°C (Figures 1-7-(d), 1-8-(d)), a peak shifted to 289 eV was observed with a strong peak at 284 eV. The former is near the position corresponding to C-F covalent bond (290 eV)[2] and the latter corresponds to C-C covalent bond of graphite itself. The F_{1s} peak observed at 688 eV was also close to that of graphite fluoride (689 eV). As $C_{7.8}F(MgF_2)_{0.002}$ (Figure 1-7-(b)) was prepared from graphitized PC at a retention temperature** of 300°C for 0.5 h, the intensity

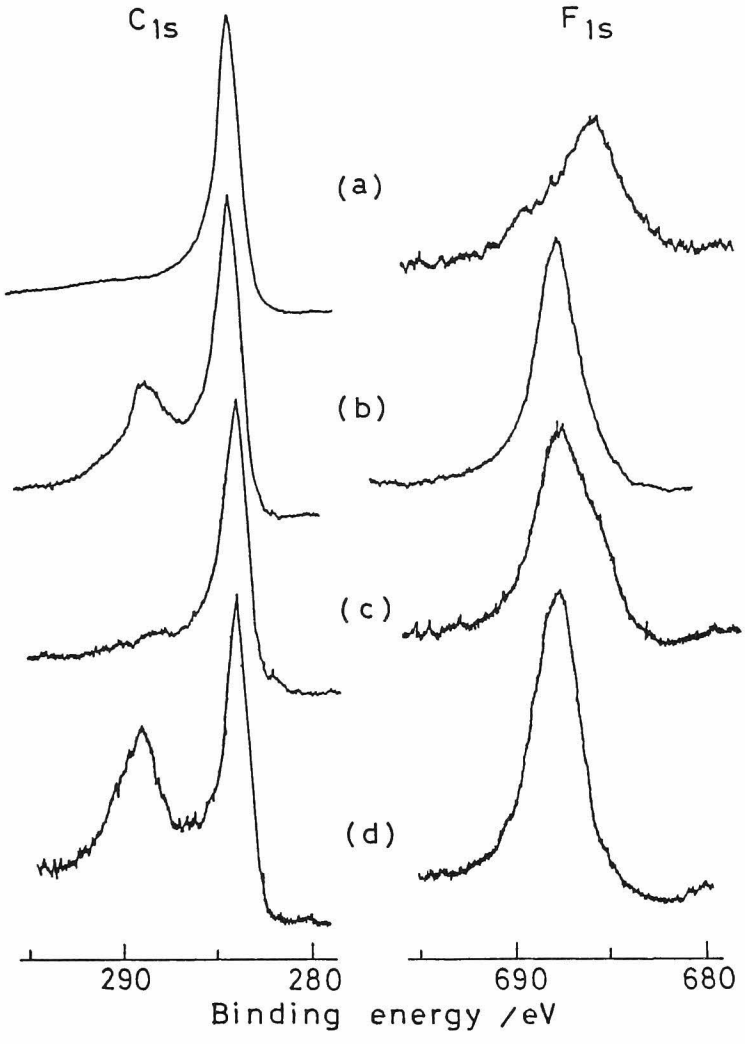

Fig. 1-7 ESCA spectra of $C_xF(MgF_2)_y$.
(a) GIC (I_c = 9.4 Å) prepared from PG at 20°C.
(b) $C_{7.8}F(MgF_2)_{0.002}$ prepared from graphitized PC at a retention temp.** of 300°C for 0.5 h.
(c) $C_{14}F(MgF_2)_{0.002}$ prepared from natural graphite at 25°C.
(d) $C_{5.5}F(MgF_2)_{0.001}$ prepared from natural graphite at a retention temp.** of 300°C for 48 h.

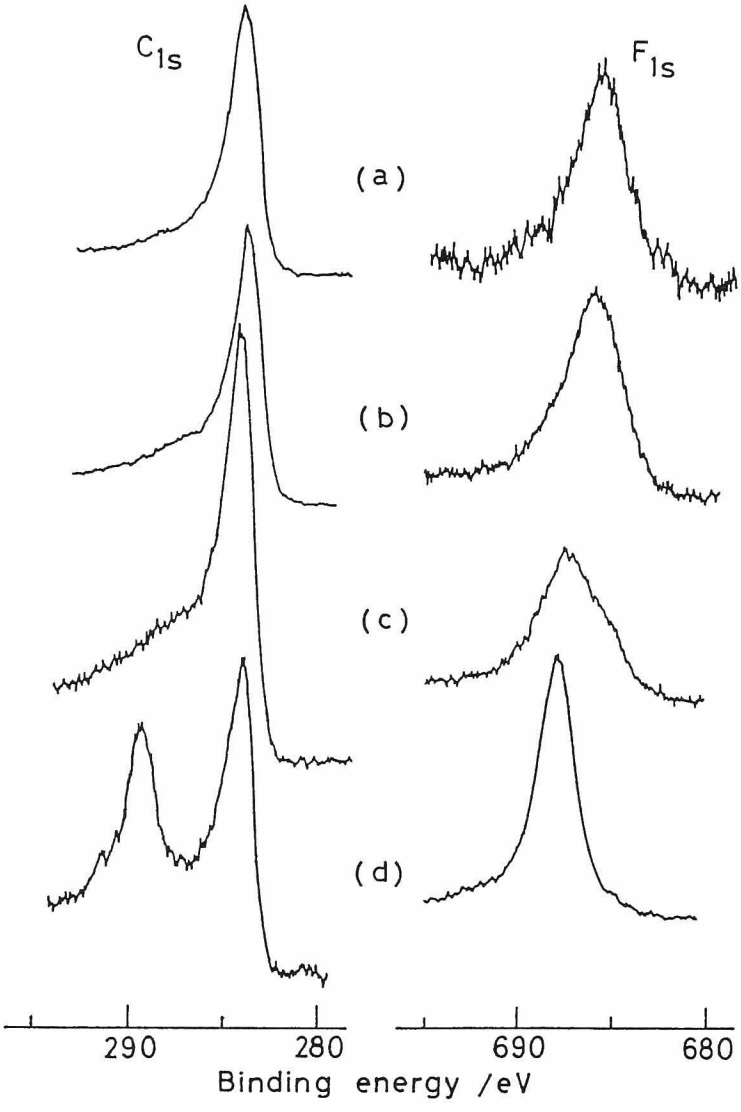

Fig. 1-8 ESCA spectra of $C_xF(CuF_2)_y$.
(a) GIC (I_c = 9.4 Å) prepared from PG at 20°C.
(b) $C_{11}F(CuF_2)_{0.0005}$ prepared from graphitized PC at a retention temp.** of 200°C for 2 h.
(c) $C_{5.2}F(CuF_2)_{0.0004}$ prepared from natural graphite at 20°C.
(d) $C_{6.7}F(CuF_2)_{0.0002}$ prepared from natural graphite at a retention temp.** of 200°C for 48 h.

of a shifted C_{1s} peak at 289 eV was not so strong as that of $C_{5.5}F(MgF_2)_{0.001}$ (Figure 1-7-(d)). In case of $C_{11}F(CuF_2)_{0.0005}$ (Figure 1-8-(b)) prepared from graphitized PC at a retention temperature** of 200°C for 2 h, only a shifted shoulder for C_{1s} electron was observed and F_{1s} peak was found at a lower binding energy (686.3 eV) than that of $C_{6.7}F(CuF_2)_{0.0002}$ (688 eV) prepared at a retention temperature** of 200°C for 48 h. $C_{14}F(MgF_2)_{0.002}$ (Figure 1-7-(c)) and $C_{5.2}F(CuF_2)_{0.0004}$ (Figure 1-8-(c)) prepared from natural graphite at room temperature showed no shifted C_{1s} peak and F_{1s} shoulder at lower binding energies than 688 eV. It was found that the chemical bond similar to C-F covalent bond was formed around the surface of the compounds prepared at higher retention temperatures** (200-300°C). On the other hand, when the bulk of the GIC was observed by cleavage of PG, F_{1s} spectra were found at lower binding energies, 685.6 eV (Figure 1-7-(a)) and 685.8 eV (Figure 1-8-(a)), which are near that of fluoride ion of ionic metal fluoride such as LiF (684.5 eV) or fluorine gas (686 eV). This result coincides with that of ^{19}F-NMR, namely, suggests that intercalated fluorines are slightly ionic or in nearly molecular state, being not strongly bonded to carbons in the bulk of the compound.

3.3 Stability of GIC

The stability of GIC in air is given in Table 1-3. The stability particularly depended on carbon materials as hosts and somewhat on metal fluorides. With regard to carbon materials, the higher stability has been found in order of the compounds of PAN-based carbon fiber, natural graphite, PG and graphitized PC. Concerning metal fluorides, order of the stability was as follows, CuF_2, AlF_3 > LiF > MgF_2, FeF_3.

GIC prepared from PAN-based carbon fiber was the most stable in these four host materials. For example, a GIC (intercalant:

Table 1-3 Stabilities of $C_xF(MF_n)_y$ prepared from several kinds of graphites and metal fluorides

A: Almost no change was observed in X-ray diffraction pattern and weight during 2 months in air.
B: (003) diffraction line shifted to lower angle by ca. 0.3 Å and several wt% of intercalant was released during 2 weeks in air. The decomposition rate decreased thereafter.
C: Original graphite line was observed in X-ray pattern and most of intercalant was released during 2 weeks in air.
A' or B' was inferior in stability than A or B, respectively.

	PAN-based carbon fiber	natural graphite	pyrolytic graphite	graphitized PC
CuF_2	A	A	A' ~ B	B'
AlF_3	—	A ~ A'	B	B'
LiF	A	B	B	B ~ C
MgF_2	—	B	A' ~ B'	B ~ C
FeF_3	A	B	B	B' ~ C

12.3 wt%, I_c = 12.7, 16.1 Å) prepared from PAN-based carbon fiber and LiF didn't show any change in its diffraction pattern for two months, and was slightly decomposed after 9 months in air, giving slightly broader diffraction lines (Figure 1-9). Almost no change was observed in its electrical conductivity and weight (Chapter 3, Figure 3-12). The better stability of GIC prepared from PAN-based carbon fiber is due to the onion-like skin and mid-random structure (Figure 1-10).

On the other hand, the most unstable GIC was that prepared from graphitized PC as host material. It was sometimes found that prepared GIC was completely decomposed within two weeks in moist air.

In case of natural graphite as a host material, the X-ray diffraction patterns of $C_xF(MF_n)_y$ showed no change after exposure to air for one day or after immersion in water overnight. However, they released a trace amount of fluorine during their storage in a glass ampule for more than 1 week. As a result the glass ampule was slightly corroded. For example, a GIC, $C_{8.1}F(MgF_2)_{0.002}$ (I_c = 9.4 Å) released a trace amount of fluorine in air for 1 week. The

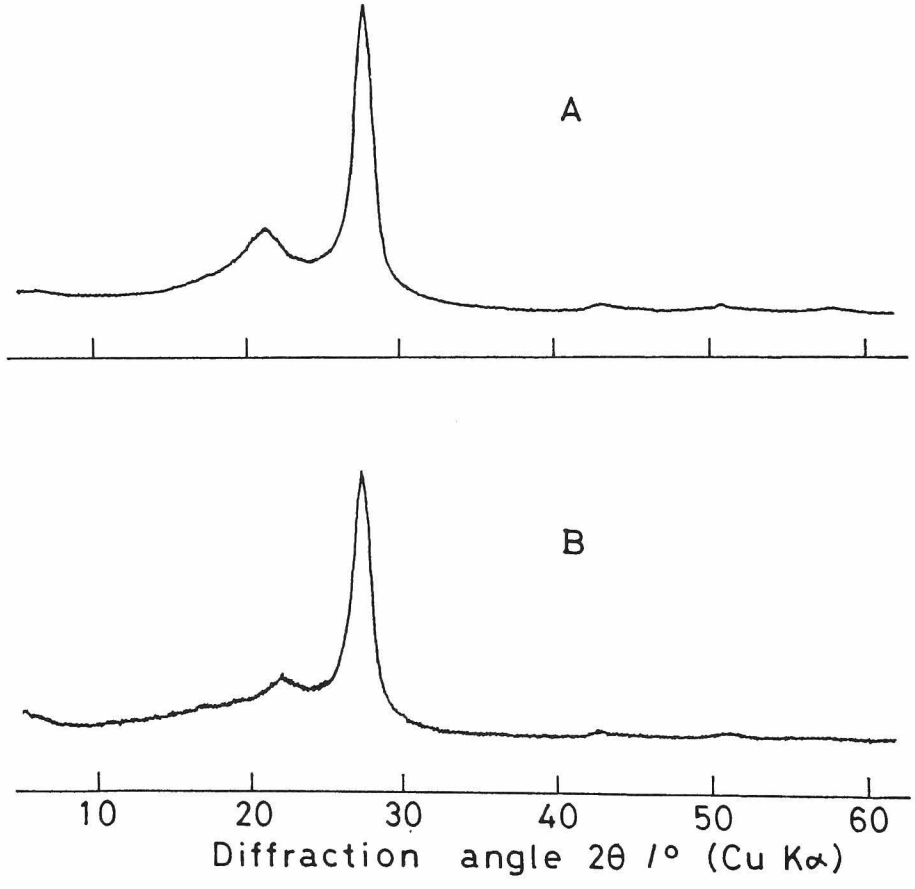

Fig. 1-9 X-ray diffraction patterns of $C_xF(LiF)_y$ prepared from PAN-based carbon fiber.
[A] Just after preparation
[B] After exposure to air for 9 months

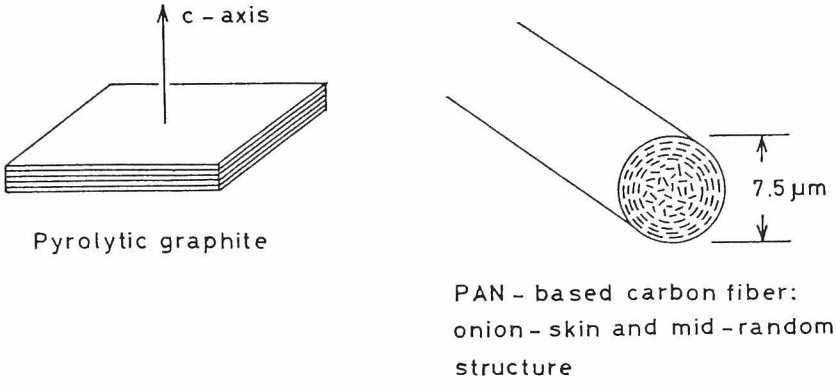

Fig. 1-10 Illustrations for structures of pyrolytic graphite and PAN-based carbon fiber.

position of (00ℓ) diffraction line shifted to lower angle by 0.3 Å and the half width increased. After exposure of $C_{8.1}F(MgF_2)_{0.002}$ to air for 3 months, its X-ray diffraction pattern gave a strong diffraction line around 26.80° corresponding to a higher stage compound owing to partial decomposition of original GIC.

Most of acceptor type GIC's containing fluorides are very hygroscopic and unstable in air. For example, C_8AsF_5 or $C_{6.5}SbF_5$ requires encapsulation to ensure the chemical stability even on measurement of X-ray diffraction pattern. However, the GIC $C_xF(MF_n)_y$ prepared from graphitized PC, which gave the most unstable GIC in all the carbon materials used in the present work, was stable in air for several days. This good stability would be first due to the strong interaction between intercalated fluorine and graphite layers. The intercalant was almost fluorine as described before. One fluorine atom contained in $C_xF(MF_n)_y$ worked equally to one AsF_5 or SbF_5 molecule as an electron acceptor from graphite (Chapter 3, 3.2), which would be owed to the large electronegativity and small size of fluorine atom. Secondly, the

low surface energy of $C_xF(MF_n)_y$ might also contribute to the high stability. It is well known that graphite fluoride has a low surface energy so that it is difficult for graphite fluoride to adsorb water in moist air.[7] The fluorine adsorbed on the graphite layer or strongly bonded to the surface of $C_xF(MF_n)_y$ would also protect the adsorption of water.

GIC had the better thermal stability also with regard to graphite host in the same order as described above. Figure 1-11-A shows DTA and TG curves in nitrogen atmosphere for a mixed stage compound (I_c = 12.8, 16.1 Å, intercalant; 13.8 wt%) prepared from PAN-based carbon fiber and LiF. Almost no weight decrease was observed up to 400°C. An endothermic peak was observed at 407°C owing to the release of intercalant from graphite layers. Figure 1-11-B shows the curves for $C_{11}F(LiF)_{0.002}$ (I_c = 9.4 Å) prepared from flaky natural graphite (833-295 μm). An exothermic reaction began at 264°C and weight decrease at ca. 150°C. Taken out after heating to 300°C, the sample was exfoliated in direction of c-axis, which means that the space among crystallites was expanded by release of intercalant during heating.

Figure 1-12 shows DTA and TG curves of a mixed stage compound (I_c = 12.8, 16.1 Å, intercalant; 11.2 wt%) prepared from PAN-based carbon fiber and reduced Fe system (A) and $C_{20}F(FeF_3)_{0.005}$ (I_c = 12.8 Å) from graphitized PC and reduced Fe (B) in nitrogen atmosphere. $C_{20}F(FeF_3)_{0.005}$ decomposed gradually with a broad endothermic peak in the range of 150-250°C owing to release of intercalant (Figure 1-12-B). At 320°C was observed an exothermic peak, just followed by an endothermic peak. Gas desorption from solid or the release of intercalant from graphite layers is generally an endothermic reaction. It is known, however, that a covalent compound $(CF)_n$ decomposes with a following exothermic reaction,

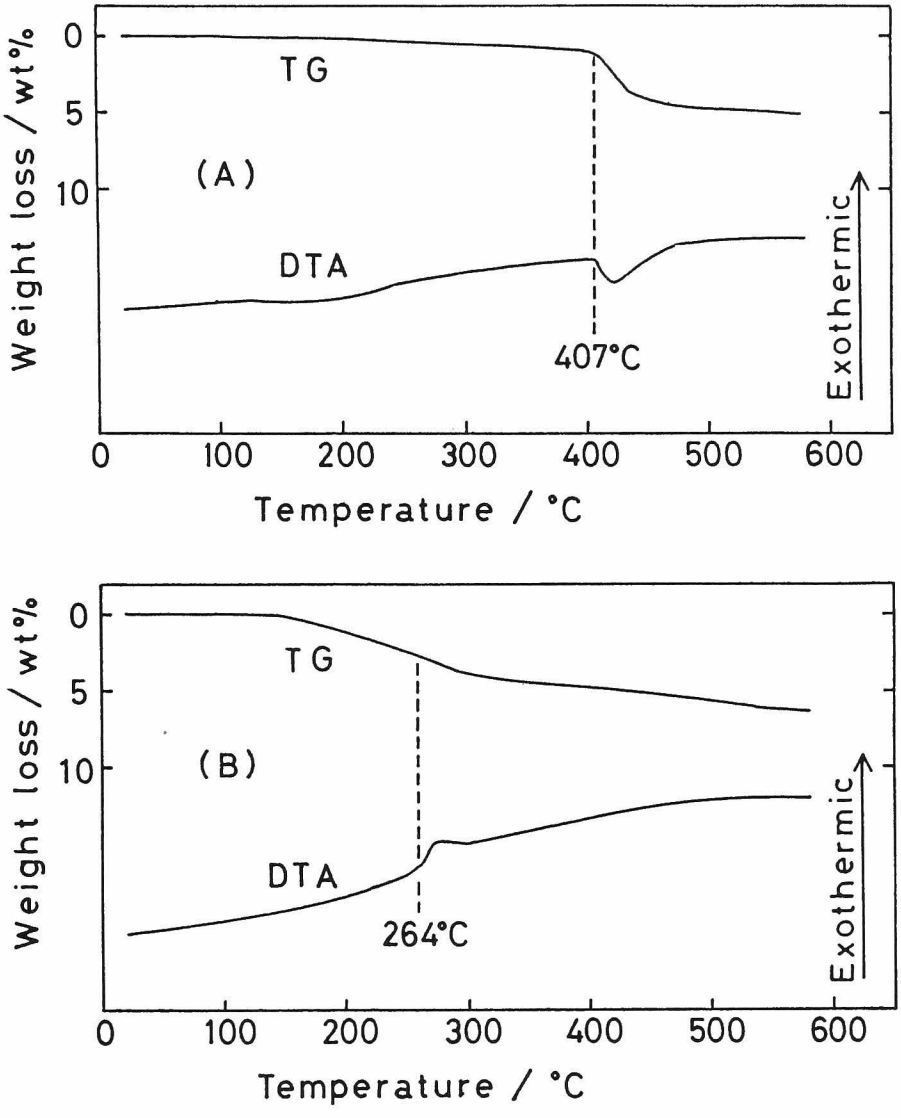

Fig. 1-11 DTA and TG curves for $C_xF(LiF)_y$ in nitrogen atmosphere.
(A) GIC (I_c = 12.8 and 16.1 Å, intercalant: 13.8 wt%) prepared from PAN-based carbon fiber
(B) $C_{11}F(LiF)_{0.002}$ (I_c = 9.4 Å) prepared from flaky natural graphite
Heating rate: 10°C/min

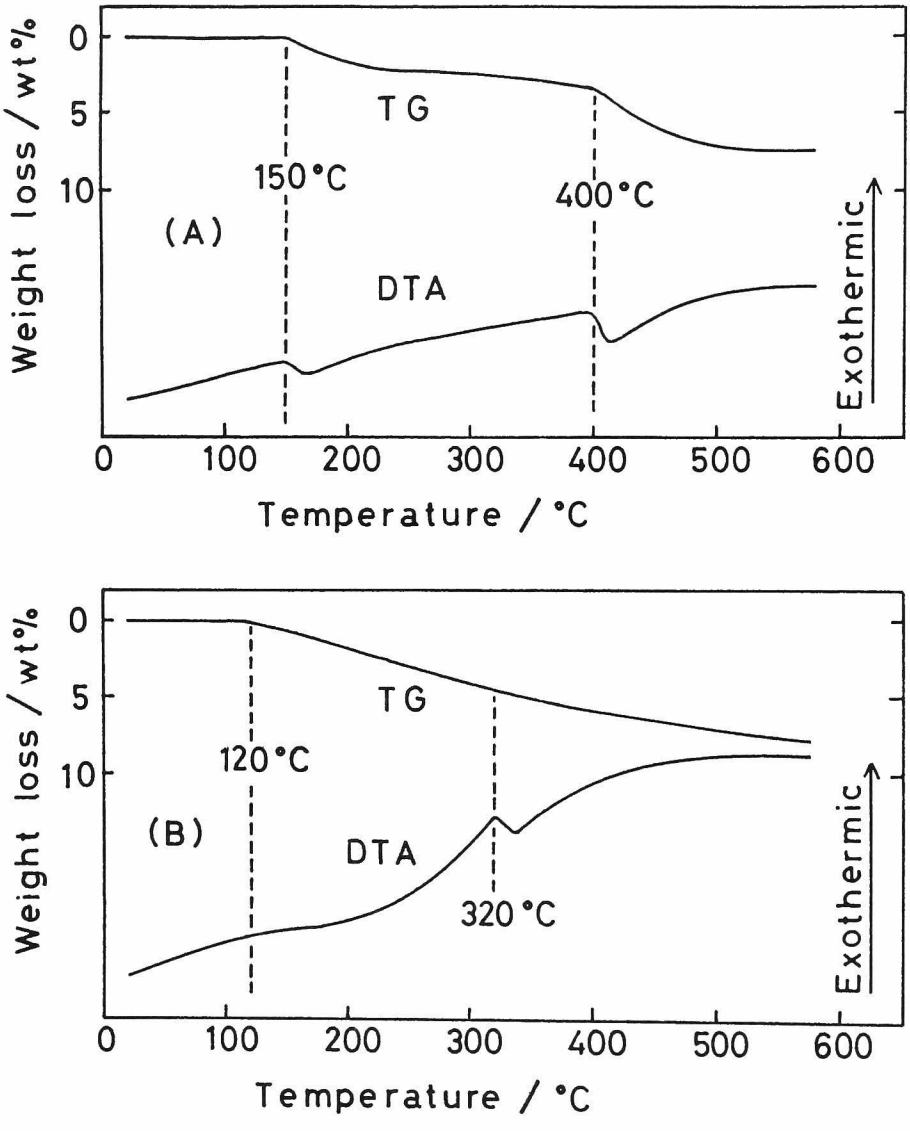

Fig. 1-12 DTA and TG curves for $C_xF(FeF_3)_y$ in nitrogen atmosphere.
(A) GIC (I_c = 12.8 and 16.1 Å, intercalant: 11.2 wt%) prepared from PAN-based carbon fiber.
(B) $C_{20}F(FeF_3)_{0.005}$ (I_c = 12.8 Å) prepared from graphitized PC.
Heating rate: 10°C/min

$$(CF)_n \longrightarrow nC + XCF_2 + YC_2F_4 \quad (1)$$

where X + 2Y = n and C is amorphous carbon.[8)]

The exothermic peak at 320°C for $C_{20}F(FeF_3)_{0.005}$ suggests that the decomposition of GIC and formation of fluorocarbon occur simultaneously. When the GIC, $C_{20}F(FeF_3)_{0.005}$ was heated up to 600°C in nitrogen atmosphere, the residue contained a small amount of fluorine, which was detected by ESCA spectra. For the curves of the GIC prepared from PAN-based carbon fiber (Figure 1-12-A), a broad endothermic peak was observed with weight decrease at 150-200°C, owing to some release of intercalant. However, the decomposition didn't proceed so continuously as that shown in Figure 1-12-B. A clear endothermic reaction started at 400°C and weight decrease was observed stepwise, corresponding to the release of intercalant without chemical reaction such as equation (1).

Figure 1-13 shows DTA curves measured in air for $C_{8.1}F(MgF_2)_{0.002}$ $C_{5.5}F(MgF_2)_{0.001}$, $C_{7.2}F(AlF_3)_{0.002}$ (I_c = 9.4 Å) and graphite fluoride, $(C_2F)_n$. These were prepared from flaky natural graphite (833-295 μm). A first exothermic broad peak appeared at 190°C for $C_{8.1}F(MgF_2)_{0.002}$ and $C_{5.5}F(MgF_2)_{0.001}$ and at 230°C for $C_{7.2}F(AlF_3)_{0.002}$. These results mean that the GIC's were oxidized at lower temperatures in air than in nitrogen atmosphere. The peaks around 830°C are attributed to the oxidative reaction of residual graphite. Graphite fluoride gave two exothermic peaks at 573 and 697°C, which correspond to the decomposition of graphite fluoride and to oxidation of residual carbon, respectively.

4. Summary

(1) New GIC's, $C_xF(MF_n)_y$ were prepared by the reaction of several kinds of graphites with fluorine and metal fluorides (M: Al,

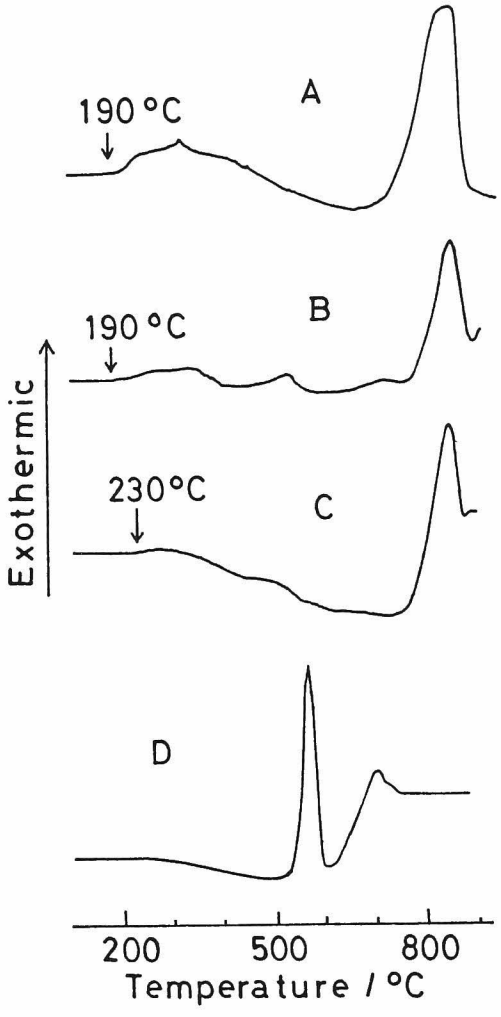

Fig. 1-13 DTA curves for $C_xF(MF_n)_y$ and graphite fluoride, $(C_2F)_n$ in air.
(A) $C_{8.1}F(MgF_2)_{0.002}$ prepared from flaky natural graphite
(B) $C_{5.5}F(MgF_2)_{0.001}$
(C) $C_{7.2}F(AlF_3)_{0.002}$
(D) Graphite fluoride, $(C_2F)_n$
Heating rate: 10°C/min

Fe, Mg, Cu or Li, n: 3, 2 or 1). The identity period in direction of c-axis (I_c) was $\{9.4 + (n - 1) \times 3.35\}$ Å (n; stage number), independent of the kind of metal fluoride. The GIC's contained a much larger amount of fluorine than metal fluoride. The chemical composition was $C_{5-12}F(MF_n)_{0.03-0.0002}$ for GIC's with I_c, 9.4 Å, and $C_{10-20}F(MF_n)_{0.02-0.0003}$ for those with I_c, 12.8 Å. It was therefore considered that the I_c was decided by the size of intercalated fluorines.

(2) ^{19}F-NMR spectra indicated that GIC contained mobile fluorines weakly interacting with graphite layer. F_{1s} ESCA spectra obtained by cleavage of GIC having HOPG host showed that the intercalated fluorines were in slightly ionized state or in nearly molecular state. It was also found that C-F covalent bond was formed around the surface of the GIC prepared by introduction of fluorine at a temperature higher than 200°C.

(3) The stability of GIC mainly depended on host graphite material. The higher stability was observed as the following order with regard to host graphite (a) and metal fluoride (b).

(a) PAN-based carbon fiber > natural graphite > pyrolytic graphite > graphitized petroleum coke

(b) CuF_2, AlF_3 > LiF > MgF_2, FeF_3

References

1) P.Kamarchik and J.L.Margrave, Acc. Chem. Res., 11, 296 (1978).

2) Y.Kita, N.Watanabe and Y.Fujii, J. Am. Chem. Soc., 101, 3832 (1979).

3) M.M.J.Mélin and A.Hérold, C. R. Acad. Sc. Paris, t.280, 641 (1975).

4) N.Bartlett, B.McQuian and A.S.Robertson, Mat. Res. Bull., 13, 1259 (1978).

5) F.L.Vogel, G.M.T.Foley, C.Zeller, E.R.Falaudeau and J.Gan, Mater. Sci. Eng., 31, 261 (1977).
6) K.Hozumi and N.Akimoto, Japan Analyst, 20, 467 (1971).
7) N.Watanabe, H.Takenaka and S.Kimura, Nippon Kagaku Kaishi, 1975, 1655 (1975).
8) N.Watanabe, S.Koyama and H.Imoto, Bull. Chem. Soc. Jpn., 53, 2731 (1980).

Chapter 2

INTERCALATION REACTION OF FLUORINE AND METAL FLUORIDE INTO GRAPHITE*

1. Introduction

Reaction of graphite with fluorine gas yields graphite fluorides, $(CF)_n$ and $(C_2F)_n$ at temperatures, 350-600°C. Below 300°C, fluorine gas is, however, so inert to graphite that no intercalation reaction occurs. Metal fluorides such as AlF_3, FeF_3, MgF_2, CuF_2 and LiF are not intercalated because they have no vapor pressures at low temperatures and are weak Lewis acids. On the contrary, as described in Chapter 1, ternary GIC's intercalated by fluorine and metal fluorides have been synthesized under coexistence of fluorine gas and the above-mentioned fluorides. These intercalation compounds, contain a large amount of fluorine compared with metal fluorides and show almost the same identity period.

In this chapter, the intercalation mechanism is discussed on the basis of reaction between fluorine and metal fluoride. Furthermore, the intercalation reaction was observed by means of thermogravimetry.

2. Experimental

A carbon material used in this study was natural graphite [(833-295 μm (20-48 mesh), purity: 99.4 %]. Commercial LiF (purity: >97 %) was dried under vacuum between 20 and 120°C for 2 days. Fluorine gas (purity: 99.7 %, most of impurities are nitrogen) was used after passing NaF pellets heated at 100°C.

Preparation and analyses of intercalation compounds were

---

* Synthetic Metals in press.

made in the same way as in Chapter 1. The weight change was monitored by using an automatic thermobalance (Figure 2-1).[1)] The apparatus was specially designed for the fluorine atmosphere. The weight sensitive portion is of a spring balance type.

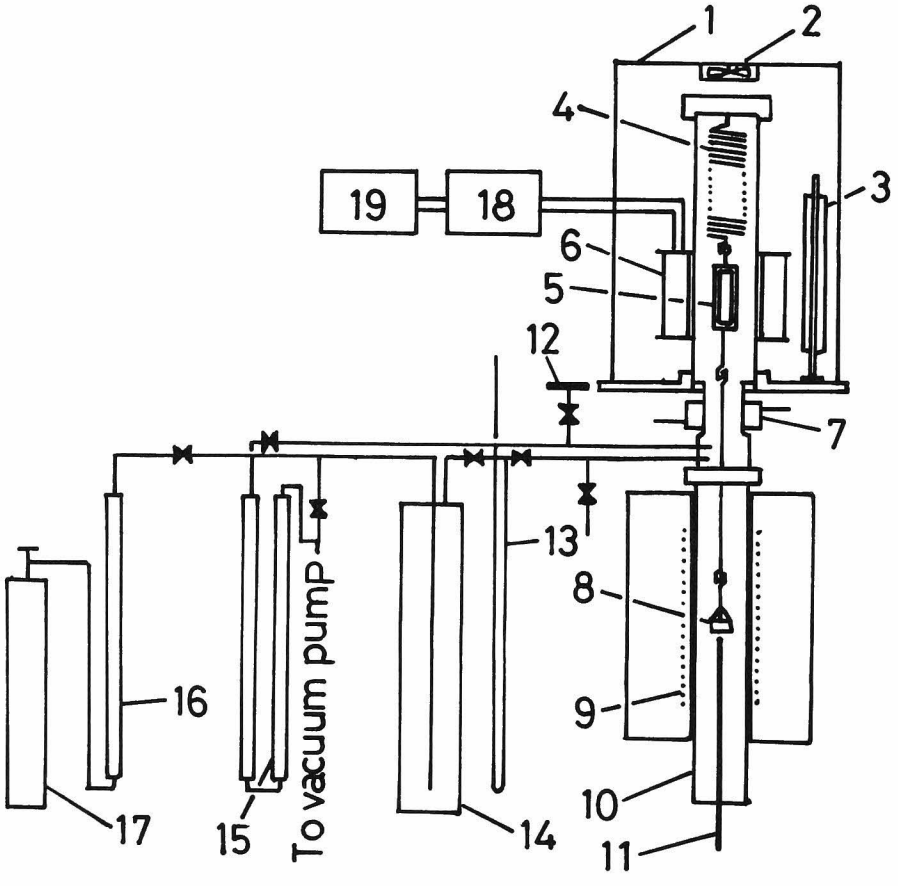

Fig. 2-1 Thermobalance specially designed for fluorination.

1. Air bath (controlled at 45°C)
2. Fan
3. Heater
4. Nickel spring
5. Ferrite core (Teflon coating)
6. Differential transformer
7. Jacket for cooling water
8. Reaction vessel
9. Furnace
10. Nickel reactor
11. Thermocouple
12. Geissler tube
13. Hg manometer
14. Buffer tank
15. F_2 absorber (Soda lime pellets)
16. HF absorber (NaF pellets heated at 100°C)
17. F_2 gas
18. Linear amplifier
19. Recorder

3. Results and Discussion

3.1 Intercalation Reaction

As is described in introduction, no intercalation occurred in the binary system of graphite and fluorine or graphite and metal fluoride such as AlF_3, FeF_3, MgF_2, CuF_2 or LiF at 20-300°C. However, as the GIC, $C_xF(MF_n)_y$ was prepared in the ternary system of graphite, fluorine and metal fluoride, it is considered that fluorine would react with metal fluoride to form a gaseous product, which would be then intercalated into graphite with fluorine.

$$\frac{m}{2} F_2(g) + MF_n(s) \longrightarrow MF_{n+m}(g) \quad (1)$$

$$\text{Graphite}(s) + MF_{n+m}(g) + F_2(g) \longrightarrow C_xF(MF_n)_y(s) \quad (2)$$

Some examples are known regarding the reaction of fluorine with other elements or compounds in which the electron orbitals have an octet structure. It was reported that a reaction of CsF or RbF with F_2 gave CsF_3 or RbF_3 complex having F_3^- anion, which was detected by means of infrared and Raman spectroscopies at 15 K,[2] K^+ cation was less able to stabilize the F_3^- anion and Na^+ could not.[3] However, the other bands in their spectra suggested the existence of $K^+F^- \cdots F_2$ and $Na^+F^- \cdots F_2$ complexes.[3] This tendency of forming complex anion would be due to the size of the cation. The large cations have great ability to stabilize F_3^- anion or F radical by using p or d orbital. The bifluoride ion HF_2^- was studied by infrared spectroscopy[4] or molecular orbital calculation.[5] Though HF_2 radical has not been detected yet, some experimental study[6] and calculation[7] suggested the existence of unstable HF_2. On the other hand, xenon fluorides and halogen fluorides are prepared at more higher temperatures. Xenon fluorides, XeF_2, XeF_4 and XeF_6 are prepared at temperatures between 300-775°C. For example, XeF_4 is formed quantitatively at

400°C by a reaction between Xe and F_2 (mole ratio 1:5).[8] IF_5 is obtained by a direct reaction of iodine with fluorine around room temperature,[9] and the further fluorination of IF_5 by fluorine yields IF_7 at 280-290°C.[10] BrF_5[11] is prepared at a temperature between 76 and 105°C by fluorination of BrF_3 which is obtained by a reaction of bromine with fluorine at a temperature between room temperature and 120°C. ClF_3 is prepared by a reaction of fluorine with chlorine at 250°C.[12]

Regarding the reaction of LiF with fluorine, it was very difficult to detect the gaseous species, LiF_{1+x} at room temperature probably because of a small equilibrium constant of equation (1), however, the reaction rate of fluorine with LiF increased with increasing temperature. The surface of LiF powder (0.2 g) was liquefied at ca. 530°C by the reaction with fluorine of 1.0×10^5 Pa and the complete liquefaction was observed around 650°C. These temperatures are lower by ca. 300-200°C than the melting point of LiF (845°C). This result suggests the following reaction of fluorine with LiF.

$$LiF(s) \xrightarrow{F_2} LiF_{1+x}'(\ell) \xrightarrow{F_2} LiF_{1+x}(g) \qquad (3)$$

The X-ray diffraction pattern of solidified LiF was that of LiF itself by the decomposition of a product, however, showing a very disordered structure of LiF crystal due to the reaction with fluorine (Figure 2-2). Solidified LiF was very hygroscopic with light yellow color, which was rapidly changed to brown in moist air.

Intercalation reaction would be initiated by gaseous LiF_{1+x}. The mobility of LiF_{1+x} between graphite layers is expected to be small due to its larger size, so it is plausible that fluorine is intercalated through LiF_{1+x} as a reaction medium.

$$LiF_{1+x} + \frac{x}{2} F_2 \longrightarrow \frac{x}{2} F_2 + LiF \cdot F_x \qquad (4)$$

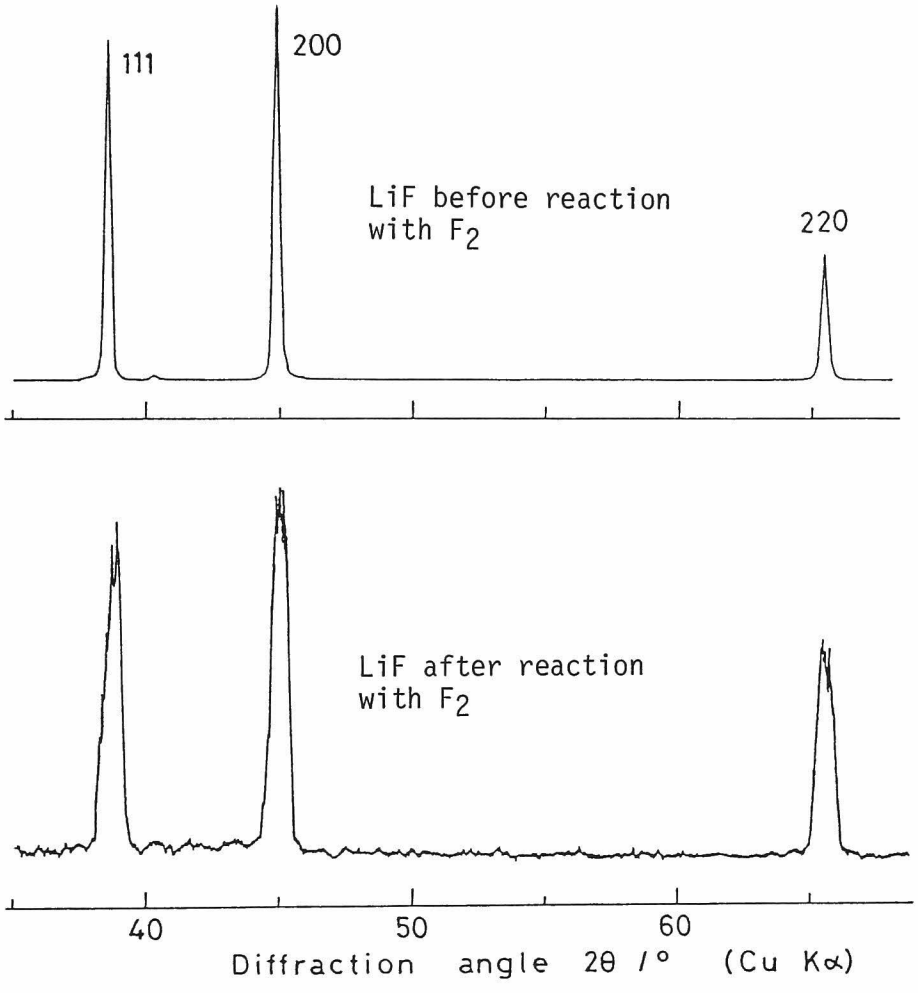

Fig. 2-2 X-ray diffraction patterns of LiF before and after reaction with F_2.

3.2 Reaction Rate for Intercalation

In general, a reaction rate increases with increasing temperature, however, the formation of an intercalation compound becomes difficult with increase in temperature since the intercalation reaction accompanies the entropy decrease and the free energy change of formation decreases with increase in temperature.

The amount of inserted substance decreased with increasing temperature and no intercalation occurred over 100°C. Table 2-1 indicates the weight increase at various temperatures in graphite-fluorine-LiF system. When fluorine gas was introduced into a reaction system at a temperature higher than 100°C, no weight change was observed at the temperature and the weight increase started after decrease in temperature below 100°C (Figure 2-3). When fluorine introduction was made between 80 and 100°C, the amount of intercalant at the temperature was smaller than that of the reaction at 20°C (Table 2-1). The lower the reaction temperature is, the more the equilibrium of equation (2) may lean to the product, $C_xF(MF_n)_y$ because the intercalation reac-

Table 2-1 Weight increase at various temperatures in graphite, fluorine and LiF system.

Temp. of fluorine introduction (T_1) °C	Weight increase at T_1 wt%	Starting temp. of intercalation (T_2) °C	Time needed for complete intercalation under T_2 h	Final weight increase wt%
355	0	20	36	8.8
302	0	61	15	18.0
252	0	89	3.5	18.0
204	0	95	3	17.8
172	0	98	2	16.0
148	0	118	4	19.8
132	0	100	3	19.0
103	0	84	2.5	16.0
101	4.2	101	2.5	18.0
93	10.9	93	4	19.8
79	11.0	79	7	17.0
20	16.5	20	13	16.5

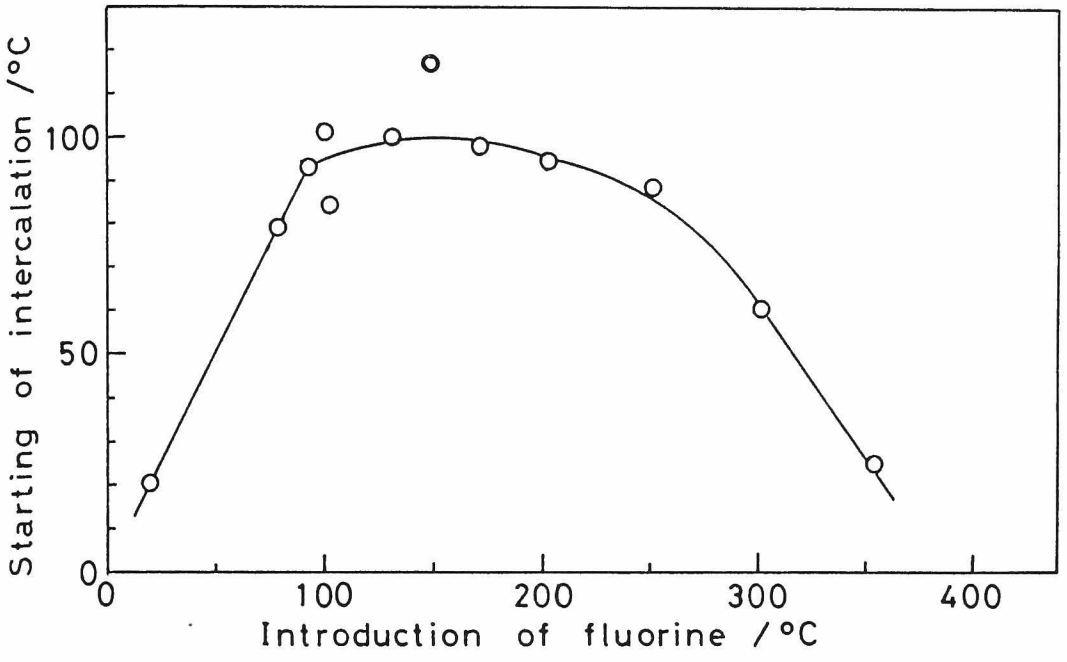

Fig. 2-3 Starting temperature of intercalation vs. the temperature of fluorine introduction.

tion occurs with decrease in the entropy and enthalpy as mentioned above. However, when fluorine was introduced at a temperature between 79-252°C, the amount of intercalant was larger than that of the product prepared at 20°C. Two factors are considered about this difference in the amount of intercalant. One is reaction temperature which generally increases the reaction rate. Another is the reaction of LiF with fluorine to produce $LiF_{1+x}(g)$ as a reaction medium because the vapor pressure of LiF_{1+x} would increase with increasing temperature. When fluorine introduction was performed above 200°C, a temperature at which intercalation started on cooling of a reaction system decreased remarkably (Figure 2-4). With increasing temperature of fluorine introduction, it would occur more easily that active sites around edge plane of graphite react with fluorine, forming C-F bond. This would make difficult

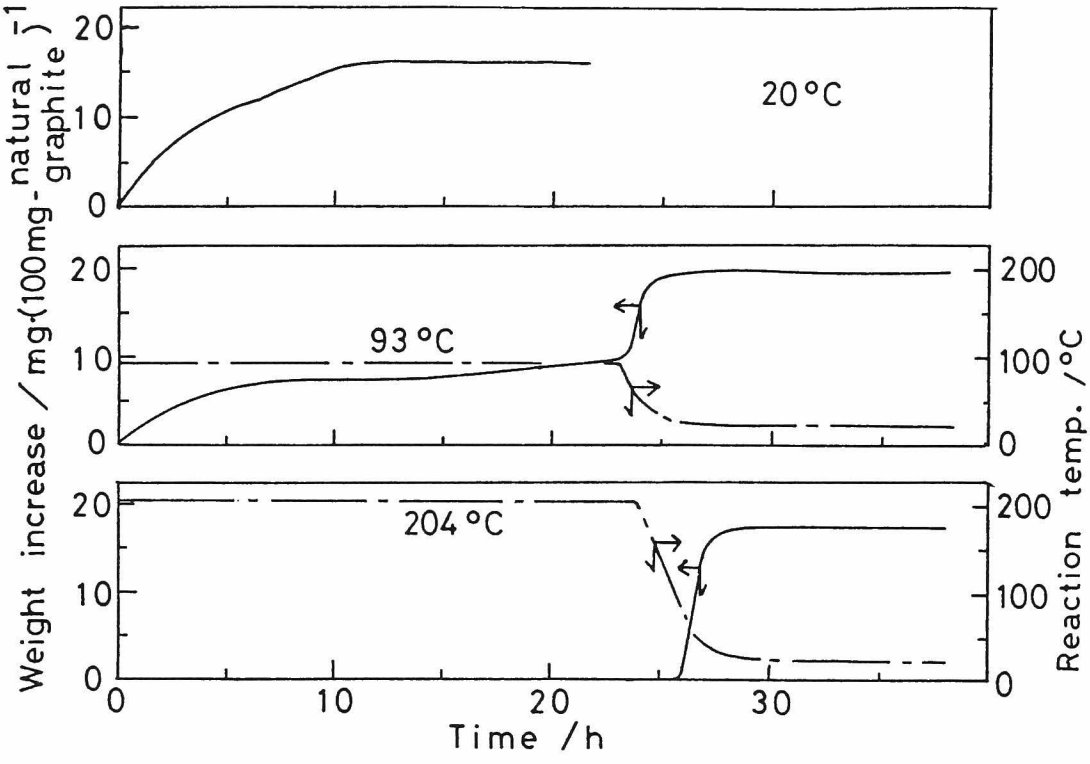

Fig. 2-4 Weight increase vs. time curves for intercalation reaction.

the electron transfer reaction between graphite and a gaseous Lewis acid formed by the reaction of fluorine with metal fluoride.

4. Summary

(1) The surface of LiF powder (ca. 0.2 g) was liquefied at about 530°C by the reaction with fluorine of 1.0×10^5 Pa and the complete liquefaction was observed around 650°C which is lower by about 200°C than a melting point of LiF (845°C). This result means that there exists a strong chemical interaction between LiF and fluorine. A gas species, MF_{n+m} formed by the

reaction of metal fluoride and fluorine would interact with host graphite and have a significant role as a medium for the subsequent fluorine intercalation.

$$\frac{1}{2}\ mF_2(g) + MF_n(s) \longrightarrow MF_{n+m}(g)$$

$$\text{Graphite}(s) + MF_{n+m}(g) + F_2(g) \longrightarrow C_xF(MF_n)_y\ (s)$$

(2) It was observed by thermogravimetry that the intercalation reaction occurred under ca. 100°C. On fluorine introduction at a temperature between 79 and 252°C, the obtained product had larger amount of intercalant than that of the GIC prepared at 20°C. However, a temperature at which intercalation started on cooling of a system decreased when the fluorine introduction temperature was over 200°C, probably because C-F covalent bond formed on active sites around edge plane of host graphite weakened the interaction between guest of gaseous Lewis acid and host of graphite.

References

1) M.Takashima and N.Watanabe, Nippon Kagaku Kaishi, 1976, 1222 (1976).
2) B.S.Ault and L.Andrews, J. Am. Chem. Soc., 98, 1591 (1976).
3) B.S.Ault and L.Andrews, Inorg. Chem., 16, 2024 (1977).
4) S.A.Macdonald and L.Andrews, J. Chem. Phys., 70, 3134 (1979).
5) P.A.Kollman and L.C.Allen, J. Am. Chem. Soc., 92, 6101 (1970).
6) B.S.Ault, J. Chem. Phys., 68, 4012 (1978).
7) S.V.O'neil, H.F.Schaefer III and C.F.Bender, Proc. Nat. Acad. Sci., 71, 104 (1974).
8) H.H.Claassen, H.Selig and J.G.Malm, J. Am. Chem. Soc., 84, 3593 (1962).

9) R.N.Haszeldine, J. Chem. Soc., 1949, 2856 (1949).
10) W.C.Schumb and M.A.Lynch Jr., Ind. Eng. Chem., 42, 1383 (1950).
11) J.Fischer, R.K.Steunenberg and W.Lechnik, U. S. At. Energy Comm., ANL-5633, p38 (1956).
12) J.W.Grisard, H.A.Bernhard and G.D.Oliner, J. Am. Chem. Soc., 73, 5724 (1951).

Chapter 3

ELECTRICAL CONDUCTIVITIES OF INTERCALATION COMPOUNDS*

1. Introduction

Since it was reported that $C_{16}AsF_5$ had a high electrical conductivity,[1] much attention has been concentrated on the electrical conductivity of graphite intercalation compound (GIC). Physical properties of GIC such as superconductivity,[2] ionization of intercalant[3] or electronic structure[4] have been also investigated.

The electrical conductivity of GIC is controlled by a carrier concentration and its mobility. The carrier is mainly a conductive free electron in a donor-type compound and a positive hole in an acceptor-type. GIC has strongly anisotropic nature as well as host graphite (Table 3-1). The electrical conductivity in direction of a-axis is about 10^5 times that along c-axis for an acceptor type, while it is about 10^3 times for a donor-type. In general, the maximum electrical conductivity is not observed for a 1st stage compound having the highest concentration of intercalant but for a higher stage compound. For the donor-type such as graphite-alkali metal compounds, the electrical conductivity in direction of a-axis doesn't depend on the kind of alkali metal and the maximum value is observed for the 5th stage compound.[6] On the other hand, for an acceptor-type compound such as graphite-AsF_5 or graphite-HNO_3, the 2nd or 3rd stage compound has the maximum electrical conductivity.[1] These phenomena are interpreted by saturation of carrier concentration and decrease of its mobility.[7] Though GIC is therefore expected as a new electroconduc-

---

* Solid State Ionics, 11, 65 (1983)

Table 3-1 Electrical conductivities of 1st stage GIC in parallel (σ_a) and in perpendicular (σ_c) to a-axis.[5)]

		σ_a(300K) $(\Omega\cdot cm)^{-1}$	σ_c(300K) $(\Omega\cdot cm)^{-1}$	σ_a/σ_c	I_c Å
	Graphite	2.5×10^4	~10	~2.5×10^3	3.35
Acceptor-type GIC	C_6HNO_3	3.0×10^5	2.0	1.5×10^5	7.78
	$C_6H_2SO_4$	1.0×10^5	0.5	2.0×10^5	7.98
	C_8AsF_5	4.0×10^5	0.2	2.0×10^6	8.11
Donor-type GIC	LiC_6	2.6×10^5	1.7×10^4	15.2	3.70
	BaC_6	$>10^5$	30	3.3×10^3	5.26
	KC_8	1.0×10^5	3×10^3	33	5.40
	RbC_8	1.0×10^5	—	—	5.65
	CsC_8	1.0×10^5	5×10^3	20	5.94

tive material, most of known compounds are hygroscopic and easily decompose in air.

Chapter 1 dealt with the preparation of ternary GIC's of $C_xF(MF_n)_y$, which were relatively stable in air. In this chapter, GIC of fluorine and MgF_2, LiF, CuF_2 or FeF_3 was prepared from pyrolytic graphite or PAN-based carbon fiber, and their electrical conductivities and stability are described.

2. Experimental

2.1 Contactless Wien Inductance Bridge

Figure 3-1 shows the principle of Wien inductance bridge.[8)] The sensing inductor for contactless conductivity measurement is L_4 with a resistance R_4. When a sample is inserted into the sensing inductor, there occurs two concomitant effects which

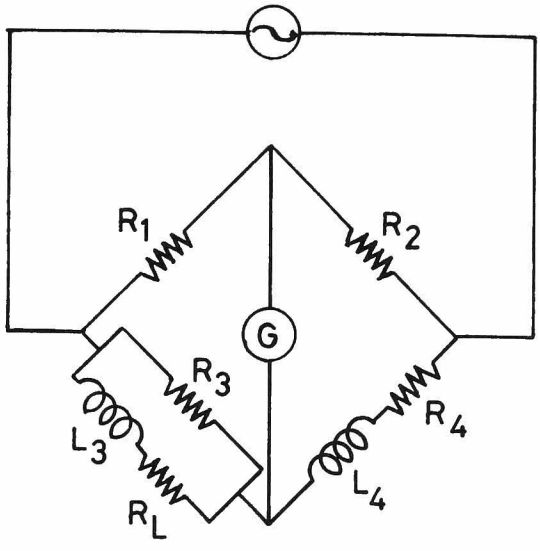

Fig. 3-1 Wien inductance bridge.[8)]

$$\omega^2 L_3 L_4 = R_4(R_L + R_3) - R_L R_3 \cdot \frac{R_2}{R_1}$$

$$\frac{L_3}{L_4} = \frac{R_1(R_L + R_3)}{R_2 R_3 - R_1 R_4}$$

ω: Wien bridge oscillator frequency

cooperate to shift the Wien bridge oscillator frequency (ω) upwards. (1) The sample couples inductively, as if in parallel, with sensing inductor to reduce L_4. (2) Eddy current occurring in the sample increases the equivalent resistance of inductor (R_4). The shift from base frequency varies directly with sample conductivity where all the samples are of exactly the same geometry.

Figure 3-2 shows the block diagram of Wien inductance bridge used in this study. The sensing inductor coil was made of TDK-H_{5A} type of ferrite core (external diameter: 50 mm, internal diameter: 30 mm, width: 13 mm), which was cut to have a 5 mm of air gap and wound by 250-turns of enamel coated copper wire (0.1 mm in diameter). A piece of talc was placed in the air gap so that a sample

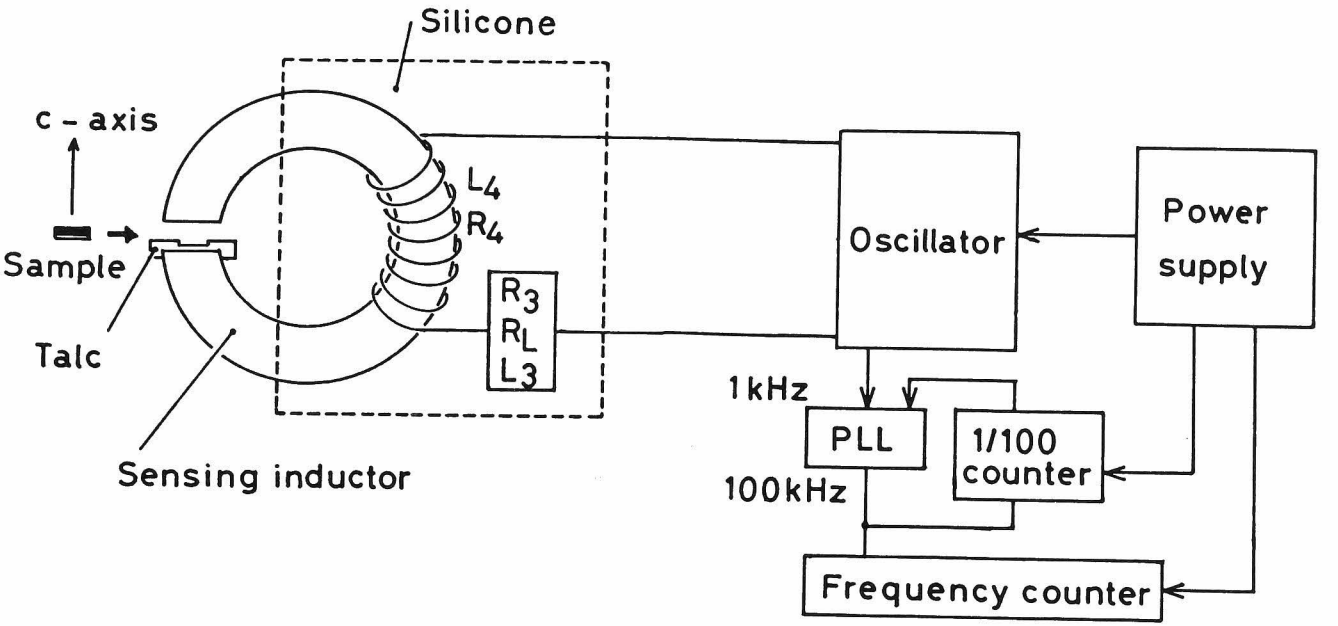

Fig. 3-2 Block diagram of contactless Wien inductance bridge.

could be fixed in the magnetic field generated in the gap. In order to match the temperature coefficient of resistors, enamel coated copper wire was wound bi-filar non-inductively. The bridge was filled with silicone rubber to maintain a temperature uniformly. Wien bridge oscillator is based on a self-balancing precision bridge circuit to make an alternating current constant. In order to magnify a detected frequency shift, a base frequency (1 kHz) was controlled to 100 kHz by phase locked loop (PLL). The observed frequency was indicated by a frequency counter.

The following relations were found from the calibration using a variety of materials having known conductivities:

(a) The frequency shift is proportional to conductivity when the geometry and thickness of samples are identical.

(b) The frequency shift is proportional to thickness of a sample between 0.2 and 2.0 mm.

Figure 3-3 shows the calibration curve for relation between observed frequency shifts and electrical conductivities of Cu, Al, Zn, Pb, Ti and isotropic graphite (5 × 5 mm in width, 1 mm in thickness).

2.2 Preparation of GIC

Host graphites of GIC were pyrolytic graphite, PG (heat-treated at 3000°C: 5 × 5 mm in width, 0.5-1.0 mm in thickness) and PAN-based carbon fiber (heat-treated at 2800°C: 60 mm in length, 7.5 ± 0.1 μm in diameter). GIC's were prepared by the same method as described in Chapter 1.

2.3 Electrical Conductivity Measurement

The electrical conductivity measurement for GIC prepared from PG was made by the contactless Wien inductance bridge method. The thickness of a sample was measured by micrometer and the electrical conductivity of the sample was obtained from the frequency

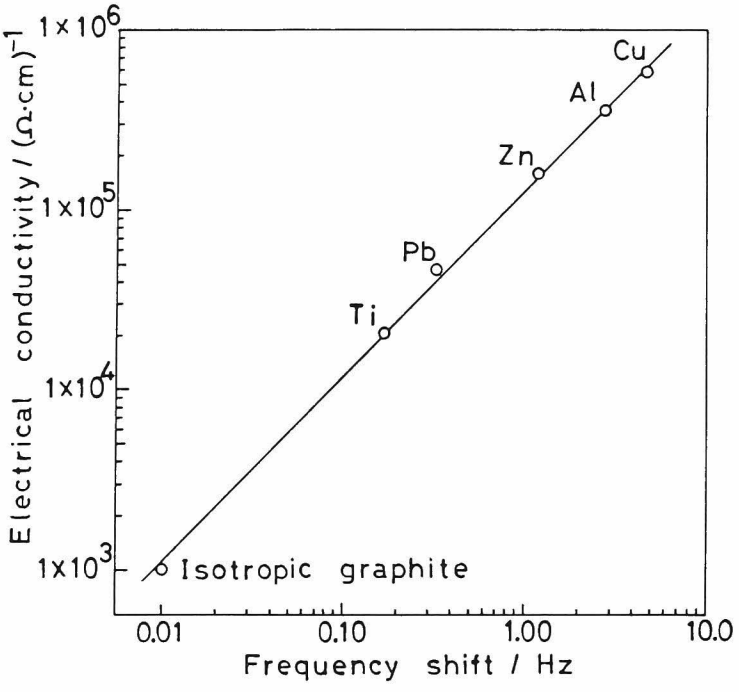

Fig. 3-3 Calibration curve for measurement of electrical conductivity by contactless Wien bridge method.

shift per 1 mm thickness.

The measurement for GIC of PAN-based carbon fiber was performed by the 4-point DC method (Figure 3-4). A fiber sample was fixed by silver paste on four platinum wires laid in parallel. The direct current of 5 μA was made to flow through the sample, and the IR drop (V) between middle two points (length: ℓ) was measured. A diameter of the sample was measured by a microscope with a ruler. The electrical conductivity was calculated by the following equation.

$$\sigma = \frac{5}{1000} \cdot \frac{1}{V} \cdot \left(\frac{2}{d} \times 10000\right)^2 \cdot \frac{\ell}{\pi}$$

σ: electrical conductivity $(\Omega \cdot cm)^{-1}$

V: IR drop (mV) ℓ: length (cm)

d: diameter (μm) π: 3.14

These measurements were carried out in air at 22 ± 2°C.

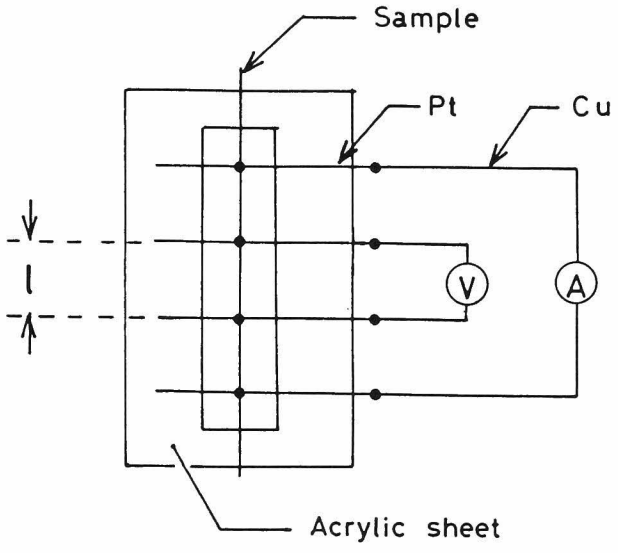

Fig. 3-4 4-point DC method used for electrical conductivity measurement of GIC prepared from PAN-based carbon fiber.

3. Results and Discussion

3.1 Electrical Conductivity of GIC Prepared from Pyrolytic Graphite

Figure 3-5, 6 and 7 show the electrical conductivities (in direction of a-axis: σ_a) of GIC's prepared from PG as a function of intercalant. At first the electrical conductivity increased rapidly with increase of intercalant to 10 wt%, where a mixed higher stage compound than that with identity period (I_c) of 16.1 Å was formed, and reached the maximum value. For $C_xF(MgF_2)_y$, the maximum conductivity was 1.9×10^5 $(\Omega \cdot cm)^{-1}$ at 8-10 wt% of intercalant corresponding to a mixed stage compound with I_c of 9.4-19.5 Å. For $C_xF(LiF)_y$, it

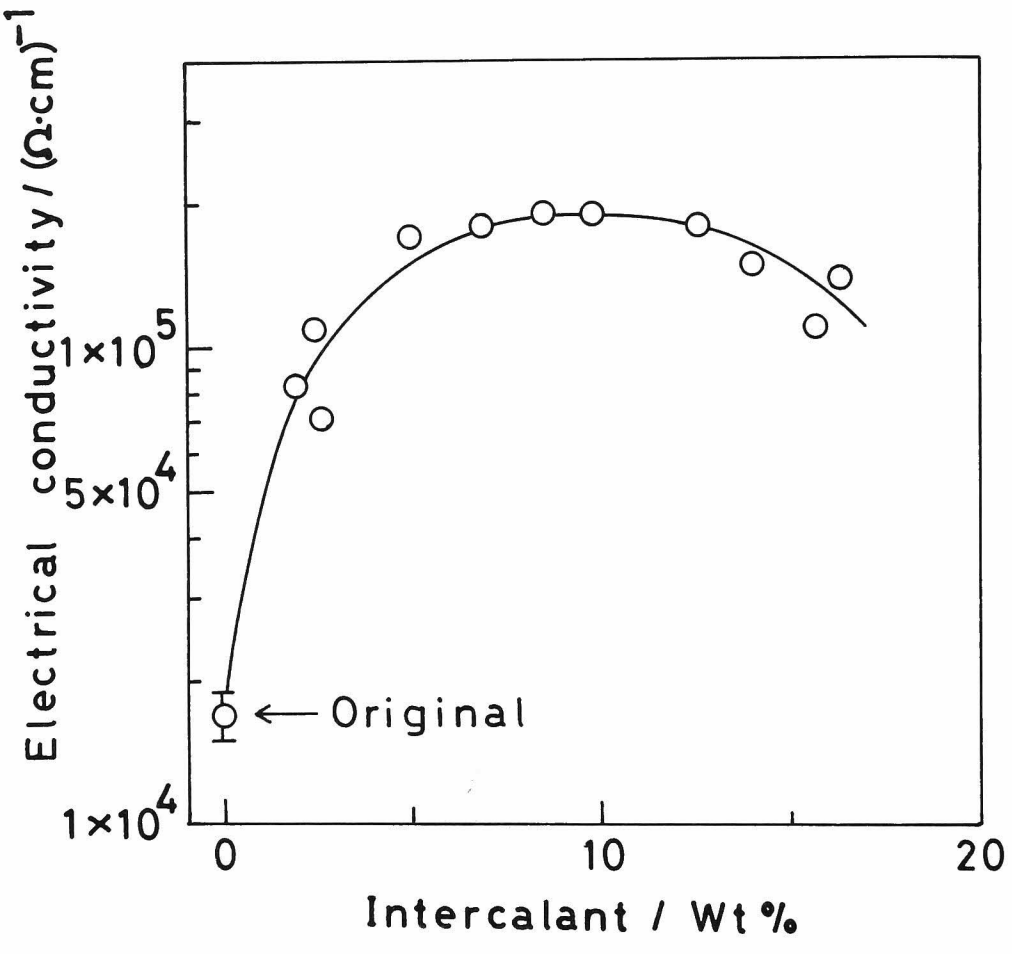

Fig. 3-5 Electrical conductivity (σ_a) of pyrolytic graphite intercalated by fluorine and MgF_2.

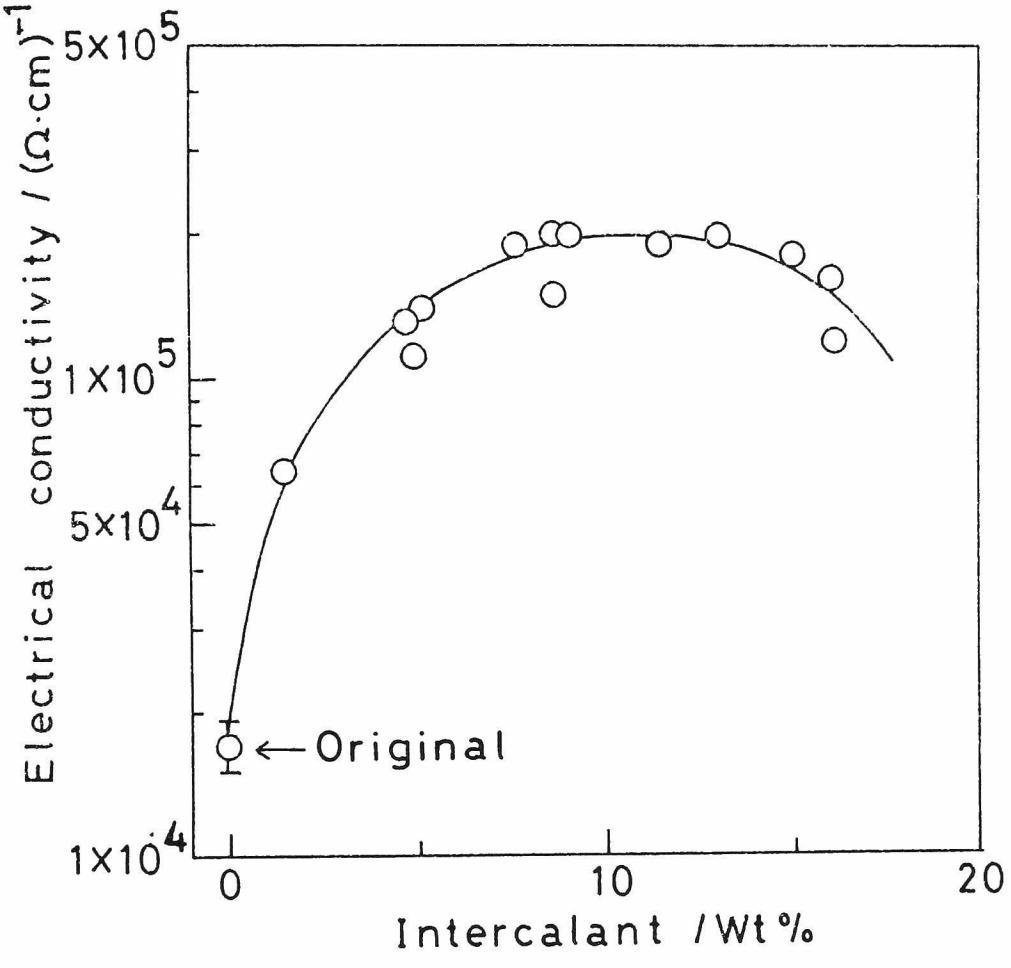

Fig. 3-6 Electrical conductivity (σ_a) of pyrolytic graphite intercalated by fluorine and LiF.

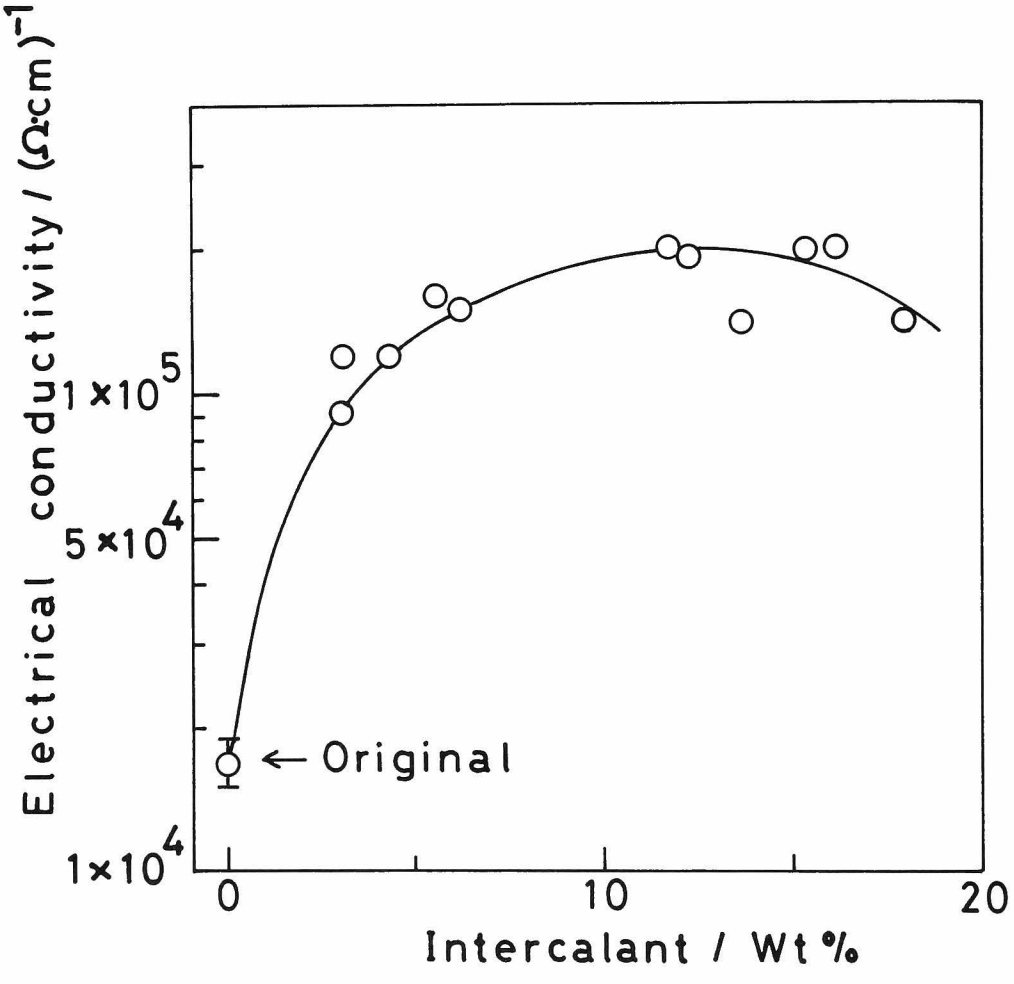

Fig. 3-7 Electrical conductivity (σ_a) of pyrolytic graphite intercalated by fluorine and CuF_2.

was 2.0×10^5 $(\Omega \cdot cm)^{-1}$ at 9-13 wt%, and that of $C_xF(CuF_2)_y$ was 2.0×10^5 $(\Omega \cdot cm)^{-1}$ at 12-15 wt% of intercalant corresponding to a mixed stage with I_c of 9.4-12.8 Å. These maximum electrical conductivities were higher by one order than that of original pyrolytic graphite, $(1.7 \pm 0.2) \times 10^4$ $(\Omega \cdot cm)^{-1}$. The electrical conductivity of the compound with I_c of 9.4 Å (1st stage compound) was lower to some extent than the maximum value. The electrical conductivity of GIC is a function of the product of number and mobility of carrier. The number of carrier increases proportionally with increase in the amount of intercalant in the range of a low concentration since the intercalants have only a weak interaction with each other and the ionicity of intercalated atoms or molecules is almost uniform. However, it is considered that the intercalants repulse each other in the higher concentration to decrease their ionicity. As a result the number of carrier doesn't increase any more with increasing intercalant. The mobility of carrier can be compared from the ^{19}F-NMR spectra. Table 3-2 indicates the peak to peak widths of ^{19}F-NMR spectra for 1st (I_c = 9.4 Å) and 2nd stage (I_c = 12.8 Å) compounds. The width of the former was 5 times that of the latter, which means that intercalated fluorine of the 1st stage compound is more strongly localized at a lattice point in more ionized state than those of the 2nd stage compound. The electrostatic force between the negatively charged fluorine and positive hole decreases the mean free path of carrier (positive hole), that is, the mobility of

Table 3-2 Peak to peak widths of ^{19}F-NMR spectra of $C_xF(MgF_2)_y$

Radio frequency: 15.00 MHz	
1st stage compound (I_c = 9.4 Å)	2.5×10^{-4} T (2.5 G)
2nd stage compound (I_c = 12.8 Å)	4.5×10^{-5} T (0.45 G)

carrier. From these reasons, the electrical conductivity of 1st stage compound is lower than that of the 2nd stage or 3rd stage.

The value of y in $C_xF(MF_n)_y$ was approximately 0.005 from the chemical analysis. By fixing y at 0.005 and calculating x from the amount of intercalant, the chemical compositions of $C_xF(MF_n)_y$ giving the maximum conductivities were obtained to be $C_{19-14}F(MgF_2)_{0.005}$, $C_{16-11}F(LiF)_{0.005}$ and $C_{12-9}F(CuF_2)_{0.005}$. In case of the GIC's of AsF_5 and SbF_5, the 2nd stage, $C_{16}AsF_5$ and $C_{12}SbF_5$ have the maximum conductivities in their series. The numbers of carbon atoms per fluorine atom of $C_xF(MF_n)_y$ are 19-14, 16-11 and 12-9, respectively, which are near the ratios of C/AsF_5 and C/SbF_5 of the above compounds. One fluorine atom of $C_xF(MF_n)_y$ is therefore almost equivalent to one AsF_5 or SbF_5 molecule as an electron acceptor from graphite.

3.2 Electrical Conductivity of GIC Prepared from PAN-based Carbon Fiber

Figure 3-8 or 3-9 shows the electrical conductivity of PAN-based carbon fiber intercalated by fluorine and LiF or FeF_3, respectively. The maximum electrical conductivity of $C_xF(LiF)_y$ was (8-9) $\times$ 10^3 $(\Omega\cdot cm)^{-1}$ in the range of 7-14 wt% of intercalant, that of $C_xF(FeF_3)_y$ was (7-8) $\times$ 10^3 $(\Omega\cdot cm)^{-1}$ in the range of 11-16 wt%. These maximum values are about 7 times that of original fiber, (1.1-1.4) $\times$ 10^3 $(\Omega\cdot cm)^{-1}$, being attained by the less amount of intercalant than in the case of pyrolytic graphite. This would be arised from the structure of host graphite. Figure 3-10 is the illustration for the structures of pyrolytic graphite and PAN-based carbon fiber. PAN-based carbon fiber has onion-skin and mid-random structure. The rapid increase in the electrical conductivity is probably because the surface area of a fiber is intercalated at first and the electric current runs mainly through the skin on the electrical conductivity measurement.

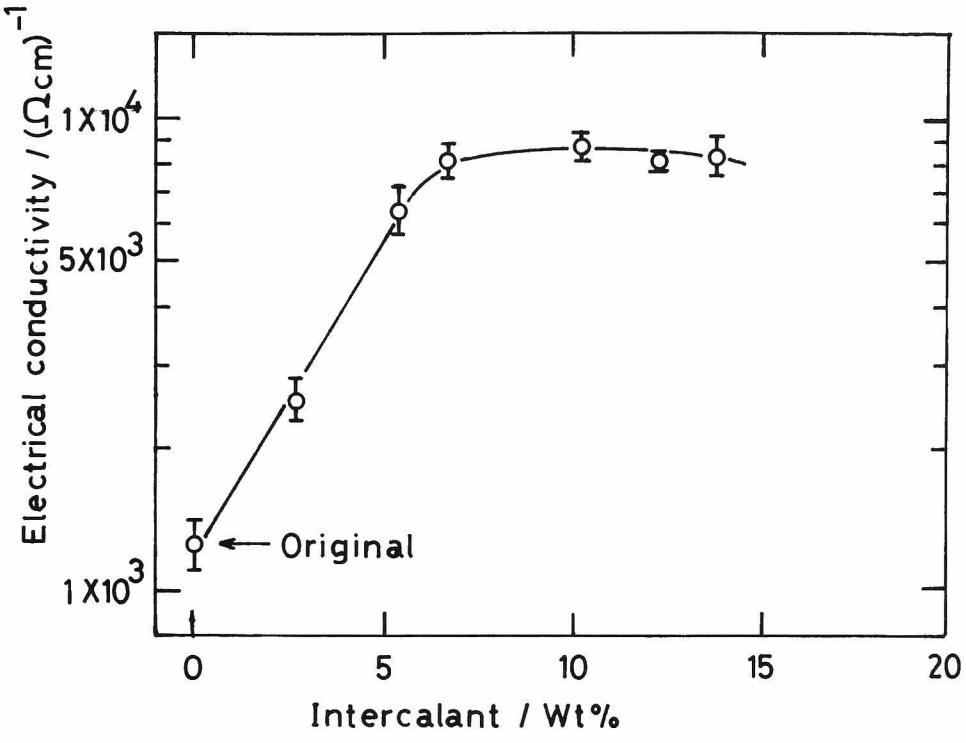

Fig. 3-8 Electrical conductivity of PAN-based carbon fiber intercalated by fluorine and LiF.

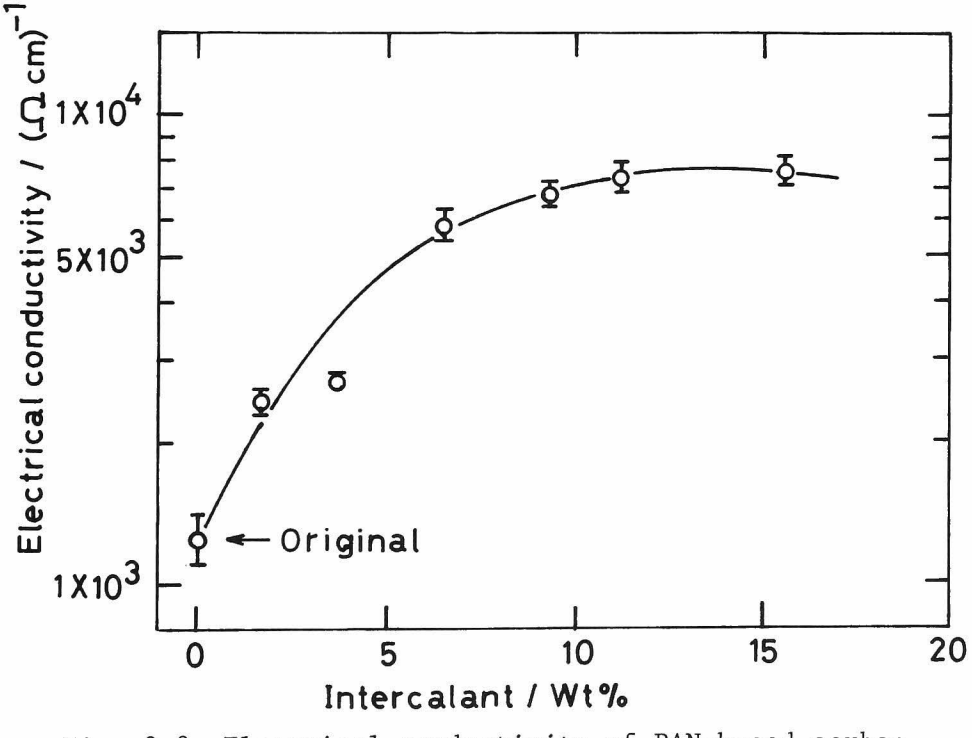

Fig. 3-9 Electrical conductivity of PAN-based carbon fiber intercalated by fluorine and FeF_3.

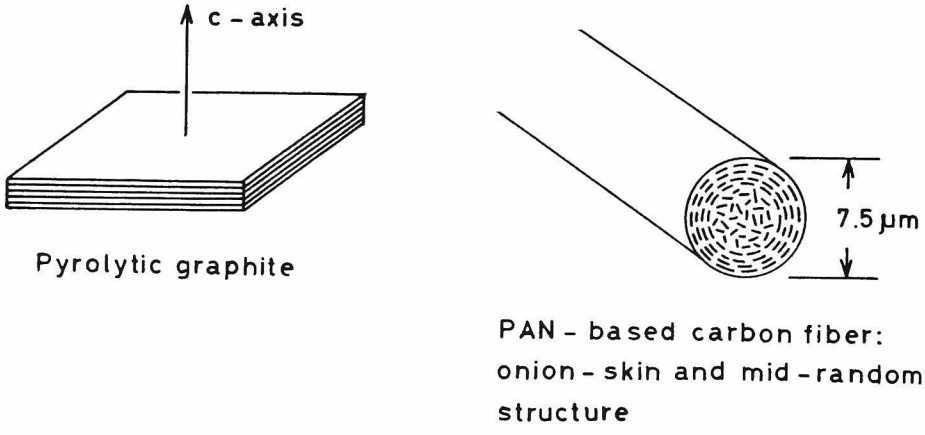

Fig. 3-10 Illustrations for structures of pyrolytic graphite and PAN-based carbon fiber.

A value of electrical conductivity is closely related with the crystallinity of host graphite. It is known that graphite with the higher crystallinity has the higher electrical conductivity. The crystallinity is estimated from a half width of a X-ray diffraction line. The half widths of (002) diffraction lines were 0.25° and 1.0° in 2θ for PG and PAN-based carbon fiber, respectively. After intercalation, those of (004) diffraction lines for 2nd stage compounds were 0.35° and 1.35°. These result indicates that the GIC of PG had the higher crystallinity than that of PAN-based carbon fiber, which led that the maximum conductivity for the compound of PG host gave the higher value than that for the PAN-based carbon fiber.

3.3 Stability of GIC's Prepared from Pyrolytic Graphite and PAN-based Carbon Fiber

Figure 3-11 shows the change in electrical conductivity and amount of intercalant in air for PG intercalated by fluorine and LiF. Slight weight increase was observed in a first few days

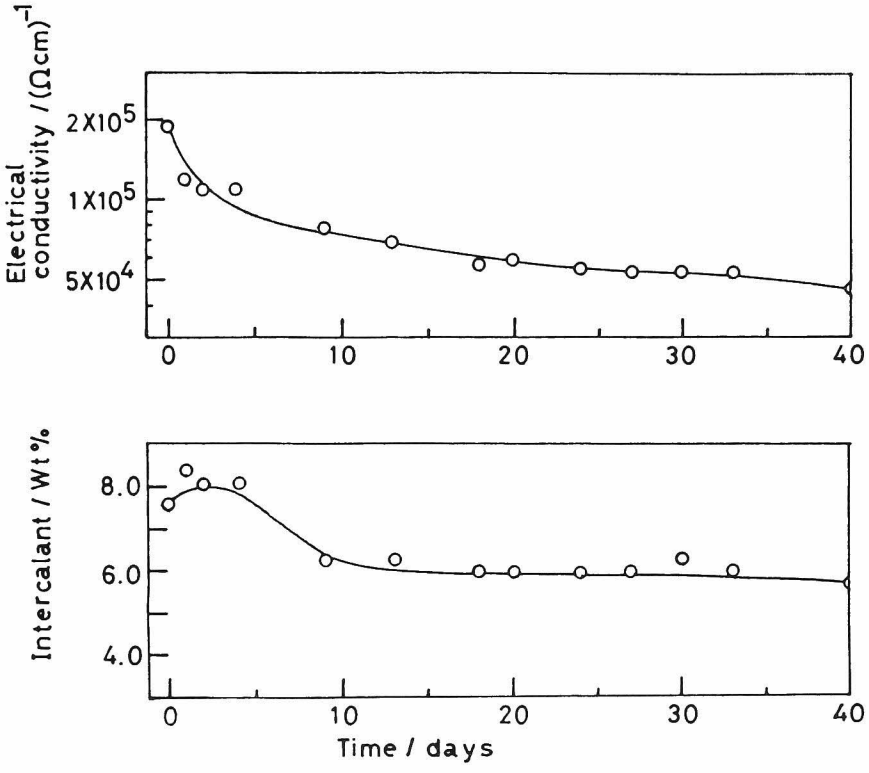

Fig. 3-11 Change in the electrical conductivity and amount of intercalant in air of pyrolytic graphite intercalated by fluorine and LiF.

probably due to the absorption of water in air. The electrical conductivity decreased with decreasing amount of intercalant in 20 days, which was caused by the release of intercalant. Thereafter almost no change was observed both in the electrical conductivity and amount of intercalant. The higher stability was found in the order of the compounds of CuF_2, LiF and MgF_2, which is the same result as indicated in Chapter 1.

Figure 3-12 is the change in the electrical conductivities of PAN-based carbon fiber intercalated by fluorine and LiF in air and in water. The decrease in electrical conductivity in air was only 7 % during 80 days. Even in water, it remained almost unchanged for 25 days, then gradually decreased to half of the

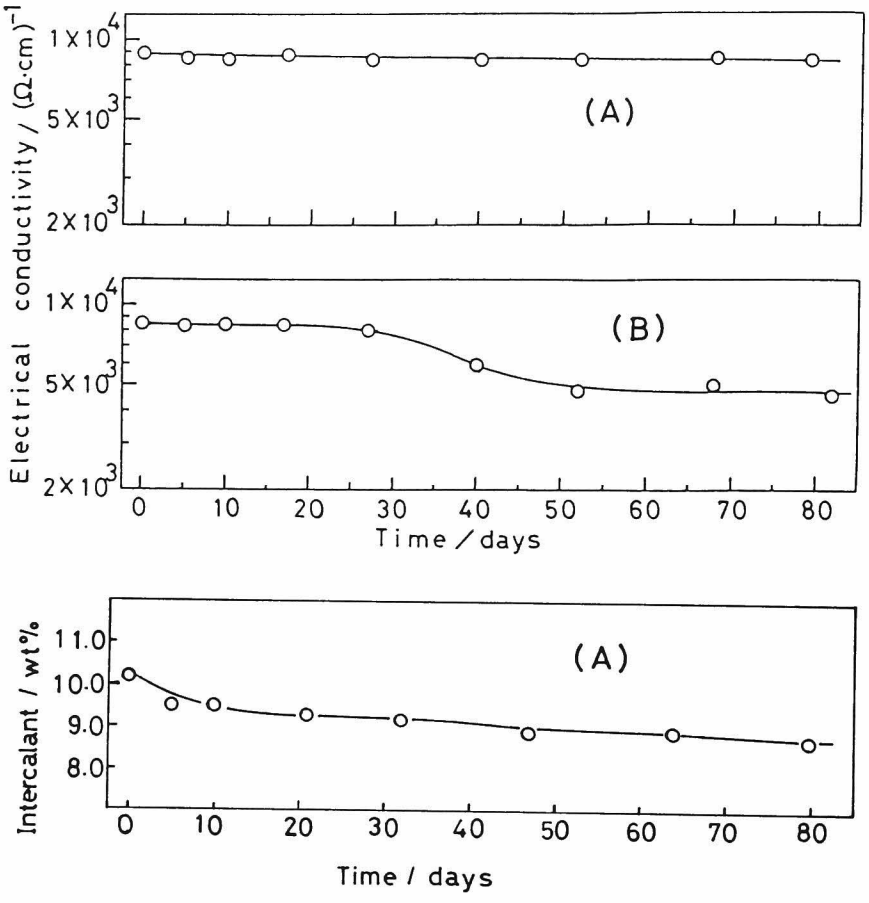

Fig. 3-12 Change in the electrical conductivity and amount of intercalant of PAN-based carbon fiber intercalated by fluorine and LiF in air (A) and in water (B).

value just after preparation. The weight decrease in air was only 2 % during 150 days. Concerning the stability, it was found that PAN-based carbon fiber was one of the good host materials.

The difference of stability between the GIC's prepared from PG and PAN-based carbon fiber is due to the structures shown in Figure 3-10. In case of PG, as the edge plane having significant role for the initial intercalation is exposed, it is easy for intercalant to be inserted or released. On the other hand, the crystallites of PAN-based carbon fiber are bound like a rope

and the inner part of the fiber is covered by onion-skin. The release of intercalant is protected more easily than in case of a PG compound.

4. Summary

(1) The electrical conductivity of GIC prepared from PG increased with increase in the intercalant and reached a maximum value of 1.9-2.0 $\times 10^5$ $(\Omega \cdot cm)^{-1}$ which was 10 times that of original PG ($1.7 \pm 0.2 \times 10^4$ $(\Omega \cdot cm)^{-1}$).

(2) GIC prepared from PAN-based carbon fiber had a maximum electrical conductivity of 7-9 $\times 10^3$ $(\Omega \cdot cm)^{-1}$ which was 7 times that of original value (1.1-1.4 $\times 10^3$ $(\Omega \cdot cm)^{-1}$).

(3) The GIC prepared from PAN-based carbon fiber was much more stable than that of PG. The decrease in the electrical conductivity was only 7 % for 80 days in air.

References

1) F.L.Vogel, G.M.T.Foley, C.Zeller, E.R.Falardeau and J.Gan, Mat. Sci. Eng., 31, 261 (1977).
2) M.Kobayashi and I.Tsujikawa, J. Phys. Soc. Jpn., 46, 1945 (1979).
3) G.Dresselhaus and M.S.Dresselhaus, Mat. Sci. Eng., 31, 235 (1977).
4) T.Inoshita, K.Nakao and H.Kamimura, J. Phys. Soc. Jpn., 43, 1237 (1977).
5) J.E.Fischer, Comments Solid State Physics, 9, 93 (1979).
6) E.Mcrae, D.Billand, J.F.Mareche and A.Hérold, Physica, B99, 489 (1980).
7) C.Zeller, J.A.Pendrys and F.L.Vogel, J. Mat. Sci., 14, 224 (1979)
8) S.C.Singhal and A.Kernick, Synthetic Metals, 3, 247 (1981).

Chapter 4

ELECTROCHEMICAL BEHAVIOR OF INTERCALATION COMPOUNDS*

1. Introduction

Graphite fluoride, $(CF)_n$ shows a high and stable discharge potential and high energy density as a cathode material of a primary battery with lithium anode.[1-4] Recently found another stable graphite fluoride, $(C_2F)_n$ has high possibilities as a new cathode material because of its higher discharge potential than that of $(CF)_n$.[5,6]

Besides these graphite fluorides of layered structures with a covalent bond between carbon and fluorine, some of the conventional graphite intercalation compounds (GIC's) of metal halides, in most cases metal chlorides, were also examined as cathode materials.[7] It is described in Chapter 1 that GIC's of fluorine and metal fluoride such as AlF_3, MgF_2 or CuF_2, prepared under fluorine atmosphere, contain many fluorine atoms with oxidizing ability. The results of ^{19}F-NMR measurement indicated that fluorine atoms were chemically adsorbed on graphite layers, being different from those in graphite fluorides. In this chapter these GIC's were used as cathode materials in lithium cells and their discharge characteristics are evaluated.

2. Experimental

2.1 Materials

Propylene carbonate (referred to as PC) as a solvent was purified by distillation below 100°C under a reduced pressure of 1.3×10^3 Pa (10 mmHg), and stored in a sealed flask with 4A

---

* Electrochimica Acta, 11, 1535 (1982)

molecular sieve. Water content in PC thus purified was determined to be less than 100 ppm by Karl Fischer titration. Lithium perchlorate, $LiClO_4$ (purity: 99.9 %) used as the electrolyte was dried at 190°C under vacuum for one day. A solution of 1 mol/dm^3 $LiClO_4$-PC was prepared and supplied as an electrolytic solution. Preparation of $C_xF(AlF_3)_y$, $C_xF(MgF_2)_y$ and $C_xF(CuF_2)_y$ used as cathode materials are as follows.

(A) Temperature increase method. Fluorine gas of 1.0×10^5 Pa (1 atm) was introduced into a nickel tube containing a mixture of natural graphite (0.3 g) and anhydrous AlF_3, MgF_2 or CuF_2 (0.3 g), purified by the same method as described in Chapter 1, at room temperature. After the reaction system was kept at room temperature for 10-60 min, the temperature of the reaction tube was raised up to 268-310°C at a heating rate of 4°C/min, and was maintained for 48 h at 268-310°C. Then the reaction system was cooled down to room temperature.

(B) Fixed temperature method. For the preparation of $C_xF(MgF_2)_y$ and $C_xF(CuF_2)_y$, another method was available. Fluorine gas of 1.0×10^5 Pa was introduced into a mixture of MgF_2 or CuF_2 and graphite at 190-350°C, and the reaction tube was maintained at the same temperature for 48 h. The system was then cooled down to room temperature.

Table 4-1 shows the results of elemental and X-ray diffraction analyses for the GIC's used in this work. Elemental analysis for C and F was performed at the Laboratory for Organic Elemental Microanalysis, Faculty of Pharmaceutical Science, Kyoto University.

2.2 Cell Assembly and Electrochemical Measurements

About 50 mg of the GIC was held between filter papers and molded into a pellet of 12.5 mm in diameter under a pressure 1800 kg/cm^2. GIC's prepared by the method (A) did not need the conductive additive and binder in molding because they had high electrical conductivity as shown in Chapter 3 and were slightly exfoliated. However, as it was difficult to mold the compounds prepared by the method (B) into a pellet, a small quantity of exfoliated graphite had to be added around the edge of a pellet as a binder. Carbon fiber as a terminal was wound around the pellet and welded with polyethylene to fix the electrode. The terminal portion of carbon fiber was covered by a polyethylene tube to avoid current leakage. Lithium metal (purity: 99 %) pressed on nickel net was used as the anode and reference electrode. Two lithium anodes having the same area as cathode were placed in parallel on both sides of the cathode in a glass container filled with 1 mol/dm^3 $LiClO_4$-PC solution. Figure 4-1 shows an illustration of the experimental cell.

Galvanostatic polarization was applied to the battery using a potentiostat/galvanostat (Hokuto Denko Ltd.) and the discharge potential of cathode was monitored by a recorder (Toa Electronics Ltd.) relative to lithium reference electrode through a Luggin capillary. Voltage measurement was made with an operation amplifier having an internal impedance of 10^{12} Ω. All the measurements were carried out in a dry box filled with dry nitrogen gas at 30°C. The discharge product was analysed by X-ray diffractometry and photoelectron spectroscopy (ESCA).

Table 4-1 Analytical data for GIC's used as cathode materials.

A: Temperature increase method
B: Fixed temperature method
** The intercalation reaction practically occurred under 100°C as described in Chapter 2. However, when used as cathode material, GIC had to be treated at a temperature between 268 and 350°C in fluorine atmosphere. This is designated as a retention temperature.

Compound[preparation method, retention temperature**]	Elemental analysis wt%	X-ray diffraction data (Cu-Kα)				
		Int.	2θ/°	d/Å	hkℓ	Identity period, I_c/Å
$C_{7.2}F(AlF_3)_{0.002}$ [A, 310°C]	C: 80.7 F: 17.8 Al: 0.06	vw, br w, br vs vw, br vw	9.2 19.6 28.42 49.6 58.86	9.6 4.5 3.14 1.8 1.57	001 002 003 005 006	9.42 ± 0.10
$C_{4.4}F(MgF_2)_{0.002}$ [A, 310°C]	C: 71.3 F: 26.0 Mg: 0.06	w m vs vw, br vw, br	9.50 19.10 28.48 48.9 59.2	9.30 4.64 3.13 1.9 1.6	001 002 003 005 006	9.34 ± 0.05

$C_{7.3}F(MgF_2)_{0.002}$ [A, 310°C]	C: 79.9 F: 17.5 Mg: 0.04	vw, br w vs vw	9.2 19.10 28.20 58.96	9.6 4.64 3.16 1.57	001 002 003 006	9.39 ± 0.10
$C_{5.5}F(MgF_2)_{0.001}$ [A, 300°C]	C: 75.2 F: 21.8 Mg: 0.02	vw w vs vw, br vw	9.38 18.94 28.28 49.0 58.90	9.42 4.68 3.15 1.9 1.57	001 002 003 005 006	9.41 ± 0.05
$C_{3.0}F(MgF_2)_{0.001}$ [B, 350°C]	C: 64.0 F: 33.4 Mg: 0.05	m, br m vs vw, br vw	9.7 18.98 28.38 48.6 59.18	9.1 4.67 3.14 1.9 1.56	001 002 003 005 006	9.38 ± 0.04
$C_{8.1}F(MgF_2)_{0.002}$ [B, 190°C]	C: 82.4 F: 16.2 Mg: 0.04	m s vs vw, br w	9.48 19.04 28.38 48.4 59.00	9.32 4.66 3.14 1.9 1.56	001 002 003 005 006	9.37 ± 0.06
$C_{7.9}F(CuF_2)_{0.0001}$ [A, 268°C]	C: 81.3 F: 16.4 Cu: 0.01	w, br s m w	20.2 26.64 ≀ 28.46 54.60	4.39 3.31 ≀ 3.13 1.68	002 for graphite mixture of higher stage compounds 003 for GIC: I_c = 9.39 004 for graphite	

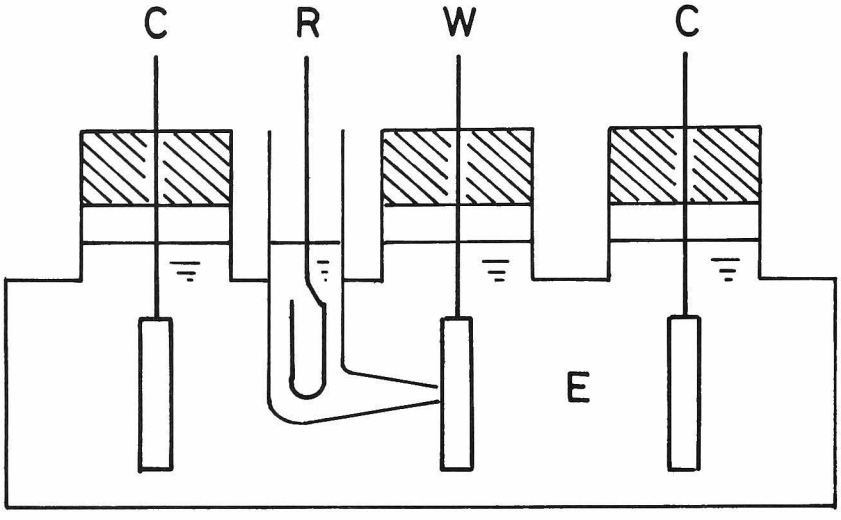

W: Working electrode
C: Counter electrode (Li)
R: Reference electrode (Li)
E: Electrolyte ($LiClO_4$ in PC)

Fig. 4-1 Experimental cell.

3. Results and Discussion

3.1 Open Circuit Voltage

The initial OCV's of GIC's were 3.4-4.2 V vs Li, which reached 3.4-3.9 V after more than 5 h. This may be because active fluorine atoms adsorbed on the surface of the GIC react with the solvent. These values are higher than for graphite fluoride (3.2-3.3 V vs Li) or graphite adsorbing oxygen on the surface. For example, the OCV of $C_{7.3}F(MgF_2)_{0.002}$ was 3.9-4.2 V vs Li at the beginning of cell construction, decreasing to 3.7-3.9 V after 8 h. After 4 and 20 % discharge, the OCV for $C_{7.3}F(MgF_2)_{0.002}$ de-

creased to 3.5 V in both cases by the discharge of active fluorine. The GIC within 2 weeks after the preparation showed a higher discharge potential by about 0.1 V below 200 $\mu A/cm^2$ than that stored in a sealed flask for 6 months. In preservation of the prepared GIC for several months, the fluorine content decreased by 2-3 %. It would be due to the release of active fluorine atoms in the GIC. It is therefore considered that the GIC just after the preparation tends to discharge the active fluorine showing a high discharge potential.

Figure 4-2 shows the potential recovery curves of $C_{7.3}F(MgF_2)_{0.002}$ electrode after 4 and 23 % utilization. It took more than 2 days until the potential reached the equilibrium value. This recovery time of OCV is longer by a half day or more than those for $(C_2F)_n$ (about 1 day) and $(CF)_n$ (about 1.5 days). As in the case of graphite fluoride, the recovery time is regarded as the time needed for that Li^+ ion inserted into the diffusion layer makes

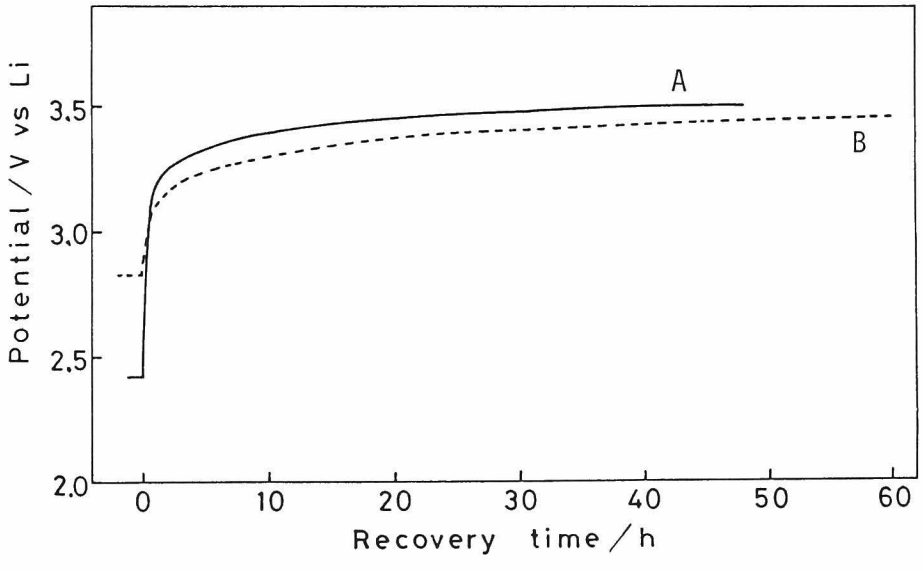

Fig. 4-2 Potential recovery curves of $C_{7.3}F(MgF_2)_{0.002}$ electrode.
A: after 23 % discharge at 800 $\mu A/cm^2$
B: after 4 % discharge at 16 $\mu A/cm^2$

an ion pair with discharged fluoride ion and the equilibrium state is attained in the cathode. As discussed later, a so-called diffusion layer formed by the discharge would be more stable in the GIC than in graphite fluoride electrode because the crystallite size of host graphite in the GIC is much larger than that in the discharged graphite fluoride. Accordingly, the transfer of Li^+ ion in the former would take more longer time than that in the latter after cut off of the circuit.

3.2 Discharge Characteristics of the GIC's

As described in Chapter 1, C-F covalent bond is formed on the surface of GIC by increasing a temperature over 200°C. Such GIC would have many cracks in itself because of the formation of $-CF_3$ and $=CF_2$ groups having covalent bonds around the surface. The flat discharge potential was observed only for this type of GIC. On the other hand, GIC prepared under 200°C had a very large overpotential without flatness and a very small energy density. For example, $C_{8.1}F(MgF_2)_{0.002}$ prepared at a retention temperature** of 190°C had only 16 % of utility in spite of high initial OCV (4.05 V). The OCV was recovered gradually after 16 % discharge, but did not reach to 3.5 V. This result suggests that the edge plane of $C_{8.1}F(MgF_2)_{0.002}$ was closed except some dischargeable crystallites as is shown in Figure 4-3.

Figure 4-4 shows galvanostatic discharge curves for $C_{7.2}F(AlF_3)_{0.002}$ prepared at a retention temperature of 310°C by the method (A). At current densities 40, 200 and 400 $\mu A/cm^2$, the cathode gave flat discharge potentials of 2.8-2.5 V vs Li

---

** The intercalation reaction practically occurred under 100°C as described in Chapter 2. However, when used as cathode material, GIC had to be treated at a temperature between 268 and 350°C in fluorine atmosphere. This is designated as a retention temperature (Cf. Chapter 1, P24).

reference electrode and its utilities were 69, 57 and 45 % (theoretical capacity: 250 Ah/kg) down to 1.2 V vs Li, respectively. Figure 4-5 is galvanostatic discharge curves for $C_{7.3}F(MgF_2)_{0.001}$ cathode prepared at a retention temperature of 310°C by the method (A). The utilities were 72, 65 and 59 % (theoretical capacity: 250 Ah/kg) at current densities 40, 160 and 400 μA/cm^2, respectively and their discharge potentials were in the range of 2.8-2.5 V vs Li as in the case of $C_{7.2}F(AlF_3)_{0.002}$. Figure 4-5 also includes the result of the discharge at 40 μA/cm^2 for $C_{3.0}F(MgF_2)_{0.001}$ prepared at a retention temperature of 350°C by the method (B). The utility was 100 % (theoretical capacity: 470 Ah/kg). Figure 4-6 shows galvanostatic discharge curves for $C_{7.9}F(CuF_2)_{0.0001}$ prepared at a retention temperature of 268°C by the method (A). This GIC gave flat discharge potentials of 2.8-2.4 V vs Li and the utilities of 66, 66 and 50 % (theoretical capacity: 230 Ah/kg) at

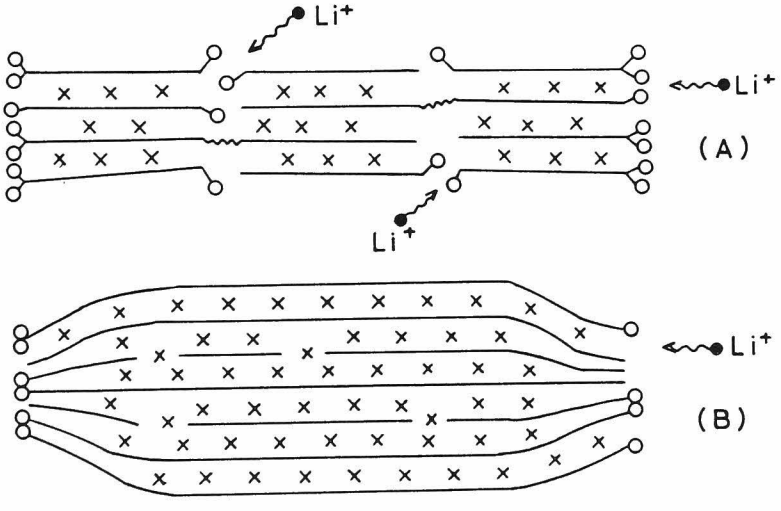

Fig. 4-3 Illustrations for GIC having C-F covalent bond around the surface and GIC prepared under 200°C.
(A) GIC prepared at a retention temperature between 268 and 350°C.
(B) GIC prepared under 200°C.
○: Fluorine atom ×: Intercalant
●: Li^+ ion 二: Graphite layer

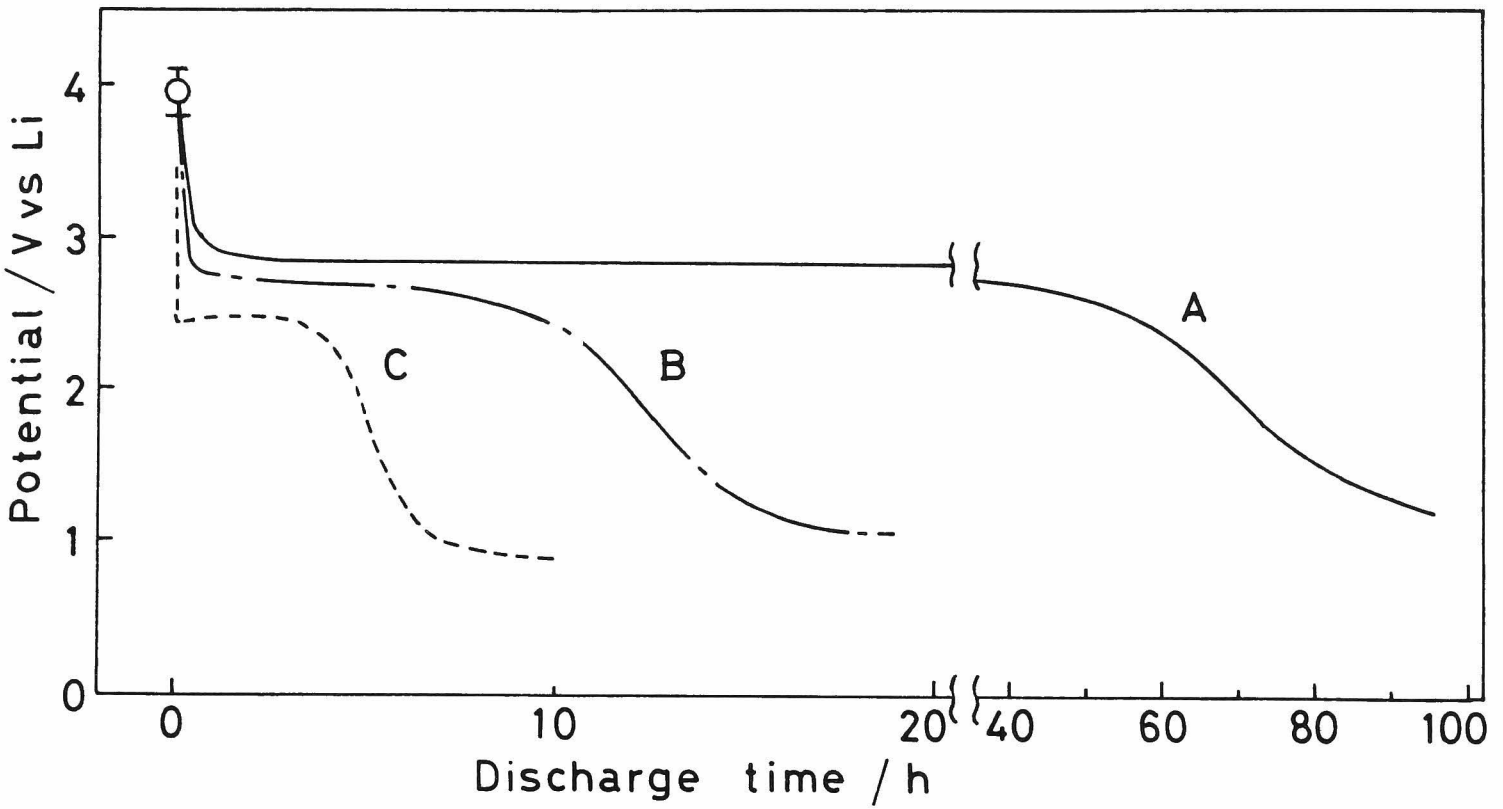

Fig. 4-4 Galvanostatic discharge curves for $C_{7.2}F(AlF_3)_{0.002}$ as cathode material.
A: 40 μA/cm^2 (54.3 mg)
B: 200 μA/cm^2 (54.3 mg)
C: 400 μA/cm^2 (54.3 mg)

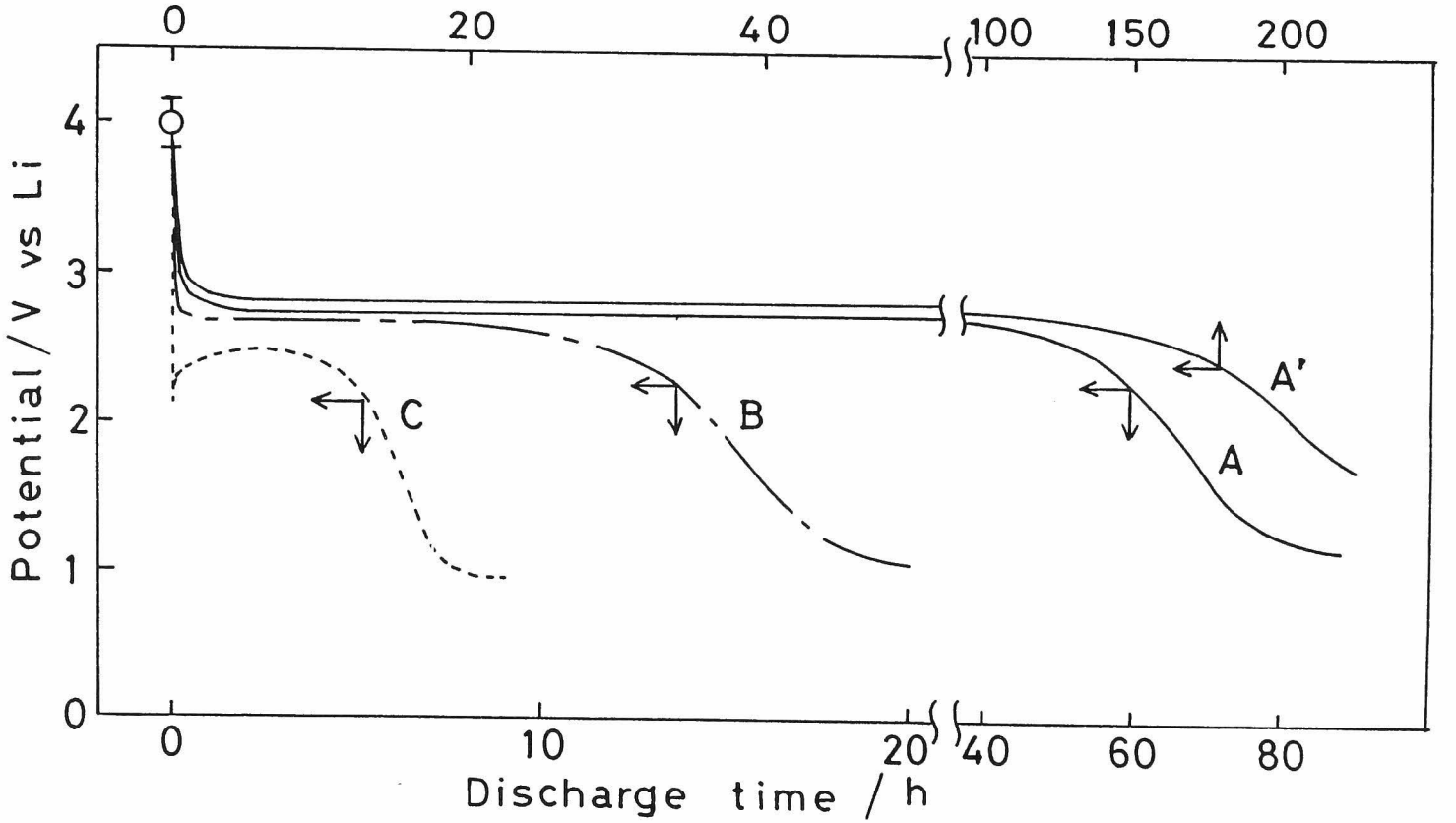

Fig. 4-5 Galvanostatic discharge curves for $C_xF(MgF_2)_y$ as cathode materials.
A: $C_{7.3}F(MgF_2)_{0.002}$ (46.5 mg) 40 μA/cm^2
B: $C_{7.3}F(MgF_2)_{0.002}$ (45.0 mg) 160 μA/cm^2
C: $C_{7.3}F(MgF_2)_{0.002}$ (47.6 mg) 400 μA/cm^2
A': $C_{3.0}F(MgF_2)_{0.001}$ (51.9 mg) 40 μA/cm^2

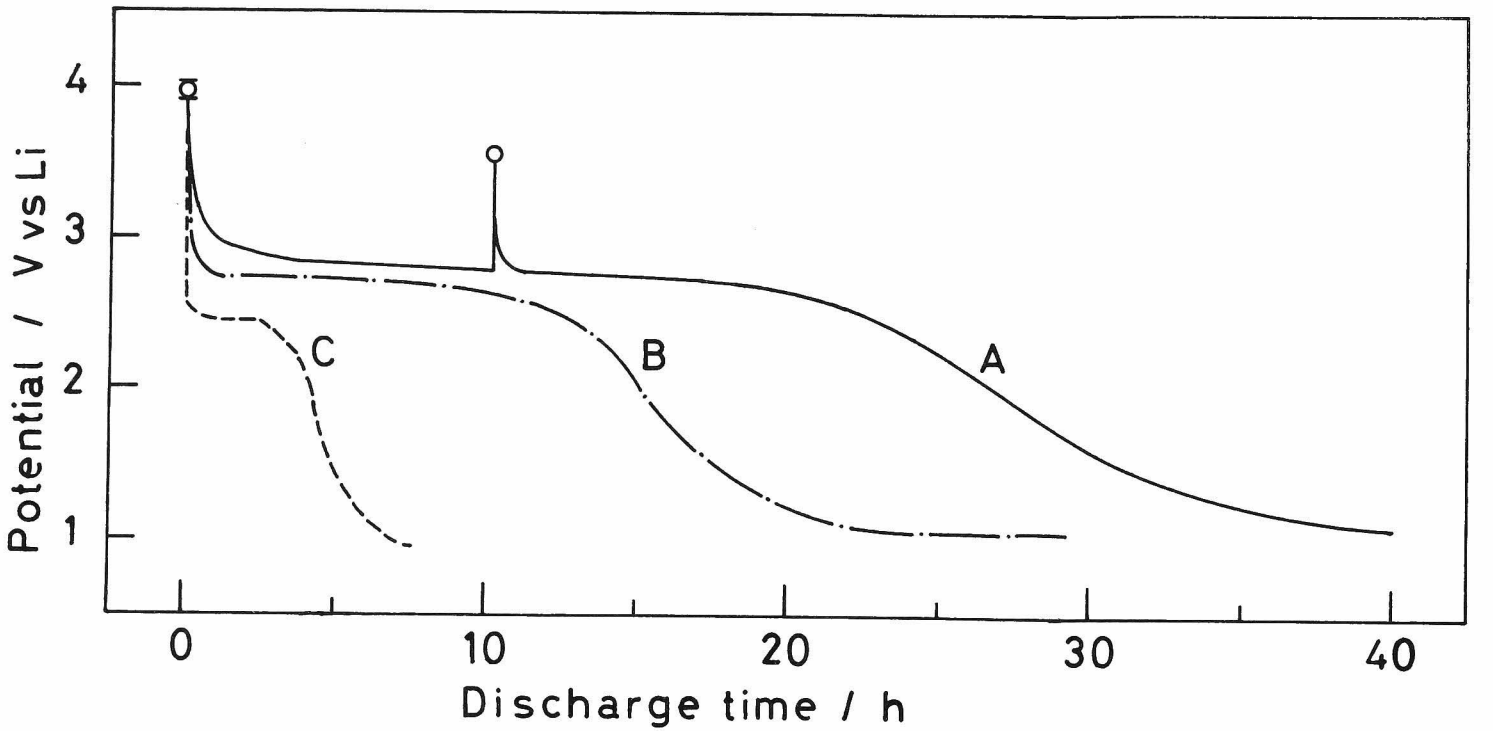

Fig. 4-6 Galvanostatic discharge curves for $C_{7.9}F(CuF_2)_{0.0001}$ as cathode material.
A: 100 $\mu A/cm^2$ (59.1 mg)
B: 200 $\mu A/cm^2$ (64.4 mg)
C: 400 $\mu A/cm^2$ (51.6 mg)

current densities, 100, 200 and 400 $\mu A/cm^2$, respectively.

The discharge potentials of GIC's and graphite fluorides are shown in Figure 4-7 as a function of the logarithm of current density.*** $(C_2F)_n$ gives by 0.2-0.3 V higher discharge potential than $(CF)_n$ at a current density in the range of 1-1000 $\mu A/cm^2$. GIC shows more higher discharge potential than graphite fluorides at a current density below 300 $\mu A/cm^2$. This would be due to more active fluorine contained in GIC than that of graphite fluoride. However, at a current density over 300 $\mu A/cm^2$, its overpotential increased rapidly and the discharge potential deviated from the linear relationship between discharge potential and logarithm of a current density.

Table 4-2 shows the discharge potentials, utilities and energy densities of GIC's at several current densities. The energy densities were proportional to the fluorine contents of GIC's as cathodes. The higher the utility and discharge potential were, the larger the energy density was.

The cathode overpotential is controlled by two factors: one is a diffusion rate of Li^+ ion in the diffusion layer formed in GIC, and another is a reaction rate for fluorine of GIC to accept

---

*** Since graphite fluoride has no electrical conductivity, acetylene black and polyethylene were added to graphite fluoride in the ratio of 1:1:1 as a conductive additive and binder, respectively. Hence, when the comparison of the current density-potential curves is made between the GIC and graphite fluoride, it is necessary to correct the electrode area of graphite fluoride. The surface area fraction of graphite fluoride in the molded electrode is calculated to be 0.2 by using the specific gravities of graphite fluoride (2.8), acetylene black (2) and polyethylene (1). Imaginary current density-potential curves are obtained by dividing the electrode area by 0.2 and are shown in Figure 4-7 with dotted line. Since a conductive additive and binder have to be mixed with graphite fluoride when it is used as a cathode material, measured I-V curves will be situated under the dotted lines in any case.

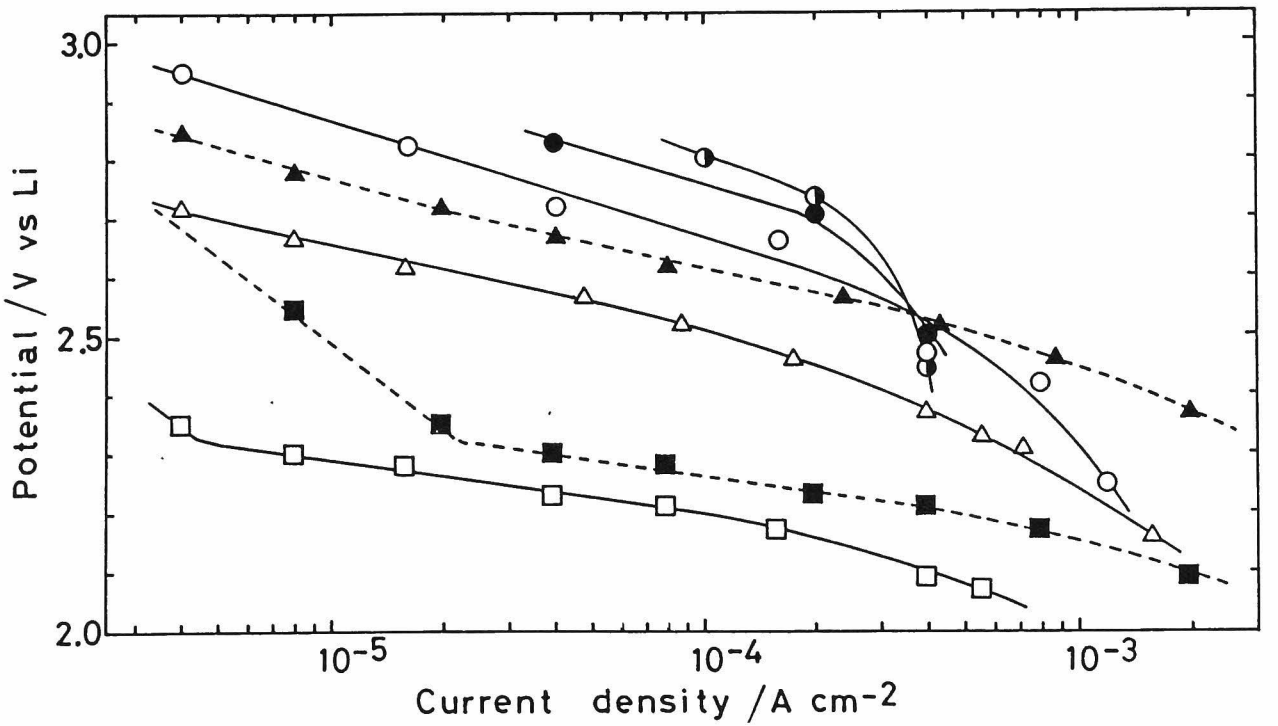

Fig. 4-7 Galvanostatic polarization curves of graphite intercalation compounds and graphite fluorides.

○: $C_{7.3}F(MgF_2)_{0.002}$

◑: $C_{7.9}F(CuF_2)_{0.0001}$ ●: $C_{7.2}F(AlF_3)_{0.002}$

△: $(C_2F)_n$ (experimentally obtained)[8)]

▲: $(C_2F)_n$ (corrected)***

□: $(CF)_n$ (experimentally obtained)[8)]

■: $(CF)_n$ (corrected)***

Table 4-2 Discharge characteristics of GIC's as cathode materials.

Compound	Current density	Discharge potential	Utility	Theoretical capacity	Energy density
	$\mu A/cm^2$	V vs Li	%	Ah/kg	Wh/kg
$C_{7.2}F(AlF_3)_{0.002}$	40	2.83	69	250	360
	200	2.70	57		300
	400	2.50	45		220
$C_{4.4}F(MgF_2)_{0.002}$	40	2.85	97	370	850
	200	2.75	82		720
	400	2.10	71		570
$C_{7.3}F(MgF_2)_{0.002}$	40	2.72	72	250	420
	160	2.66	65		380
	400	2.47	59		320
$C_{5.5}F(MgF_2)_{0.001}$	200	2.61	65	310	480
	400	2.57	63		450
$C_{3.0}F(MgF_2)_{0.001}$	40	2.80	100	470	1100
	200	2.56	100		850
	400	2.50	100		810
$C_{8.1}F(MgF_2)_{0.002}$	200	—	16	230	—
$C_{7.9}F(CuF_2)_{0.0001}$	100	2.80	66	230	360
	200	2.73	66		360
	400	2.44	50		250

an electron. The cathode overpotential would be decided mainly by the diffusion rate of Li^+ ion in the diffusion layer because of the long recovery time of OCV as is shown in Figure 4-2. As shown in the next section, the diffusion layer would consist of an new GIC, $C_x(LiF)(MF_n)_y$. The diffusion rate of Li^+ ion is closely related with the decomposition rate of the diffusion layer to graphite, LiF and MF_n. If the intermediate compound, $C_x(LiF)(MF_n)_y$ which is responsible for the cathode potential, is stable, in other words, if its decomposition is slow, the cathode overpotential would increase. It is likely that the stability of discharge products depends on their crystallite size, which is estimated from the half width of the highest line in X-ray diffraction pattern. For example, graphite fluorides, $(CF)_n$ and $(C_2F)_n$ have much smaller crystallites than original graphite. Their average half widths of (001) diffraction lines were very broad, ca. 2° in 2θ for $(CF)_n$ and 3° for $(C_2F)_n$ (by Cu-Kα). The (002) diffraction lines of graphite were observed in the discharge products of graphite fluorides, being ca. 6° in 2θ. However, the half widths of the highest diffraction lines of GIC's used as cathode materials were very sharp (0.5-0.7° in 2θ). And a new GIC was observed by X-ray diffractometry for the discharge products of GIC's (Figure 4-8). Their half widths were in the range of 1.1-1.3° in 2θ, much smaller than those for graphite fluorides. These results showed that the discharge products with large crystallites were more stable than those with small ones. From this point of view, the difference in the discharge characteristics and utilities of graphite fluorides and GIC's can be discussed. At a current density under 200 $\mu A/cm^2$, the discharge potentials of $C_{4.4}F(MgF_2)_{0.002}$ and $C_{7.9}F(CuF_2)_{0.0001}$ cathodes were higher than the corrected value*** of $(C_2F)_n$ by about 0.2 V which corresponds to the difference between OCV's of GIC and

$(C_2F)_n$ cathodes. It is considered that the diffusion layer of GIC cathode was as thick as that of $(C_2F)_n$ cathode at such a low current density. With increasing current density, the formation rate of the diffusion layer increases both in GIC and graphite fluoride cathodes. However, the decomposition rate would be faster in graphite fluoride than in GIC because of the smaller crystallites of graphite fluoride and its discharge product. As a result, the thickness of diffusion layer and the overpotential would increase in GIC cathode much more than in graphite fluoride cathode. The utility of fluorines in GIC was lower than that for graphite fluoride even on the discharge at a low current density. The discharge was done at a constant current using galvanostat. However, it is expected that the true current density increases near the end of the discharge due to the decrease in the electrode surface. Because of this effect, the discharge potential of GIC would decrease to ca. 1 V vs Li with undischarged fluorines in the cathode. This tendency would be more distinctive with increasing current density. In fact, the utilities of fluorines in GIC decreased with an increase in the current density.

3.3 Discharge Reaction

Figure 4-8 shows a typical X-ray diffraction pattern of a discharge product. The diffraction line with the highest intensity is situated at 27.40° in 2θ, being different from (003) diffraction line for the original GIC, $C_xF(MF_n)_y$ or (002) line of natural graphite, which suggests the formation of a new GIC, $C_x(LiF)(MF_n)_y$ (M: Al, Mg or Cu, n: 3 or 2). The weak lines at 39° and 45° in 2θ are attributed to LiF, suggesting the partial decomposition of the new GIC produced by discharge. The intensities of these lines for LiF became much stronger after evacuation at room temperature. Furthermore, when the discharge product was heated to 800°C under vacuum, host graphite was considerably exfoliated

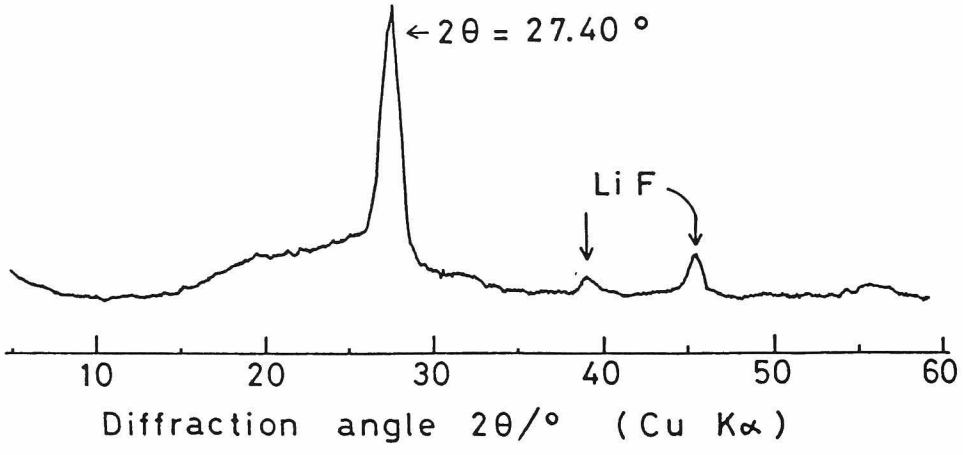

Fig. 4-8 X-ray diffraction pattern for discharge product.

in the direction of c-axis and the residual substance showed a diffraction pattern of graphite with high crystallinity (half width: 0.45° in 2θ for (002) diffraction line) probably because of a complete decomposition of the GIC, $C_x(LiF)(MF_n)_y$ formed by the discharge. Though such a GIC was proposed as the discharge product in graphite fluoride-lithium battery based on the thermodynamic calculation[8] and ESCA measurement,[9] only amorphous carbon was observed by means of X-ray diffractometry because of the higher decomposition rate of the discharge product for graphite fluoride cathode than that for the GIC, $C_xF(MF_n)_y$ cathode.

Figure 4-9 is the ESCA spectra of a discharge product after washing with PC and drying under vacuum. F_{1s} peak for the discharge product lies between those for LiF and the GIC used as a cathode material. It seems that the fluorine in the discharge product had a nearly ionic interaction with Li^+ ion inserted into graphite layers, retaining the interaction also with carbon atom. C_{1s} spectrum for the original cathode material had two strong peaks at 289 eV corresponding to C-F covalent bond and 284 eV for

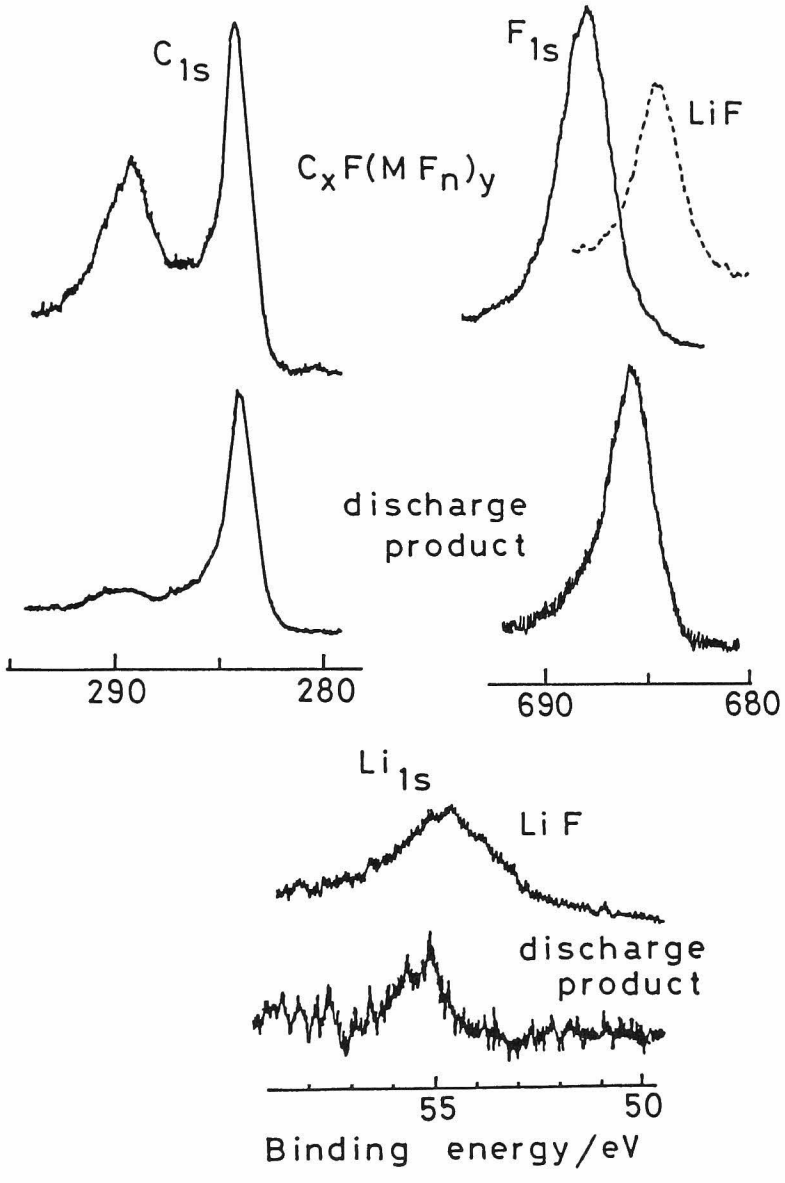

Fig. 4-9 ESCA spectra for $C_xF(MF_n)_y$ and its discharge product.

C-C covalent bond, however, that for the discharge product showed a strong peak at 284 eV and a broad shoulder in the range of 288-291 eV. It is also shown from C_{1s} spectra that the discharge product did not have so strong interaction as C-F covalent bond between intercalant and carbon layer, which coincides with the result of F_{1s} spectra. Li_{1s} spectrum is very weak and almost the same position as that for LiF. From these results, it is considered that the discharge reaction progressed with forming the following GIC:

$$\text{Anode reaction:} \quad Li \longrightarrow Li^+ + e^-$$

$$\text{Cathode reaction:} \quad C_xF(MF_n)_y + e^- \longrightarrow C_x(MF_n)_yF^-$$

$$\text{Cell reaction:} \quad C_xF(MF_n)_y + Li \longrightarrow C_x(LiF)(MF_n)_y$$

where M is Al, Mg or Cu and n is 3 or 2.

The electromotive force of lithium-fluorine cell is 6.1 V from the free energy change of formation for LiF at 30°C. The initial OCV observed in this work was 4.2-3.4 V being lower by 1.9-2.7 V than the theoretical value. Two kinds of contribution are considered regarding the decrease in the free energy. One is the free energy change of formation for GIC, $C_xF(MF_n)_y$ (ΔG_I in Figure 4-10) from graphite, fluorine and metal fluoride, and another is the free energy change of formation for a new GIC, as a discharge product, which decomposes subsequently to graphite, LiF and MF_n.

4. Summary

(1) GIC's used as cathode materials had higher OCV's of 3.5-3.6 V vs Li after 20 % discharge than that of $(CF)_n$ or $(C_2F)_n$, which is due to more active fluorine atoms intercalated in graphite layers.

(2) The flat discharge potential was observed only for GIC's

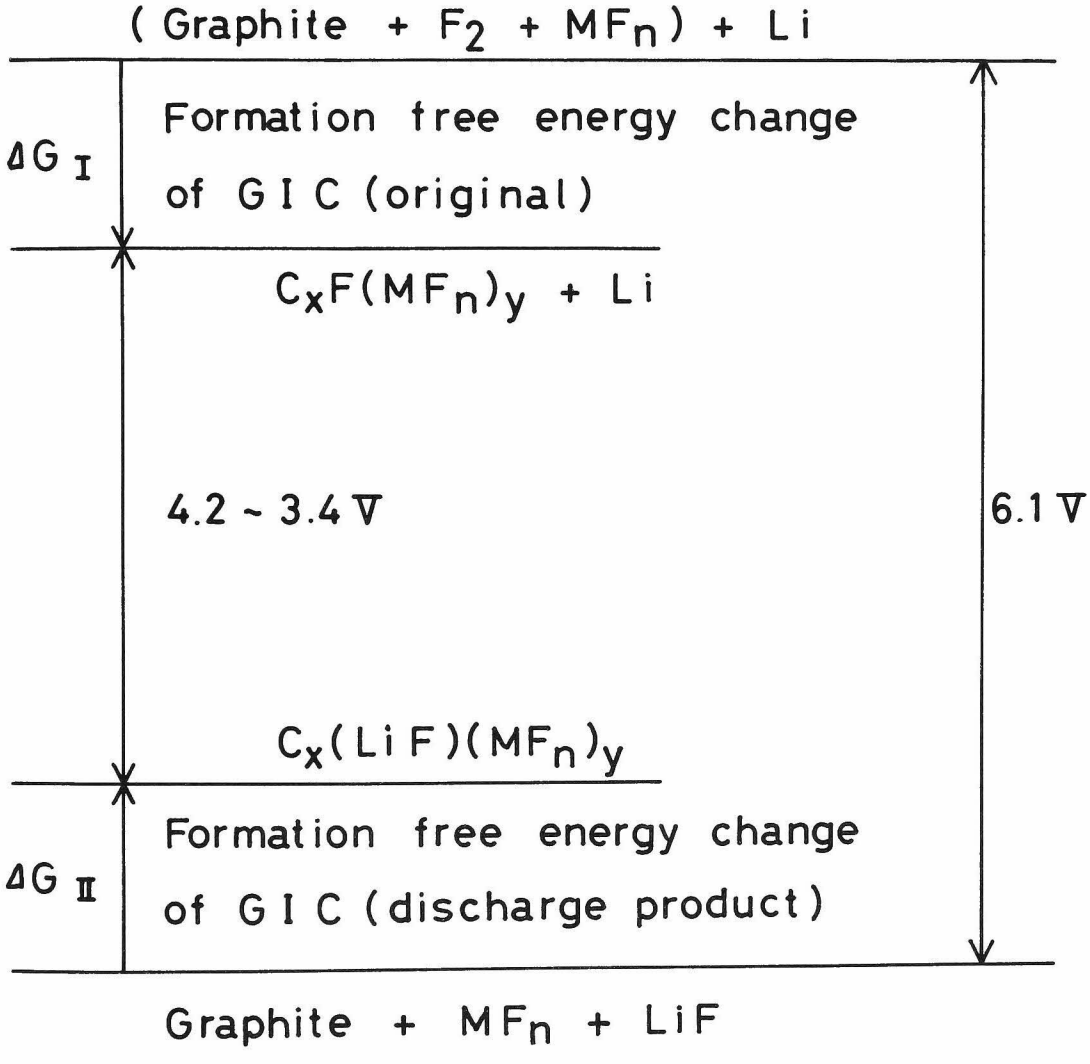

Fig. 4-10 Free energy change in $C_xF(MF_n)_y$-Li cell.

treated in fluorine gas at a retention temperature between 268 and 350°C. Such a GIC showed a higher discharge potential than $(CF)_n$ or $(C_2F)_n$ at a current density lower than 300 $\mu A/cm^2$. The overpotential increased with increase in current density probably because a thickness of a diffusion layer consisting of $C_x(LiF)(MF_n)_y$ increased.

(3) X-ray diffraction analysis and ESCA measurement indicated that the discharge reaction proceeded as follows,

$$C_xF(MF_n)_y + Li \longrightarrow C_x(LiF)(MF_n)_y$$

where M is Al, Mg or Cu and n is 3 or 2.

References

1) N.Watanabe and M.Fukuda, U. S. Pat., 3,536,532 (1970); N.Watanabe and M.Fukuda, ibid., 3,700,502 (1972).
2) M.Fukuda and T.Iijima, Prog. Batt. Solar Cells, 1, 26 (1978).
3) J.Watanabe, H.Ogawa and R.Okazaki, ibid., 1, 39 (1978).
4) J.Watanabe, E.Kawakubo, T.Shinagawa and Y.Kajikawa, ibid., 3, 74 (1980).
5) Y.Kita, N.Watanabe and Y.Fujii, J. Am. Chem. Soc., 101, 3832 (1979).
6) N.Watanabe and K.Morigaki, Denki Kagaku, 47, 169, 174 (1979).
7) M.Armand and P.Touzain, Mat. Sci. Eng., 31, 119 (1977).
8) N.Watanabe, R.Hagiwara, N.Kumagai, T.Sakai and T.Nakajima, Denki Kagaku, 51, 183 (1983).
9) M.S.Whittingham, J. Electrochem. Soc., 122, 526 (1975).
10) N.Watanabe, Solid State Ionics, 1, 87 (1980).

Chapter 5

APPLICATION TO THE SYNTHESIS OF $(C_2F)_n$*

1. Introduction

There are two kinds of graphite fluorides, poly(carbon monofluoride), $(CF)_n$ and poly(dicarbon monofluoride), $(C_2F)_n$.[1] When natural graphite is used as a starting material, $(CF)_n$ is prepared at about 600°C and $(C_2F)_n$ at 350-400°C. At a temperature between 400 and 600°C, a mixture of both compounds is formed.

Natural graphite + F_2 —
- ca. 600°C → $(CF)_n$
- 400-600°C → A mixture of $(CF)_n$ and $(C_2F)_n$
- 350-400°C → $(C_2F)_n$

As described in General Introduction and Chapter 4, $(CF)_n$ is now commercially available and is used as a cathode material of lithium battery and as a solid lubricant. $(C_2F)_n$ also has high possibilities as a new active mass for lithium battery because it shows a higher discharge potential than $(CF)_n$,[2] however, compared with $(CF)_n$, it takes a significantly longer time to prepare $(C_2F)_n$ due to the low formation temperature. In order to facilitate the reaction rate of carbon with fluorine, exfoliated graphite[3] was employed as a starting material; the results indicated that $(C_2F)_n$ was prepared at lower temperatures, 335-374°C, with a higher reaction rate than in the case of flaky natural graphite.[4] It was described in Chapter 1 that metal fluorides, such as AlF_3 and MgF_2, with a high sublimation or boiling point were intercalated into graphite layers with large amount of fluorine. It is reported in this chapter that $(C_2F)_n$ is formed through the decomposition and subsequent fluorination of these

---

* Bull. Chem. Soc. Jpn., 56, 455 (1983)

GIC's in more higher reaction rate.

2. Experimental

2.1 Preparation of $(C_2F)_n$ from Graphite-F_2-AlF_3 System

The starting materials are Madagascar natural graphite [279-149 μm (50-100 mesh), purity: 99.4 %], petroleum coke heat-treated at 2800°C (graphitized PC), commercial aluminum fluoride (purity: >98 %), and high-purity fluorine gas (purity: 99.7 %). The fluorination reaction was carried out using an automatic thermobalance, as shown in Chapter 2. Aluminum fluoride (50 mg) and graphite (50 mg) were placed in a nickel vessel hung by a nickel spring. After fluorine gas had been introduced into the nickel reaction vessel, the reaction system was kept at room temperature for 1 or 2 h; the temperature was then increased to 357-393°C at a rate of 16°C/min, followed by a reaction at that temperature until no weight increase was observed. The graphite fluoride thus prepared was analyzed by means of X-ray diffractometry and elemental analysis. The reaction was stopped prior to the complete fluorination of graphite, and the reaction rate was compared with that in the fluorination of exfoliated graphite by analysing the intermediate products.

2.2 Preparation of $(C_2F)_n$ from Graphite-F_2-MgF_2 System

The starting materials are Madagascar natural graphite [purity: 99.4 %, 833-295 μm (20-48 mesh), 74-61 μm (200-250 mesh), 41-37 μm (350-400 mesh)], petroleum coke heat-treated at 2800°C (graphitized PC) commercial MgF_2 (purity: >98 %) and fluorine gas. MgF_2 (ca. 0.2 g) and graphite (ca. 0.2 g) were placed in a nickel reaction tube and the system was evacuated by a rotary pump at 100-200°C for 12 h. After fluorine gas of 1.0×10^5 Pa had been introduced into the system at room temperature, the reaction system was kept

at room temperature for 5 h. The temperature was then increased to 350-400°C at a rate of ca. 4°C/min, followed by a reaction at that temperature for 12-48 h. The graphite fluoride prepared was analysed by means of elemental analysis, X-ray diffractometry and ESCA.

3. Results and Discussion

3.1 Formation Process of $(C_2F)_n$ via GIC

A typical thermogravimetric curve is shown in Figure 5-1. Almost no weight change was detected in the AlF_3-F_2 system at temperatures between room temperature and 400°C, however, in the ternary system of natural graphite, AlF_3, and F_2, a weight increase due to the formation of a GIC was observed at room temperature. The increase in temperature to 350-400°C caused the de-

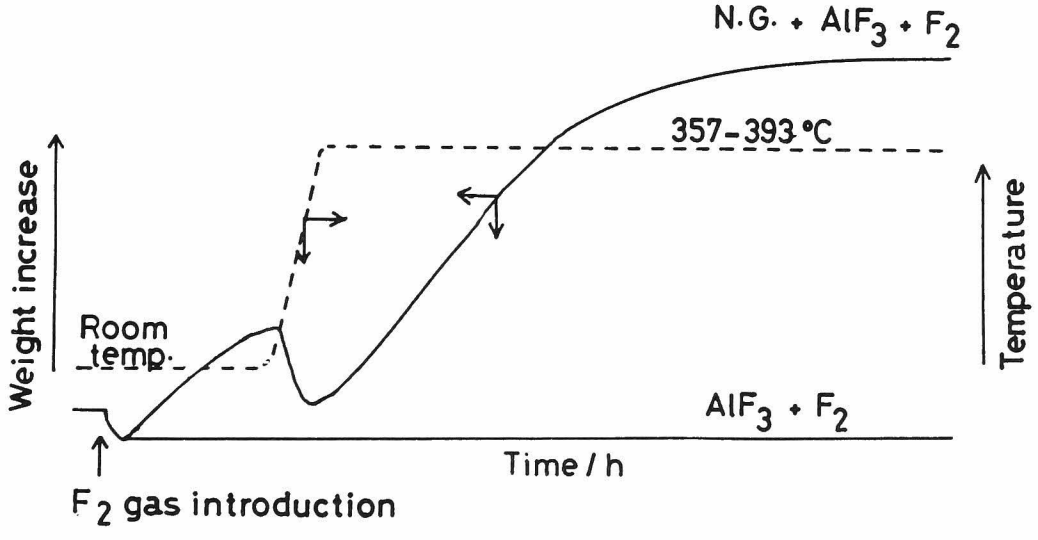

Fig. 5-1 Thermogravimetry for the reactions of AlF_3 with F_2 and of natural graphite (N.G.) + AlF_3 with F_2.

composition of the GIC with an accompanying weight decrease, when natural graphite was expanded along the c-axis by release of the intercalant. A large weight increase was observed due to the subsequent fluorination of exfoliated graphite at temperatures between 350 and 400°C:

$$\text{Graphite} + AlF_3 + F_2 \xrightarrow[\text{Room temperature}]{} C_xF(AlF_3)_y \longrightarrow \xrightarrow[350\text{-}400°C]{F_2} \text{Formation of exfoliated graphite} \xrightarrow[350\text{-}400°C]{F_2} \longrightarrow \text{Graphite fluoride}$$

Figure 5-2 shows X-ray diffraction patterns of GIC, exfoliated graphite formed by decomposition of GIC in fluorine atmosphere and $(C_2F)_n$ prepared by this method. Graphite fluoride, $(C_2F)_n$ prepared has the same appearance in shape as exfoliated graphite (Figure 5-3). "Exfoliated graphite" is generally prepared by the thermal decomposition of the residual compound of GIC prepared from flaky natural graphite and mixture of HNO_3 and H_2SO_4. Graphite is expanded largely in the direction of the c-axis when the thermal decomposition occurs because the intercalant is released rapidly from graphite layers or grain boundary during heating. Exfoliated graphite therefore has a larger surface area and volume than flaky natural graphite. Similar to this mechanism, the GIC, $C_xF(MF_n)_y$, prepared from natural graphite began to decompose with increasing temperature and host graphite was exfoliated under 300°C in fluorine atmosphere. As a result, the carbon-carbon bonds connecting crystallites of host graphite together would be cut in various places. Such division of crystallite particles would increase a surface area having significant role for initial intercalation of fluorine. Each crystallite would be further divided by subsequent fluorination. Figure 5-4 shows a microphotograph of $(C_2F)_n$ thus prepared. It was detected by ESCA measurement that the GIC contained a small amount of fluorine even after

heating to 600°C in nitrogen atmosphere. The intercalated fluorine was not therefore completely released from graphite layers during heating, contributing to the subsequent fluorination reaction. It took more than 100 h to finish the fluorination of the flaky natural graphite (833-295 μm) by direct fluorination in fluorine atmosphere of 1.0×10^5 Pa (1 atm) at 400°C. However, it took less than 10 h by the present method under the same condition.

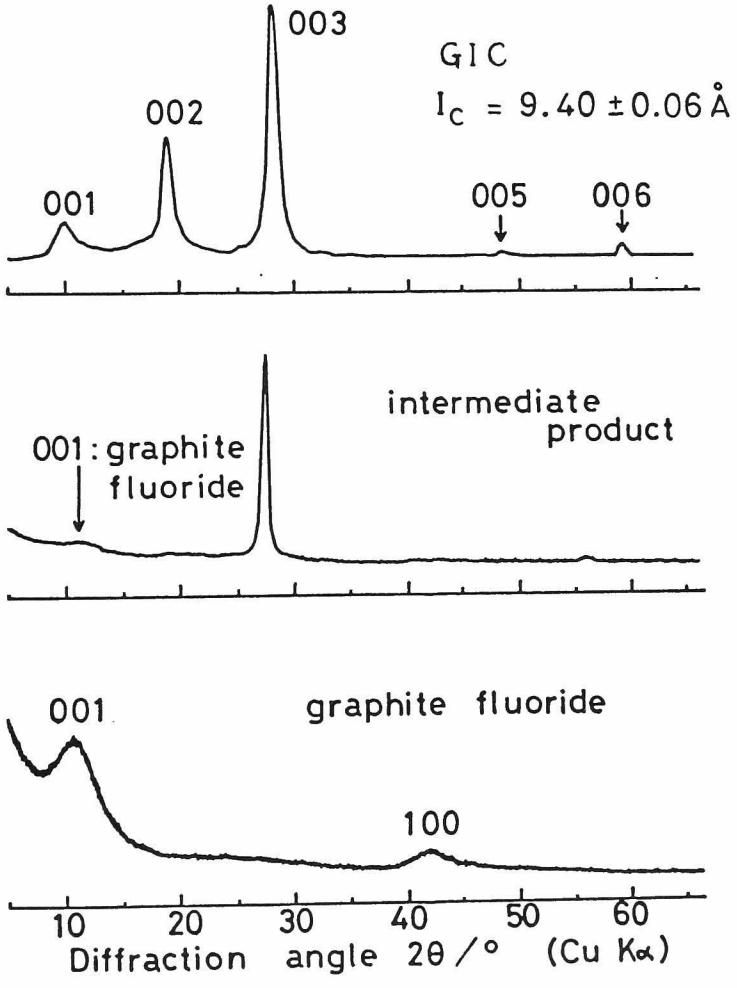

Fig. 5-2 Change in X-ray diffraction patterns of the products.

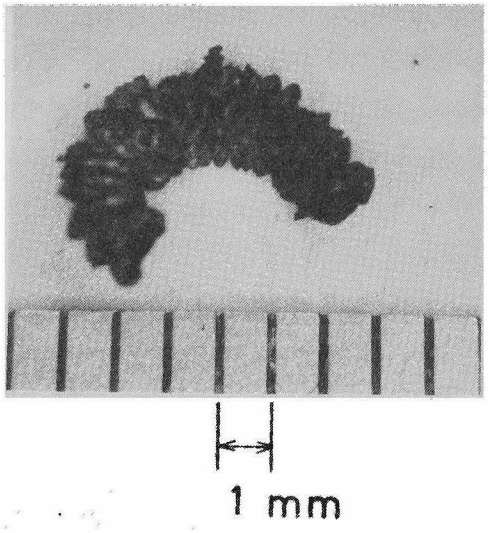

Fig. 5-3 Exfoliated graphite fluoride.

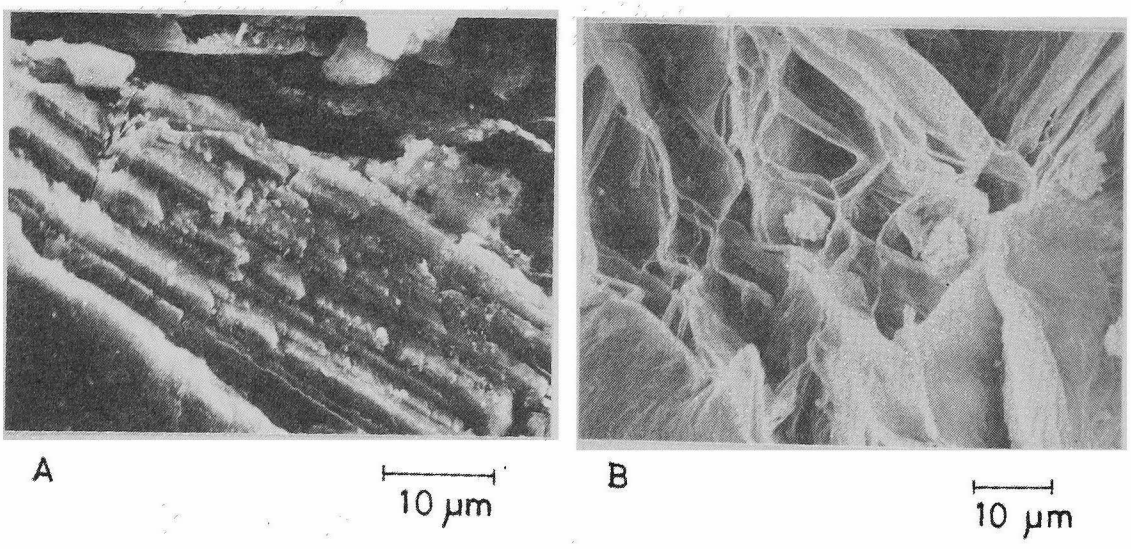

Fig. 5-4 Scanning electron micrographs of flaky natural graphite (A) and exfoliated $(C_2F)_n$ prepared via GIC (B).

3.2 Comparison of Reaction Rates between Exfoliated Graphite and Graphite with AlF_3 Systems

In order to compare the reaction rate of exfoliated graphite with that of flaky natural graphite-AlF_3 system, the fluorination was stopped at the initial stages of the reaction and the intermediate products were analysed. The reaction times for graphite with an AlF_3 system were those when the reaction system was above 335°C, while for the reaction of exfoliated graphite, fluorine gas was introduced into the thermobalance maintained at a reaction temperature and the elapsed time after fluorine introduction was adopted as the reaction time. The results of elemental analyses of the products are shown in Table 5-1. The products obtained from graphite with an AlF_3 system contained more fluorines than those from exfoliated graphite, though the complete combustion of the products was difficult in analysis by the conventional oxygen-flask method. Figure 5-5 shows the X-ray diffraction patterns of these products. The small peaks between 10° and 15° in 2θ (by Cu-Kα) are due to graphite fluoride, while the strong ones around 26° are due to the unreacted graphite. Since much

Table 5-1 Composition of intermediate products prepared from natural graphite + AlF_3 and from exfoliated graphite at 357°C

Reaction time	Natural graphite + AlF_3	Exfoliated graphite
h	F/C	F/C
0.3	0.06	0.03
1	0.17	0.05
2	0.15	0.07
4.5	0.40	0.16

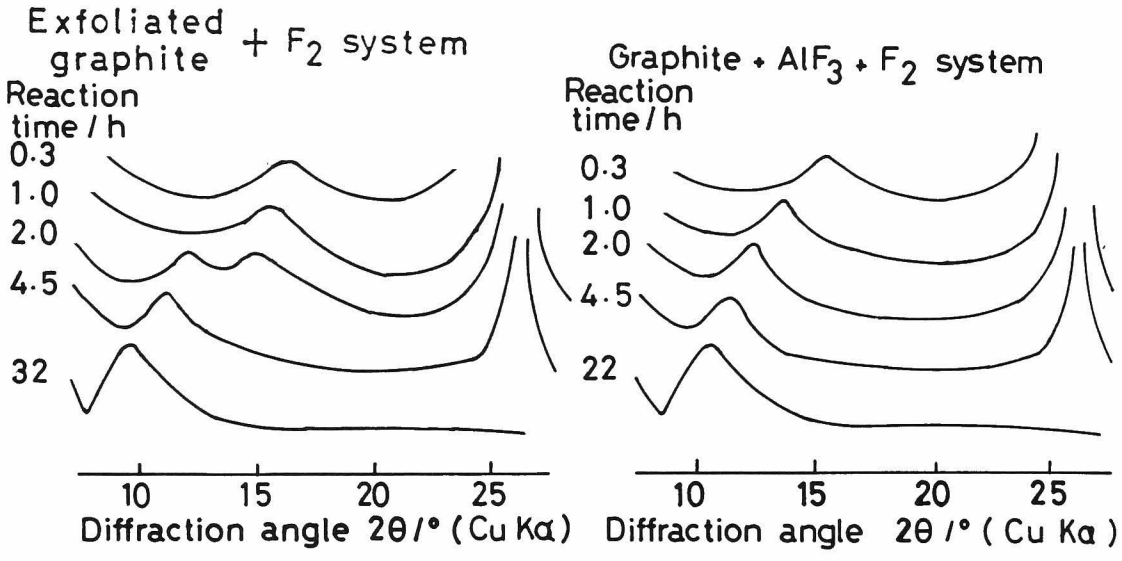

Fig. 5-5 Variation of (001) diffraction patterns of graphite fluoride prepared at 357°C as a function of reaction time.

unreacted graphite remained at the initial stage of the reaction, the intensities of the X-ray diffraction peaks for graphite fluoride was much weaker than those of unreacted graphite, though they gradually increased with the progress in the fluorination reaction. With an increase in the reaction time, the diffraction peak shifted from a higher angle due to $(CF)_n$ to a lower one due to $(C_2F)_n$ for both exfoliated graphite and graphite with AlF_3 systems, which means that $(CF)_n$ is first formed around the surface with disordered structure, followed by the formation of $(C_2F)_n$ in the bulk. The movement of the diffraction peak to a lower angle was faster in graphite with an AlF_3 system than for exfoliated graphite. Table 5-2 gives the analytical data of the products as a function of the reaction time at room temperature and also the reaction temperatures after the temperature-increase to 350-400°C. The time required for completing the reaction was 22 h for graph-

Table 5-2 Reaction time and structural parameters of graphite fluoride prepared from natural graphite + AlF_3 system (F_2: 267×10^2 Pa)

Reaction temperature °C	Reaction time at room temperature h	Reaction time at 357-393°C h	d_{001} Å	β_{001} °	F/C ratio
357	1	49	8.6	3.4	0.55
357	2	22	8.1	3.5	0.69
376	2	16	8.4	3.8	0.64
393	2	9	8.3	3.9	0.71
357**	—	32	8.9	2.9	0.57

** Prepared from exfoliated graphite

ite with an AlF_3 system, while it was 32 h for exfoliated graphite at 357°C. The fluorination of graphite proceeds faster via the GIC than that of exfoliated graphite. Another advantage is that the former process includes the formation of exfoliated graphite and its fluorination.

The amount of F_2 and AlF_3 intercalated into graphite depends on the reaction time at room temperature. When that reaction time is short, only a small amount of F_2 and AlF_3 is intercalated into graphite. As a result, graphite is not fully expanded in the temperature-increase process and it takes a longer time to finish the fluorination of graphite. However, the product contains a larger amount of $(C_2F)_n$ because of the lower expansion of graphite. The reaction time decreased with an increase in the reaction temperature between 357 and 393°C. Compared with graphite fluoride prepared from exfoliated graphite at 357°C, the interlayer spacing, d_{001}, of that prepared from graphite with an AlF_3 system decreased by 0.5-0.8 Å, while the half-width and the F/C ratio increased by 0.6-1° in 2θ (Cu-Kα) and 0.07-0.14 respectively, which means that the latter graphite fluoride contains a larger amount of $(CF)_n$ than the former. These results are attributed to the larger expansion of the graphite formed by the decomposition of the GIC than that of the exfoliated graphite used for comparison; this attribution was confirmed by the analytical data (Table 5-2) of the expanded products.

3.3 Effect of Fluorine Pressure on the Reaction Rate

The time required for completing the reaction did not give a linear relationship, but a minimum point around 267×10^2 Pa against the fluorine pressure. The reaction times were almost the same above 667×10^2 Pa of fluorine, whereas under 133×10^2 Pa it was about twice that under 267×10^2 Pa (Figure 5-6). On the contrary, the F/C ratio of the products had a maximum value

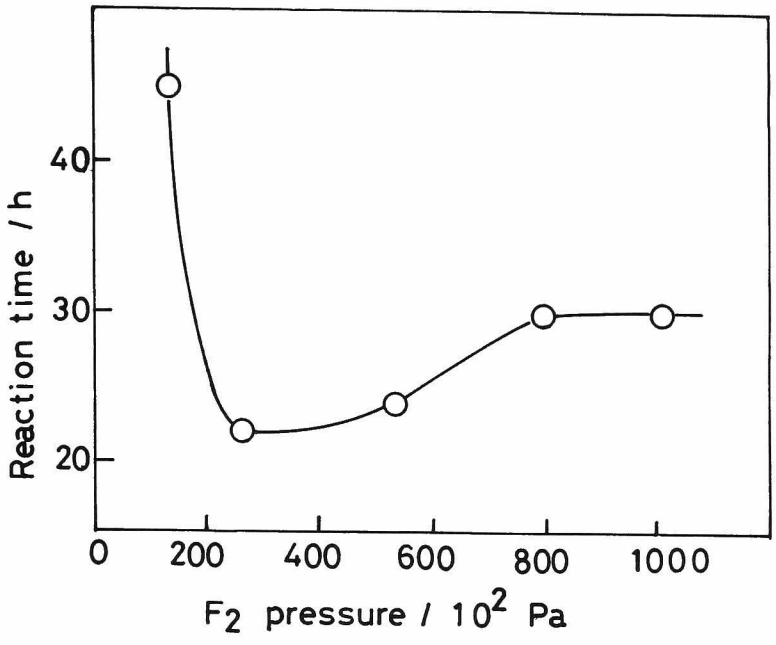

Fig. 5-6 Variation of reaction time of graphite fluoride as a function of F_2 pressure. (Reaction temperature: 357°C)

under 267×10^2 Pa of fluorine (Figure 5-7). It was reported that the $(C_2F)_n$ contained in graphite fluoride can be related to the F/C ratio by representing the amounts of $(C_2F)_n$ and $(CF)_n$ as x and 1 - x respectively: $F/C = 1 - \frac{1}{2}x$.[3] The values calculated by the above equation are as follows: $(C_2F)_n$, 76-78 % (F_2: 800×10^2 - 1013×10^2 Pa); $(C_2F)_n$, 70 % (F_2: 133×10^2, 533×10^2 Pa); $(C_2F)_n$, 62 % (F_2: 267×10^2 Pa). With a decrease in the content of $(C_2F)_n$ in graphite fluoride, the interlayer spacing, d_{001}, decreases, while the half-width, β_{001}, increases much as in graphite fluoride with a low crystallinity (Figure 5-8). These results show that the highest reaction rate observed under 267×10^2 Pa of fluorine is attributable to the rapid decomposition of the GIC, accompanied by the large expansion of graphite. The fluorine uptake by graphite was almost the same at room tempera-

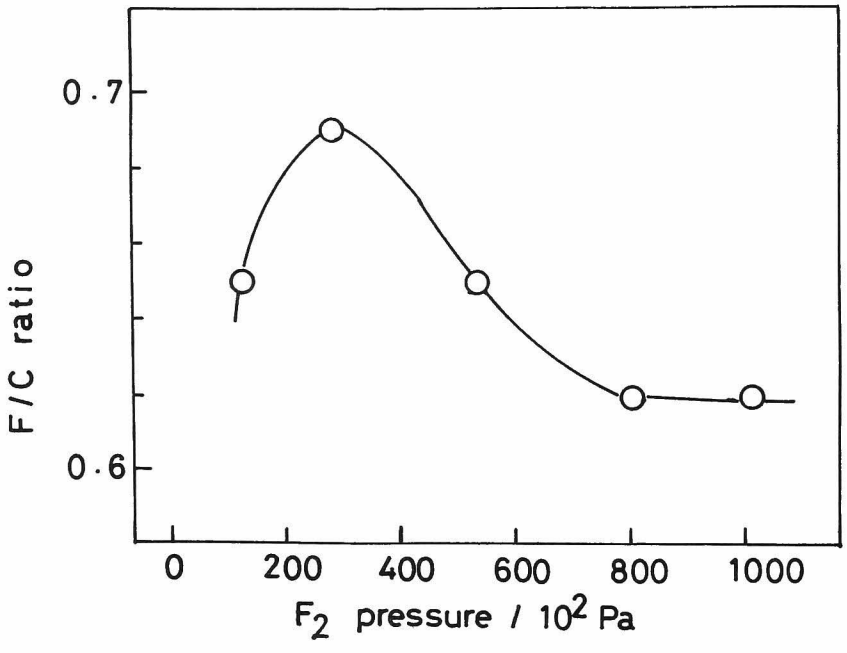

Fig. 5-7 Variation of F/C ratio of graphite fluoride as a function of F_2 pressure. (Reaction temperature: 357°C)

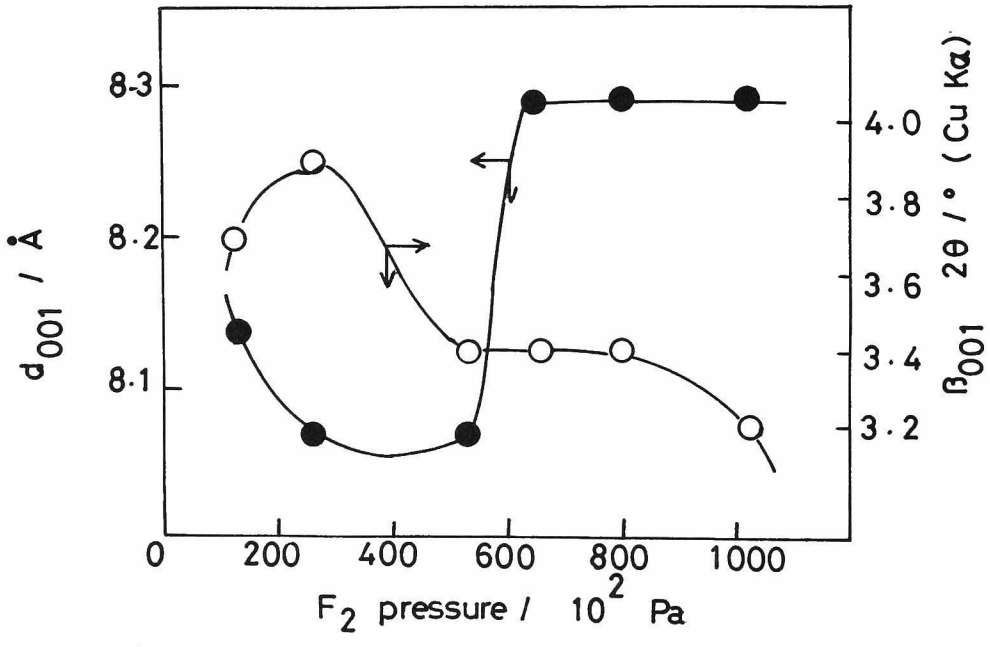

Fig. 5-8 Variation of d_{001} and β_{001} of graphite fluoride as a function of F_2 pressure. (Reaction temperature: 357°C)

ture, even under fluorine pressures of higher than 267×10^2 Pa, however, in the same range of fluorine pressure, a smaller expansion of graphite was observed, probably because the release of fluorine by the decomposition of the GIC was restrained by the higher atmospheric pressure in the temperature-increase process. As a result, the reaction rate of graphite with fluorine is slower under fluorine pressures above 267×10^2 Pa. On the other hand, under a fluorine pressure of 133×10^2 Pa, the amount of fluorine absorbed by graphite at room temperature was much smaller than in other cases and the graphite was not largely expanded on the temperature-increase, which would lead to a slow reaction rate under a low fluorine pressure.

3.4 Preparation of $(C_2F)_n$ from Graphitized Petroleum Coke

Table 5-3 shows the data for graphite fluoride prepared from graphitized PC. As in the case of natural graphite, the reaction time decreased in the presence of AlF_3. The addition of MgF_2 also gave a similar result. The F/C ratios and half-widths of the (001) diffraction lines were slightly larger than those for

Table 5-3 Preparation of $(C_2F)_n$ from graphitized PC

Reaction system	Reaction temperature °C	Reaction time h	F/C ratio	d_{001} Å	β_{001} °
PC + AlF_3	385	7	0.71	7.6	4.4
PC + MgF_2	383	9	0.73	8.1	4.4
PC	380	33	0.71	8.7	4.3
PC	380	13	0.67	8.6	4.3

(F_2 pressure: 1013×10^2 Pa)

graphite fluorides prepared by the direct fluorination of graphitized PC whereas the interlayer spacing, d_{001}, had an opposite relation.

As is shown in Figure 5-7, graphite fluoride prepared under a fluorine pressure of 267×10^2 Pa contained the maximum amount of $(CF)_n$ in the case of natural graphite. A comparison of this graphite fluoride with that prepared from graphitized PC in the presence of AlF_3 or MgF_2 reveals that $(C_2F)_n$ is preferentially formed from natural graphite with large crystallites. The $(C_2F)_n$ content is estimated to be 54-58 % for graphitized PC with an AlF_3 or MgF_2 system and 59-66 % for a graphitized PC system.

3.5 $(C_2F)_n$ Content and Chemical Bond in the Graphite Fluoride Prepared from MgF_2 System

Graphite fluoride prepared by the present method was a mixture of $(C_2F)_n$ and $(CF)_n$. It is known that the interlayer spacing, d_{001} of $(C_2F)_n$ is ca. 9 Å** and that of $(CF)_n$ is ca. 6 Å.** When graphite fluoride contains some amount of $(CF)_n$ with $(C_2F)_n$, the diffraction line appears at a higher position than that for $(C_2F)_n$ because the strong peak for $(C_2F)_n$ is overlapped with a small one for $(CF)_n$. The interlayer spacing, d_{001} of graphite fluoride prepared by the present method decreased and the half width, β_{001} increased with increasing reaction temperature, which means that the graphite fluoride contained larger amount of $(CF)_n$ in the same way as described above with increasing the reaction temperature (Figures 5-9 and 5-10). Figures 5-9 and 5-10 also indicate that $(CF)_n$ content in graphite fluoride tends to increase with decreasing particle size of starting graphite material. These results mean that the reaction rate increases with increase in the reaction temperature and the surface area. Figure 5-11

** These values were obtained from the (001) diffraction line without correction of Lolenz-polarization factor.

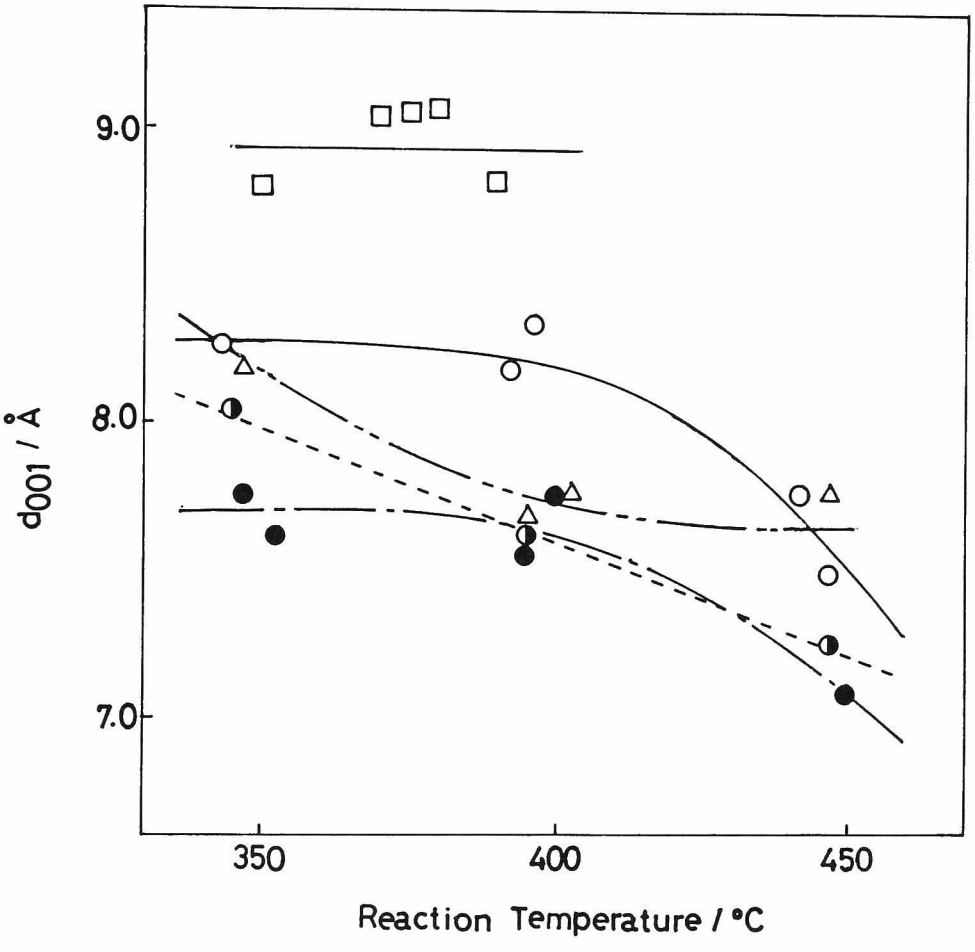

Fig. 5-9 Variation of d_{001} of graphite fluoride prepared via GIC as a function of reaction temperature.
—○—prepared from natural graphite, 833-295 μm
---◐--from natural graphite, 74-61 μm
-—●-from natural graphite, 41-37 μm
---△--from graphitized PC
—□—from natural graphite (74-61 μm) by the conventional method

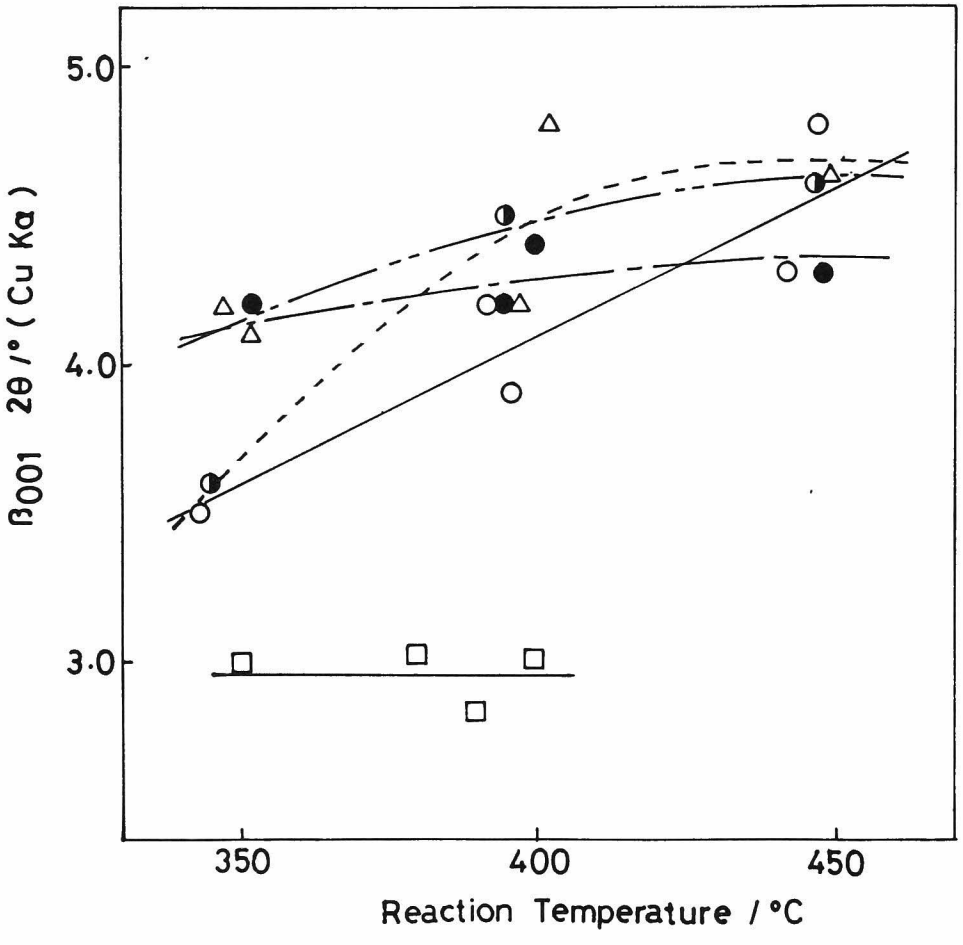

Fig. 5-10 Variation of β_{001} of graphite fluoride prepared via GIC as a function of reaction temperature.
—○— prepared from natural graphite, 833-295 μm
---◐--- from natural graphite, 74-61 μm
-●- from natural graphite, 41-37 μm
--△-- from graphitized PC
—□— from natural graphite (74-61 μm) by the conventional method

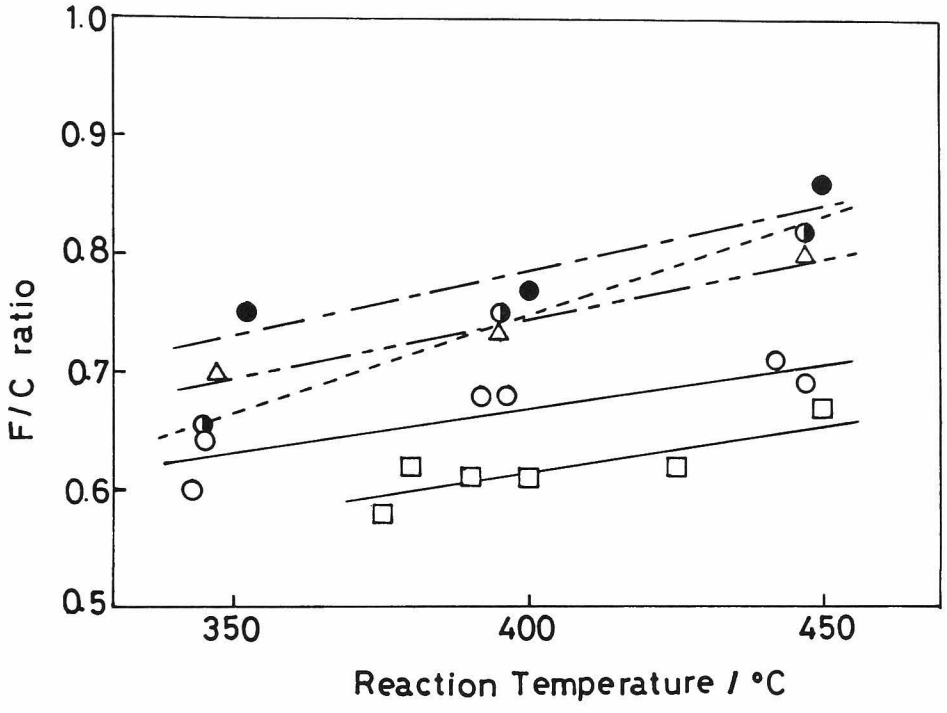

Fig. 5-11 Variation of F/C ratio of graphite fluoride prepared via GIC as a function of reaction temperature.
—○— prepared from natural graphite, 833-295 μm
--◑-- from natural graphite, 74-61 μm
·—●— from natural graphite, 41-37 μm
--△-- from graphitized PC
—□— from natural graphite (74-61 μm) by the conventional method

shows the variation of F/C ratio as a function of reaction temperature. The F/C ratio is inversely proportional to $(C_2F)_n$ content in graphite fluoride, namely decreasing with increase in the $(C_2F)_n$ content. It was found together with the results in Figures 5-9 and 5-10 that $(C_2F)_n$ content decreased with increasing reaction temperature.

Table 5-4 indicates the C_{1s} peak positions in ESCA spectra of graphite fluoride prepared by the present method in comparison with that prepared by the conventional method. In case of natural graphite, the peak position corresponding to C-F covalent bond was observed at a lower binding energy for the former than for the latter. This result suggests that the fluorine atom is bound with carbon layer more strongly in the latter than in the former. It is considered from this result that some amount of fluorine atom of the former is chemically adsorbed on carbon layer having many defects in crystallite. However, C_{1s} peak position of graphite fluoride prepared from graphitized PC was almost the same as that prepared by the conventional method. The present method is more effective for graphite having large particle size such as flaky natural graphite because the host graphite holds the intercalant so tightly at low temperature that the space among the crystallites might expand largely by rapid decomposition on heating. On the other hand, for graphite with small particle size, for example, graphitized PC, GIC was not so stable even at a low temperature as described in Chapter 1 that it decomposed smoothly on heating. Accordingly, the surface area would not increased so much by the present method. Therefore, the $(C_2F)_n$

Table 5-4 C_{1s} and F_{1s} binding energies of graphite fluoride.

Starting material of natural graphite	Graphite fluoride prepared by the present method		Graphite fluoride prepared by the conventional method	
μm	eV		eV	
	C_{1s}	F_{1s}	C_{1s}	F_{1s}
833-295	289.4	688.8	290.2	689.3
74-61	289.4	688.9	289.9	688.8

prepared from graphitized PC by the present method would have similar nature as that prepared by the conventional method.

4. Summary

(1) It was found that graphite fluoride, $(C_2F)_n$, was prepared via GIC at a higher reaction rate than by the conventional method. This process consisted of the decomposition of GIC with fluorine and metal fluoride and the subsequent fluorination of exfoliated graphite formed by the decomposition at 350-400°C.

(2) The reaction rate was maximum at a fluorine pressure of 267×10^2 Pa where the decomposition of GIC would occur most easily.

(3) $(C_2F)_n$ prepared by the present method contained more $(CF)_n$ than that prepared by the conventional method because of the disordered and large surface area of the exfoliated graphite formed by the decomposition of GIC. However, the purity of $(C_2F)_n$ increased with decrease in the reaction temperature.

References

1) Y.Kita, N.Watanabe and Y.Fujii, J. Am. Chem. Soc., **101**, 3832 (1979).

2) N.Watanabe and K.Morigaki, Denki Kagaku, **47**, 169 (1977).

3) Y.Kita and T.Kawaguchi, Nippon Kagaku Kaishi, **1977**, 191 (1977).

4) N.Watanabe, A.Izumi and T.Nakajima, J. Fluorine Chem., **18**, 475 (1981).

5) K.Hozumi and N.Akimoto, Bunseki Kagaku, **20**, 467 (1971).

CONCLUSION

Graphite intercalation compounds (GIC's) have been extensively studied in the fundamental fields. However, only a covalent compound $(CF)_n$ is now in practical use because of less stability of the electroconductive GIC's in moist air. In the present study, new GIC's, $C_xF(MF_n)_y$ (M: Al, Fe, Mg, Cu or Li, n: 3, 2 or 1) were prepared from a ternary system of graphite, fluorine and metal fluorides having high melting or boiling points, and their physicochemical properties were investigated.

In Chapter 1 was dealt the preparation of GIC's, $C_xF(MF_n)_y$ from some kinds of graphites, fluorine and metal fluorides (AlF_3, FeF_3, MgF_2, CuF_2, LiF). The identity period in direction of c-axis (I_c) was $\{9.4 + 3.35 \times (n-1)\}$ Å (n; stage number), independent of the kind of metal fluoride. The GIC's contained a much larger amount of fluorine than metal fluoride. The typical composition was $C_{5-12}F(MF_n)_{0.03-0.0002}$ for GIC's with I_c, 9.4 Å, and $C_{10-20}F(MF_n)_{0.02-0.0003}$ for those with I_c, 12.8 Å. It was therefore considered that the I_c was decided by the size of intercalated fluorines. ^{19}F-NMR spectra indicated that GIC contained mobile fluorines weakly interacting with graphite layer. F_{1s} ESCA spectra obtained by cleavage of GIC having HOPG host showed that the intercalated fluorines were in slightly ionized state or in nearly molecular state. It was also found that C-F covalent bond was formed around the surface of the GIC prepared by introduction of fluorine at a temperature higher than 200°C. The stability of GIC mainly depended on host graphite material. The higher stability was observed as the following order with regard to host graphite (a) and metal fluoride (b).

(a) PAN-based carbon fiber > natural graphite > pyrolytic graphite > graphitized petroleum coke

(b) CuF_2, AlF_3 > LiF > MgF_2, FeF_3

In Chapter 2, intercalation mechanism was discussed on the basis of the results of the reaction between fluorine and LiF and the thermogravimetric curves on intercalation reaction. The surface of LiF powder (ca. 0.2 g) was liquefied at ca. 530°C by the reaction with fluorine of 1.0×10^5 Pa and the complete liquefaction was observed around 650°C which is lower by about 200°C than the melting point of LiF (845°C). This result means that there exists a strong chemical interaction between LiF and fluorine. A gas species, MF_{n+m} formed by the reaction of metal fluoride with fluorine would interact with host graphite and have a significant role as a medium for the subsequent fluorine intercalation.

$$\frac{1}{2} mF_2(g) + MF_n(s) \longrightarrow MF_{n+m}(g) \quad (1)$$

$$\text{Graphite}(s) + MF_{n+m}(g) + F_2(g) \longrightarrow C_xF(MF_n)_y(s) \quad (2)$$

The reaction (1) would proceed more easily with increasing temperature, however, the intercalation reaction (2) prefers the lower temperatures. It was observed by thermogravimetry that the intercalation reaction occurred under ca. 100°C.

Chapter 3 dealt with the electrical conductivities of GIC's, $C_xF(MF_n)_y$. The electrical conductivity of GIC in direction of a-axis prepared from pyrolytic graphite (PG) increased with increase in the intercalant and reached a maximum value of 1.9-2.0 $\times 10^5$ $(\Omega \cdot cm)^{-1}$ which was 10 times that of original PG ($1.7 \pm 0.2 \times 10^4$ $(\Omega \cdot cm)^{-1}$). On the other hand, GIC prepared from PAN-based carbon fiber had the maximum electrical conductivity of 7-9 $\times 10^3$ $(\Omega \cdot cm)^{-1}$ which was 7 times that of original value (1.1-1.4 $\times 10^3$ $(\Omega \cdot cm)^{-1}$). However, GIC prepared from PAN-based carbon fiber was much more stable than that of PG. The decrease in the electrical conductivity was only 7 % for 80 days in air.

In Chapter 4, the discharge characteristics of GIC's, $C_xF(MF_n)_y$ were discussed in comparison with those of $(CF)_n$ and

$(C_2F)_n$. GIC's used as cathode materials had higher OCV's of 3.5-3.6 V vs Li after 20 % discharge than that of $(CF)_n$ or $(C_2F)_n$, which is due to more active fluorine atoms intercalated in graphite layers. The flat discharge potential was observed only for GIC's treated in fluorine gas at a retention temperature between 268 and 350°C. Such a GIC showed a higher discharge potential than $(CF)_n$ or $(C_2F)_n$ at a current density lower than 300 $\mu A/cm^2$. The overpotential increased with increase in current density probably because a thickness of a diffusion layer consisting of $C_x(LiF)(MF_n)_y$ increased. X-ray diffraction analysis and ESCA measurement indicated that the discharge reaction proceeded as follows,

$$C_xF(MF_n)_y + Li \longrightarrow C_x(LiF)(MF_n)_y$$

where M is Al, Mg or Cu and n is 3 or 2.

Chapter 5 dealt with an application of the GIC to the synthesis of graphite fluoride, $(C_2F)_n$. It was found that $(C_2F)_n$ was prepared via GIC at a higher reaction rate than by the conventional method. This process consisted of the decomposition of GIC with fluorine and metal fluoride and the subsequent fluorination of exfoliated graphite formed by the decomposition at 350-400°C. The reaction rate was maximum at a fluorine pressure of 267×10^2 Pa where the decomposition of GIC would occur most easily. $(C_2F)_n$ prepared by the present method contained more $(CF)_n$ than that prepared by the conventional method because of the disordered and large surface area of the exfoliated graphite formed by the decomposition of GIC. However, the purity of $(C_2F)_n$ increased with decrease in the reaction temperature.